Worcester Polytechnic Institute
Digital WPI

Major Qualifying Projects (All Years) | Major Qualifying Projects

April 2010

FORCE PLATE RELIABILITY AND DYNAMICS FOR AMBULANCE VIBRATION SUPPRESSION

Nicole Courtney Klegraefe
Worcester Polytechnic Institute

Follow this and additional works at: https://digitalcommons.wpi.edu/mqp-all

Repository Citation
Klegraefe, N. C. (2010). *FORCE PLATE RELIABILITY AND DYNAMICS FOR AMBULANCE VIBRATION SUPPRESSION.* Retrieved from https://digitalcommons.wpi.edu/mqp-all/3157

This Unrestricted is brought to you for free and open access by the Major Qualifying Projects at Digital WPI. It has been accepted for inclusion in Major Qualifying Projects (All Years) by an authorized administrator of Digital WPI. For more information, please contact digitalwpi@wpi.edu.

FORCE PLATE RELIABILITY AND DYNAMICS FOR AMBULANCE VIBRATION SUPPRESSION

A Major Qualifying Project Report

Submitted to the Faculty

of the

WORCESTER POLYTECHNIC INSTITUTE

in partial fulfillment of the requirements for the

Degree of Bachelor of Science

in Mechanical Engineering

by

Nicole Klegraefe

_____

Date: April 29, 2010

Approved:

_____

Prof. M.S. Fofana, MQP Advisor

ABSTRACT

This Major Qualifying Project used experimental methods, mathematical analysis tools and solid modeling applications to determine the dynamic characteristics and reliability of a force plate design as a solution to attenuate disruptive and harmful road-induced vibrations experienced in the patient-care compartment of an ambulance. Vibration data were collected experimentally from four different tests, each including a different ambulance traveling over four distinct road surfaces in three different speed ranges. The data were processed and analyzed for correlations to safety and patient care. Additionally, the vibrations characterized through experimentation were used to determine an appropriate mathematical modeling solution to attenuate the mast harmful vibrations experienced in the ambulance patient compartment. Finally, the model was applied to discover the ability of a supplemental force plate suspension design that would support and protect passengers in the back of the ambulance through the use of both passive mechanical springs and dampers, and an active, controllable attenuation device.

ACKNOWLEDGMENTS

I would like to give my appreciation to the UMASS Memorial Emergency Medical Service, the Putnam CT Emergency Medical Service, and the Woodstock CT Volunteer Fire Association for allowing access to emergency medical vehicles for this project. In particular I would like to thank the following individuals who gave their time to help facilitate test runs in the vehicles: Steve Haynes (UMASS Memorial), David Lyons (UMASS Memorial), Nathan Campbell (Putnam EMS), and Susan Calaman (Woodstock VFA).

Last I would like to extend my heartfelt gratitude towards my mentor, Paul Cotnoir, and my advisor, Dr. Mustapha S. Fofana, both for inviting me to work with them in this academic undertaking and for their guidance throughout the year.

Table of Contents

List of Figures and Tables

CHAPTER 1: INTRODUCTION

According to the National Hospital Ambulatory Medical Care Survey, over 18 million ambulance transports to United States emergency departments alone occurred in 2006. Standard emergency medical service procedure is to stabilize and transport the patient to the nearest hospital as quickly as possible, which requires that a variety of diagnostic and treatment procedures be carried out while the ambulance is in transit. However, the ability of emergency medical personnel to carry out such procedures is made difficult during patient transport in the back of an ambulance. With the health of the patient already at risk in an emergency situation, and the limitations on treatment caused by the environment of the moving ambulance, the need to examine and improve on existing emergency medical services has become a focus of both behavioral and administrative studies as well as a motivation for engineering innovation.

Much of the literature available about emergency transport is focused on injuries and fatalities caused by accidents involving emergency vehicles. The high risk associated with ambulance transportation has led to enhanced safety policies, such as more rigorous crash test requirements for the vehicles and more extensive driver training and practice. Despite the implementation of these policies, there are still additional risks to the health and safety of both injured or ill patients and emergency medical personnel. These risks are generated from potentially dangerous shocks and vibrations transmitted through the ambulance as it travels over uneven road surfaces. Whole-body shocks and vibrations that are felt while in a traveling vehicle can have possible negative effects on a variety of human physiological systems and may affect human sensory perceptions and motor functions.

Although studies to determine the direct physical effects, if any, which are caused by whole-body shock and vibration have resulted in unclear and indefinite conclusions, it is

generally understood that such shocks and vibrations do have potential to be dangerous to human health. In addition, it has been established that diagnostic and treatment activities are limited and difficult for emergency medical personnel to perform while traveling in an ambulance. The disturbances caused by vibrations may also interfere with diagnostic equipment and their use, particularly those which require the use of human sensory interpretation or sensitive electrical signals. It is apparent that ambulance patient care and comfort would benefit from a reduction in shocks and vibrations currently transmitted through the ambulance suspension system.

The recurrent vibrations that occur in typical ambulance travel vary over a wide range of frequencies. These frequencies can be correlated to various road surface profiles and travel velocities based on studies found in literature and developed mathematical road models. Several methods for predicting discomfort caused by vehicle shocks and vibrations have been developed and are used in the automotive industry to aid in the design of vehicle suspensions to reach optimum passenger comfort. One mathematical model commonly used as a tool in designing suspension systems, with concern for comfort as the main objective, is the quarter-car model. This model can be used to accurately measure the ability of an ambulance suspension system to support the required load and isolate road excitations.

Using the quarter-car method, it has been shown that a standard ambulance chassis suspension does not sufficiently suppress significant road-induced vibrations that can be harmful to patients and emergency medical personnel traveling in the ambulance. The vibrations present in the ambulance during travel can directly affect the health of injured or ill patients and also hinder the performance of the emergency medical personnel responsible for their care. The ultimate goal of this project was to develop and model an active force plate design that would

work to suppress the most harmful vibrations transmitted through the current standard ambulance suspension system.

CHAPTER 2: BACKGROUND

Road Surfaces and Vehicle Vibrations

Techniques for characterizing road surfaces and measuring the vibrations transmitted to vehicle passengers have been used in multiple studies on the subject of occupational hazards caused by continual vibration exposure as well as to aid in the evaluation of suspension design for ride comfort. Many of these studies make use of mathematical models to simulate, test, and analyze approximate road surface excitations. In their study, Tamboli and Joshi compared the power spectrum density of imitation road excitations, created by the application of oscillatory functions, and actual road excitations and were able to conclude that their sinusoidal model was an accurate approximation of actual measured displacements (Tamboli & Joshi, 1999). Figure 1 below shows a diagram of the power spectrum density comparison.

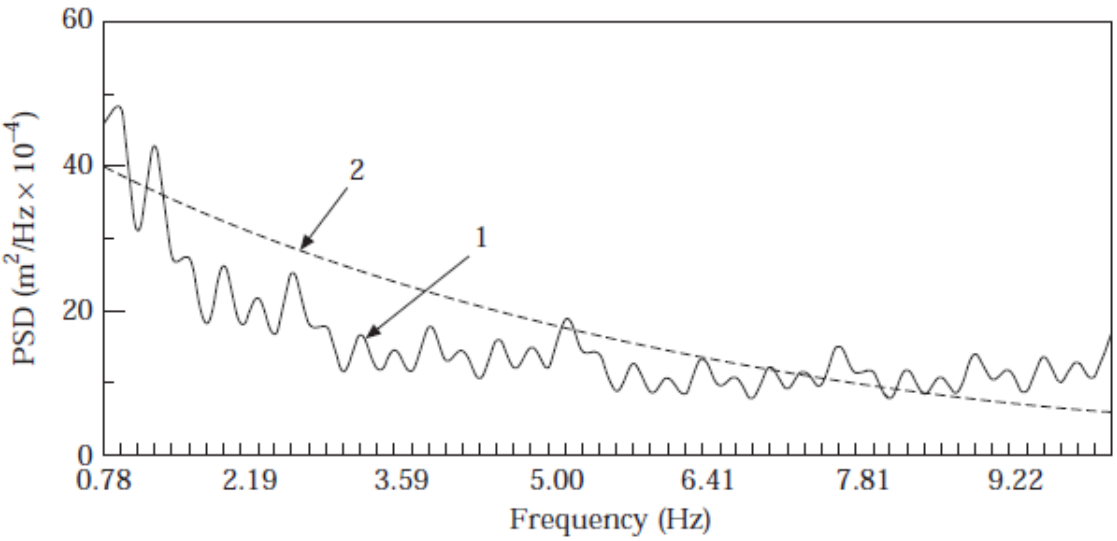

Figure 1: Comparison of power spectrum density of actual (1) and formulated (2) road excitations (Tamboli & Joshi, 1999, p.200)

Other vehicle vibration studies only use actual vibration data collected directly from measurement in actual traveling vehicles. Exposure severity and limits have historically been measured by several methods, including the use of shake tables, ride simulator experiments, ride measurement in vehicles, and subjective ride assessment (Barak, 1991). In their study, Paddan and Griffin measured vibration data from 100 different vehicles tested over 461 experimental trials (Paddan & Griffin, 2002). Figure 2 displays the power spectrum curves for the 25 cars that were evaluated as part of this study. Although the road excitations experienced by each of these vehicles were diverse, the variability and range of the power spectrum curves is fairly tight. Although many methods have been employed in the study of vehicle vibrations, the power spectral density measurement method shows significant consistency across many studies, even with variable frequencies and amplitudes of road excitations.

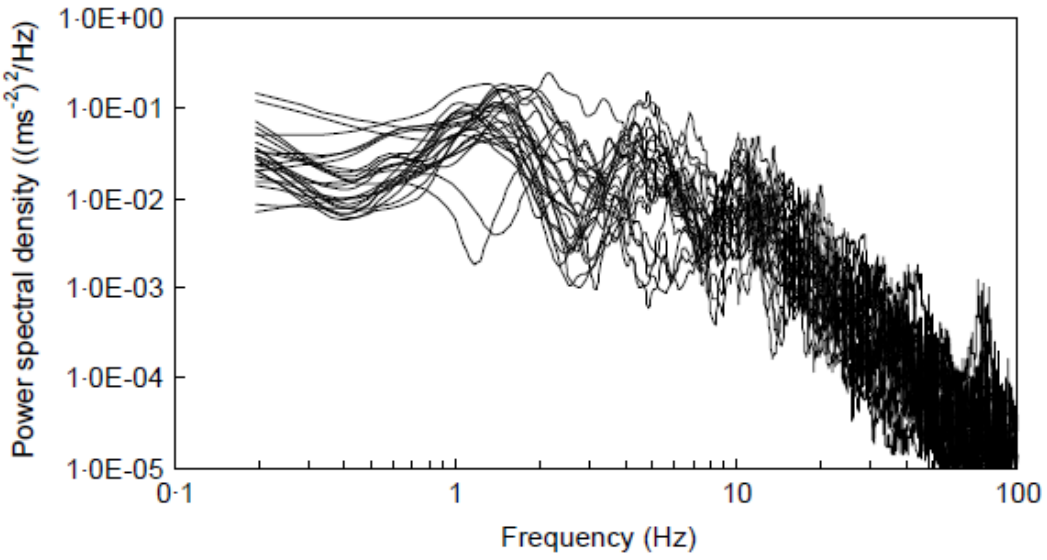

Figure 2: Power spectrum density of vertical vibration measurement on seats of the 25 cars tested by Paddan and Griffin (2002, p203)

Human Response to Vibration

Two international vibration standards can be applied to vibration studies: the International Organization for Standardization (ISO) 2631 (International Organization for Standarization, 1997) and the British Standard Institution 6841 (British Standards Institution, 1987). Both of these standards require vibration magnitude data to be calculated using vibration dose value, which accounts for the frequency, magnitude and length of the exposure to the vibration under investigation. However, acceleration information is obtained for three axes and the resultant axis under the British Standard, while only the most severe axis acceleration is obtained for the ISO standard. Both standards express vibration exposure limits in terms of time, establishing these limits based on comfort levels and decreased proficiency due to fatigue.

In the Paddan and Griffin study that measured vibrations in 100 different vehicles, results were assessed relative to both ISO and British standards (Paddan & Griffin, 2002). The range of vibration amplitudes for all the vehicles tested ran from 0.14 m/sec^2 to 1.52 m/sec^2. Paddan and Griffin found that the majority of the measurements indicated that the location which measured the worst frequency-weighted accelerations was the vertical axis of the seat pan. The vibration evaluations that were calculated in accordance with the ISO standard resulted in lower values than those calculated with the British standard, which consequently resulted in a lower likelihood of exceeding the "health guidance caution zone" proposed in the ISO standard versus reaching the "action zone" of the British standard. The lack of uniformity between the international standards used to evaluate the potential hazard of vehicular vibrations makes it difficult for conclusions to be made about the physical characteristics of vibrations or how vibrations can be harmful.

Although conclusions cannot be drawn about the direct effects of vibrations on human health, some general observations can be made about how the human body can be affected by shocks and vibrations. Effects from vibrations are frequency, magnitude, direction, and duration dependent. Relative discomfort or danger related to a specific magnitude vibration must also be correlated to the frequency, direction and duration of that vibration. Table 1 below displays the natural frequencies of the human body as summarized by Paschold (2008, p.54). Human biological systems are most sensitive to vibrations which resonate that the same frequencies as their natural frequencies. This means that the effects of vibrations are dependent on factors both external and internal to the human body.

Table 1: The natural frequencies of the human body and its various parts as summarized by Paschold

Study authors	**Natural frequency (Hz)**	**Body, part or organ**
Randall, Matthews & Stiles, 1997	12	Whole body, standing
Brauer, 1994	4 -6	Whole body, seated
Brauer, 1994	3- 4	Whole body, supine
Wasserman, 1996	4- 8	Whole trunk, vertical
Kroemer and Grandjean, 1997	4*	Lumbar vertebrae
Brauer, 1994	20-30	Head, relative to body
Kroemer and Grandjean, 1997	5-30*	
SafetyLine Institute	20- 30	
Mansfield, 2006	20	Eyes
Kroemer and Grandjean, 1997	20- 70*	
SafetyLine Institute, 2007	20- 90	

Kroemer and Grandjean, 1997	5*	Shoulder girdle
Kroemer and Grandjean, 1997	3- 6*	Stomach
SafetyLine Institute	4- 5	
Kroemer and Grandjean, 1997	4- 6*	Heart
Kroemer and Grandjean, 1997	10-18*	Bladder

*seated posture

Effect of Vibrations on Ambulance Patients

While there is substantial literature and international standards to back up claims made about vehicle comfort, there are few studies that link vehicle vibration to health or injury risks. In the case of ambulance patients, physiological effects of exposure to shocks and vibrations are generally limited to the short-term, acute effects of ambulance travel, which are difficult to define because of the patients' compromised health conditions which are pre-existing. While there have been an array of experimental studies that have attempted to characterize the effects of ambulance vibrations on patients being transported, the human physiological responses to vehicular vibrations are not well enough understood to draw concrete conclusions.

In their study involving the monitoring of patients being transported in ambulances, Waddell, Scott, Lees and Ledingham discovered that the direct physiological stimuli from riding in the ambulance, including the vibrations felt and noise from sirens, as well as the limited ability of emergency medical service personnel to perform diagnostic and care procedures while in the moving vehicle caused a variety of cardiovascular and respiratory effects in patients (Waddell, Scott, Lees, & Ledingham, 1975). In another study, 7 percent of patients diagnosed with either myocardial infarctions or unstable angina prior to transport experienced arrhythmias, chest pain,

hypotension, and cardiac arrest during ambulance transport (Schneider, Borok, Heller, Paris, & Stewart, 1988). In a similar study by Griffin, vertical vibrations in the 1-20 Hz range were shown to cause increases in heart rate and blood pressure measurements, which could be potentially dangerous to individuals with existing cardiovascular conditions (Griffin, 1990).

While drawing conclusions from these experimental studies is difficult, it is apparent that there are some significant effects on critically ill patients caused by the stress and physiological stimuli during ambulance transport. The studies have also shown that the vertical vibrations experienced in the ambulance patient compartments often exceed the limits in place for healthy adults, which could likely have adverse effects on pediatric and ill patients travelling in ambulances. More studies should be done to further understand the possible direct physiological effects of whole-body vibrations on patients.

Effect of Vibrations on Emergency Medical Service Personnel and Patient Care

Vibrations can have several effects on the ability of emergency medical service personnel to care for patients in the back of a moving ambulance, ranging from physical limitations to equipment malfunction. Important medical procedures that require high perception, motor and control skills are often completed before transport because of the impact that shocks and vibrations can have on these functional skills. In addition to the physical difficulties in performing medical procedures in a moving ambulance, some medical equipment used to aid in the diagnosis or treatment of patients can also malfunction as a result of the vibrations felt in the patient compartment of the ambulance.

Visual perception is one of the most effected of the senses when exposed to shocks and vibrations. Movement of the observer, of what is being observed, or a combination of both can

cause blurred vision. Vibrations below 2 Hz do not typically effect visual perception because of the ability of the eye to move and follow moving objects. However, vision becomes compromised as vibration frequencies reach around 10 Hz because the human vision system can no longer accurately adjust for the displacement of the image on the retina. Vibrations with frequencies about 20 Hz also begin to effect resonances within the human eye muscles and can cause even more distortion of visual perception (Griffin, 1990).

According to Griffin, there are three causes of vibration-affected manual skills: (1) vibration-correlated error, (2) input-correlated error and, (3) remnant. Vibration-correlated error is caused by vibrations that are transmitted through the body to the arm and hand. Vibrations reach a maximum affect around 4-5 Hz when transmitted through the human body (Griffin, 1990). Figure 3 shows the vibration transmission to an outstretched hand when in a seated position. The random vertical vibrations produced large displacements of the hand in the x and z axes in the range of 2-6 Hz frequencies. The largest displacements occurred between 4-8 Hz in the y axis. The graphs show curves for hands outstretched to different distances and also holding weight.

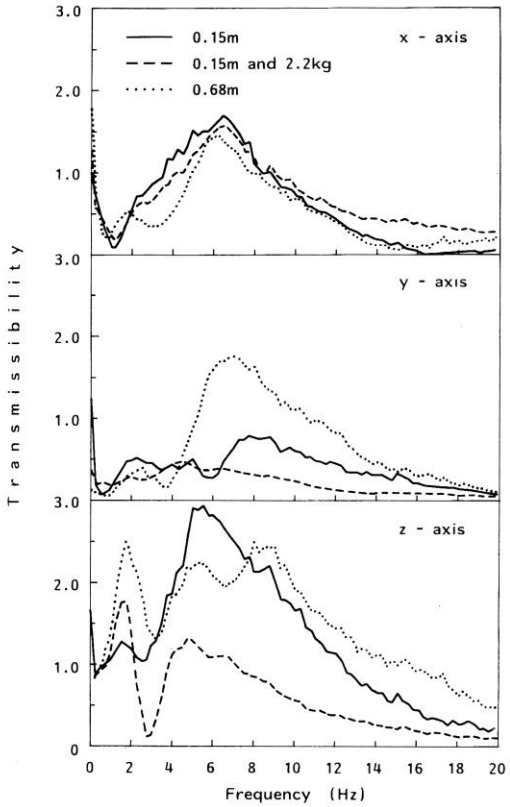

Figure 3: Transmissibility to the hand of vertical vibrations applied to a seated subject as measured by Griffin

In input-correlated error described by Griffin relates to the error due to limitations of the human visual and motor system. These errors are present even in the absence of shocks and vibrations, but can become more apparent when skills are affected by vibrations. Also, the remnant error is an inherent error that accounts for human and biological control systems acting in a non-linear fashion when completing a complex visual-motor function. An example of remnant error is the tendency for a person to slow down the execution of a task to improve the accuracy of completing that task (Griffin, 1990).

The total positioning error is the sum of all of the types of errors described above. This total error can be expressed as a root mean square tracking error, in dimensions of length. The total error in visual-motor tasks reaches a peak value at 4-8 Hz frequencies, which is the range

that causes the highest values of vibration-correlated error. Vibration-correlated error and total error both increase with increasing acceleration magnitudes. This is shown in Figure 4 which depicts a handwriting legibility test during which participants were asked to write on a hand-held clipboard while subject to whole-body vibrations at increasing amplitudes and frequencies (Griffin, 1990).

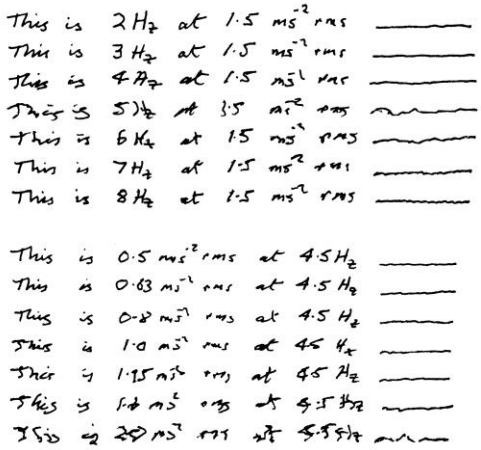

Figure 4: Handwriting samples of individuals subjected to whole-body vibrations as presented by Griffin (1990)

Figure 5 also depicts a study that demonstrates the frequency range of vibration-correlated errors. In this study a tracking task was performed by seated individuals subjected to sinusoidal vertical vibrations at 3.15 and 5.0 Hz (Griffin, 1990).

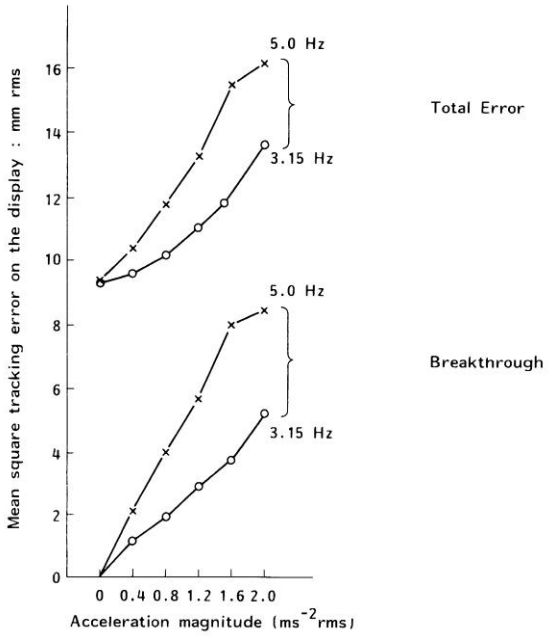

Figure 5: Total and breakout error in visual motor tasks as a function of vibration amplitude as reported by Griffin (1990)

The physical effects of shocks and vibrations on the perception, motor and control skills of emergency medical personnel performing in the back of an ambulance cause much of the important and sensitive medical procedures to be performed before transport begins, to avoid unintentional errors or unnecessary stress.

The limitations of emergency medical personnel are not only limited by the physiological effects of shocks and vibrations, but also are inhibited by the malfunctioning of sensitive medical equipment when subject to vibrations in the back of an ambulance. When speaking with emergency medical personnel at UMass Medical Center in Worcester, MA, equipment malfunction was a major factor in degradation of patient care in an ambulance. Personnel discussed the limitations associated with using any medical instrument that required auditory perception, such as using a stethoscope to hear heart and chest sounds or to make blood pressure measurements. Portable electrocardiogram machines used as a major diagnostic tool by

emergency medical personnel was also said to be unreliable when used in the moving vehicle, historically giving false readings.

Electrocardiogram machines are used to take a "snapshot" of how the human heart is functioning, and are often considered the most powerful and important piece of diagnostic equipment on the ambulance. An electrocardiogram has twelve electrodes, or leads, are attached to the body across the chest, abdomen, legs and arms to detect and measure electrical signals coming from the heart (Healthwise, Inc., 2008). The signals are then translated into outputs, usually digital or printed graphs. Malfunction of this equipment is affected by vibrations in several ways, but most apparent in the sensitivity of the electrodes and connecting wires. When the wires and electrodes are exposed to shocks and vibrations, it correlates to incorrect heart measurements because the machine cannot distinguish the external "noise" factors present. False outputs of this machine can have drastic effects on patient diagnosis and treatment.

Blood pressure, a basic triage measurement taken for all patients, can be measured both manually and automatically. However, both methods of measurement are affected by exposure to vibrations in a moving ambulance. Manual blood pressure measurement makes use of a inflator cuff which cuts off circulation in the arm until no blood is flowing through to the lower arm. A stethoscope is used to hear when the first beat is heard as the cuff deflates (Pickering, et al., 2005). Auditory perception is a necessary element in taking a manual blood pressure measurement, which can be made very difficult because of the noise associated with the moving ambulance, as well as outside of the ambulance. Automatic blood pressure measurement devices also use an inflation cuff to cut off blood circulation to the lower arm. As the cuff deflates, the machine records when it detects the pressure to no longer be steady, but pulsating. This pulsating pressure indicates the systolic blood pressure number, and a return to steady pressure indicates

the diastolic pressure measurement. This device can easily malfunction if vibrations caused by transport affect the pressure measures in the cuff as the arm is jostled (Kinast, 2005). Personnel at UMASS indicated that the use of automatic blood pressure monitors have had limited success being used in ambulances because of their sensitivity to shocks and vibrations.

Summary

Many experimental studies have shown the relationship whole-body vibrations and degraded perception and motor skills. In addition, it is accepted that whole-body vibrations have negative health effects on the human body at certain magnitude and frequencies, and can cause high levels of discomfort in individuals with extended exposure. A reduction in the vibrations that are transmitted to the patient compartment of an ambulance would allow for emergency medical service personnel to perform more effectively and lead to better diagnosis and treatment of patients during transport, subsequently reducing the time it takes for a patient to reach the hospital. Reductions in vibrations would also ensure better patient comfort and reduce the health risks that may be associated with exposure to vibrations while being transported.

CHAPTER 3: METHODOLOGY

The goal of this project was to develop and model an active force plate design that would work to suppress the most harmful vibrations transmitted through the current standard ambulance suspension system. The project will be completed in three steps: (1) experimentally characterize vibrations experienced during a typical ambulance ride, (2) process and analyze the vibration data collected to correlate the human physiological effects, and (3) analytically determine a model force plate design that would successfully attenuate harmful vibrations experienced in the ambulance.

Ambulance Vibration Characterization

In order to characterize the vibrations experienced in the back of an ambulance, experimental testing was done on four different ambulances in the New England area. Each of the ambulances was driven over four different types of road surfaces within three different speed ranges.

Vehicle selection

The four ambulances tested for this project included both Type I and Type II model configurations. The ambulances were built on four different chassis, including a Chevrolet C-4500, a Ford E-450, an F-450, and an F-550. Three of the ambulances featured classic leaf spring and shock absorber suspension systems and one featured an air ride suspension system. All four of the ambulances were manufactured in different years, including two newer ambulances and two older ones. All of the ambulances were also built to KKK-A-1822 star-of-life standards. Characterization of the four ambulances is outlined in Table 2 below.

Table 2: Test Vehicle Characteristics

	Date of test	EMS	Body mfg.	Mfg. Yr. Chassis	Suspension	Type	Class	GVW (lbs)	Tires
1	12/2009	UMASS Memorial EMS	Horton	2005 Ford F450	Standard leaf spring & shock absorber	I	1	16000	225/70 R19.5
2	12/2009	Putnam, CT EMS	Lifeline	2001 Ford E450	Standard leaf spring & shock absorber	III	1	14050	225/75 R16
3	12/2009	UMASS Memorial EMS	Braun	2008 Chevy C4400	Standard leaf spring & shock absorber	I	1	16500	225/70 R19.5
4	12/2009	Woodstock, CT EMS	Lifeline	2009 Ford F550	Air ride	III	5	17950	225/70 R19.5

Photographs of each of the vehicles tested as well as detailed specifications for each can be found in Appendix A of this report.

Road surface selection

The four common road surfaces found in the New England area were characterized as highway, secondary road, city street, and unpaved road. The four different road surfaces were used in this experiment to ensure comprehensive results that included a broad range of vibrations. Photographs of each of the four road surfaces are shown in Figure 6 below.

Figure 6: Photographs of local road surfaces including: (a) unpaved roads, (b) city streets, (c) secondary roads, and (d) highways

In addition to the typical road surfaces, random shocks due to road surface irregularities were also included when testing the ambulances on each type of road surface described above. These irregularities included potholes, speed bumps, and severely worn or crowned road surfaces.

Speed range selection

The three different speed ranges used during experimentation in the ambulances were speeds less than or equal to 35 miles per hour, speeds anywhere between 36 and 64 miles per hour, and speeds greater than or equal to 65 miles per hour. Not all vehicle speeds were tested over each of the road surfaces because drivers were limited by posted speed limits as well as road surface conditions. Table 3 outlines the road surface and speed range combinations that were tested to obtain the most comprehensive results.

Table 3: Road surface and speed range combinations for testing

Road Surface	Speed ≥ 65 mph	36-64 mph	≤ 35 mph
Highway	✓	✓	✓
Paved secondary road		✓	✓
Paved city street		✓	✓
Unpaved road			✓

Experimental Set-Up

Steps were taken to ensure that the experimental set-up was the same in each of the four ambulances tested. Each test included appropriate loading to mimic the loading of a real ambulance service run by the use of a Laerdal Nursing Anne full-body, articulated training manikin strapped to the standard transport stretcher of the ambulance being tested. Loading of the emergency medical technicians in the ambulance were mimicked by individuals conducting the experiments riding the back of the ambulance with the stretcher and manikin. The experimental set-up with and without the loaded stretcher are depicted in Figure 7 below.

Figure 7: Experimental set-up before and after loading the manikin on the stretcher

The accelerometer used to take measurements for the experiment was attached to the floor of the ambulance using 2 inch wide, 0.012 inch thick, Shurtape DF 550 double-stick carpet tape, and was located approximately 50 inches (+/- 5 inches depending on the ambulance configuration) from the back of the ambulance compartment and 35 inches (+/- 5 inches) from the side of the ambulance compartment. This position was chosen because of its rough orientation with the location of where the patient's chest would be located. Orientation of the axes of the accelerometer was set-up as shown in Figure 8 below.

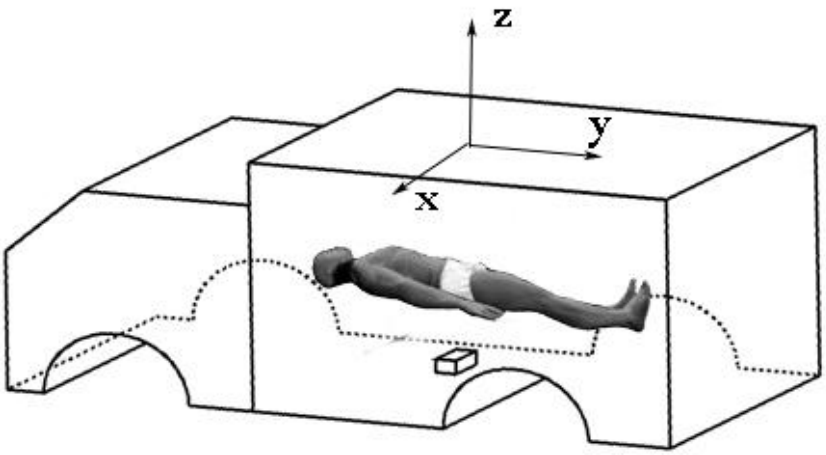

Figure 8: Axes orientation in ambulance compartment

The accelerometer axes location with respect to the vehicle where such that the x-axis extended side-to-side of the ambulance, the y-axis extended from front to back of the ambulance, and the z-axis extended from the floor to the ceiling of the ambulance.

Acceleration recorder

The accelerometer used during these experiments was an Instrumented Sensor Technology EDR-3C-10 Shock & Vibration Sensor/Recorder. This recording device is equipped

with a built-in tri-axial accelerometer for simultaneous measurement of accelerations in all three axes. The device also features three piezo resistive elements which provide the low frequency response (true DC) which was required to collect vibration data at the frequencies of interest during this experiment. Detailed specifications for the device can be found in Appendix B of this report. The sensor is shown in Figure 9 below.

Figure 9: Photograph of IST EDR-3C-10 Sensor

Each road type and vehicle speed range combination was sampled multiple times for each ambulance in discrete ten second intervals called events. In addition to providing acceleration data, the device also captured and recorded the date and time for each of the measured events. Approximately 70, 10-second events were recorded for each vehicle. All events were sampled 498.8 times per second (498.8 Hz) for acceleration values. Additionally, a remote trigger switch was used to manually initiate recording of the acceleration data for each event. The start time of each event was logged on data sheets which could later be inspected to match the acceleration data to the road type and vehicle speed range being tested.

Other instruments used with the accelerometer included a Toshiba Satellite L-305 laptop computer running EDR3CCOM and IST Dynamax software to set-up and calibrate the accelerometer and a wired remote toggle switch which allowed for data to be recorded only

when traveling over the road surfaces being tested. The computer was connected to the accelerometer via a serial cable at the start of each experimental run in order to download set-up parameters and engage the unit. The device was set to auto-calibrate before the recording of each event. Data stored in the memory of the recorder was downloaded to a computer after each ambulance was tested for long-term storage and analysis.

Data Processing and Analysis

The vibration data collected from the accelerometer after testing included time domain accelerations from all three axes as well as the root mean square acceleration. Using the Dynamax proprietary software provided by IST, peak acceleration values from all three axes and the RMS accelerations were also obtained. In order to characterize the vibrations experienced in the ambulances in relation to their impacts on passengers according to the ISO measurement standards, two additional data sets were generated using Microsoft Excel. This data included mean RMS acceleration values for each measured axis and mean peak accelerations in each axis. Mean RMS values specified the overall vibration levels experienced when traveling over certain roads within certain speed ranges, while the mean peak values showed the magnitudes of the vibrations likely caused by the road irregularities, such as potholes.

Force Plate Model Development and Analysis

For the last portion of this project, a model force plate design was developed and analyzed. Using the vibration data collected experimentally, forcing functions were derived and used as inputs to the model to discover the feasibility and reliability of the force plate design as a solution to attenuating the harmful vibrations experienced in the ambulance.

CHAPTER 4: RESULTS AND DISCUSSION

Event Description

For this experiment each ambulance was tested on certain road surfaces within certain speed ranges in 10 second intervals called events. The event numbers for each vehicle categorized by road surface and vehicle speed range are given in Table 4 below.

Table 4: Test and Event Numbers

Amb #	Total # events	Event[1] #'s							
		Highway			Secondary road		City street		Un-paved road
		≤35 mph	36-64 mph	≥65 mph	≤35 mph	36-64 mph	≤35 mph	36-64 mph	≤35 mph
1	64	1-3	4-6; 15-20	7-14	21-23; 27-29	24-26; 30-32	41-64	38-40	33-37
2	63	1-3	4-6; 10-15	7-9; 16-18	25-27; 50-52	31-33; 58-60;	19-24; 44-49; 61-63	28-30	34-43
3	71	1-3	4-6	7-15	16-18; 22-24	19-21	34-58	31-33	25-30
4	93	16-18	19-24; 31-35	25-30	4-6; 10-12	1-3; 13-15; 41; 43-45	7-9; 34-36; 49-58; 68-70; 77-82; 91-93	37-39; 59-67	71-76

[1]Each event represents a 10 second recording interval.

Vibration Amplitude Data

The data collected as part of the experiment for this project provide characterizations such as magnitude and frequency spectra necessary to evaluate the effects of the vibrations experienced in the patient compartment of an ambulance according to ISO standardized measures. Acceleration data was collected for the x, y, z, and resultant axes, with both peak axis data and total vibration values reported. However, for the purposes of this project, vibrations

experienced in the z-axis, or vertical axis, were the focus of the analysis. The raw vibration amplitude data collected from the experiment are presented in Appendix C of this report. The data includes z-axis, worst axis and resultant, tri-axial accelerations for overall vibrations (mean RMS), and shock accelerations (maximum peak and mean peak).

Characterization of ambulance vibration amplitude data by vehicle

The data collected from each ambulance test was analyzed to evaluate the differences between the vibrations experienced from vehicle to vehicle. Table 5 below lists the overall magnitude of the z-axis vibrations as well as the magnitudes of the average peak vibrations for each separate ambulance in terms of the mean rms acceleration values and the mean peak acceleration values. The results are also shown graphically in Figure 10.

Table 5: Vibration magnitudes separated by vehicle

Overall magnitude of vibrations z-axis					Magnitude of bumps and shocks z-axis				
Mean RMS (m sec-2)					Mean peak (m sec-2)				
For ambulance #1, all speeds, all road surfaces									
$\bar{x}$	Min	Max	s	n	$\bar{x}$	Min	Max	s	n
1.15	0.60	2.41	.55	64	6.08	3.44	13.56	3.2	64
For ambulance 2, all speeds, all road surfaces									
$\bar{x}$	Min	Max	s	n	$\bar{x}$	Min	Max	s	n
0.83	0.62	1.05	0.16	63	3.88	2.88	5.36	0.96	63
For ambulance #3, all speeds, all road surfaces									
$\bar{x}$	Min	Max	s	n	$\bar{x}$	Min	Max	s	n
1.34	0.71	2.55	0.56	71	7.03	3.90	15.45	3.64	71
For ambulance #4, all speeds, all road surfaces									
$\bar{x}$	Min	Max	s	n	$\bar{x}$	Min	Max	s	n
0.64	0.46	0.96	0.16	93	3.20	1.87	4.40	0.86	93

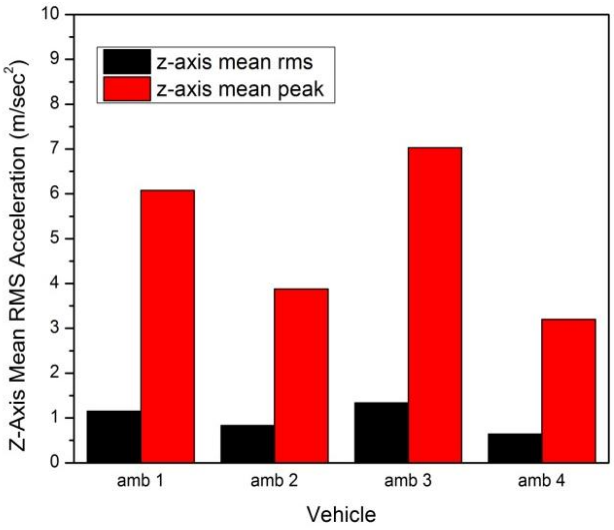

Figure 10: Graph of z-axis mean rms acceleration and mean peak acceleration for each ambulance at all speeds and road surfaces

Figure 10 shows that ambulances 1 and 3 (the two ambulance tests run in Worcester, MA) experienced higher average and peak accelerations than ambulances 2 and 4 (the two ambulance tests that were run in Connecticut). Looking further at the data, which is presented in Appendix C of this report, there do not appear to be significant differences between measured vibrations taken on the same road surfaces within the same speed ranges in different ambulances. This means that the differences between the ambulances that appear in the graph in Figure 10 are likely caused by another factor, such as driver handling or road conditions and could be deemed insignificant for the purposes of this project.

Characterization of ambulance vibration amplitude data by road surface

The data collected for each ambulance was then analyzed to evaluate the differences between the vibrations experienced over the four different road surfaces. Table 6 lists the magnitudes of the overall average z-axis vibrations and of the average peak z-axis vibrations experienced separated by the four different types of road surfaces tested. The results are also shown graphically in Figure 11.

Table 6: Vibration magnitudes separated by road surface

Overall magnitude of vibrations z-axis					Magnitude of bumps and shocks z-axis				
Mean RMS (m sec-2)					Mean peak (m sec-2)				
For all speeds, all ambulances, highway travel									
$\bar{x}$	Min	Max	s	n	$\bar{x}$	Min	Max	s	n
0.89	0.59	1.63	0.31	73	4.28	3.07	7.25	1.20	73
For all speeds, all ambulances, secondary road travel									
$\bar{x}$	Min	Max	s	n	$\bar{x}$	Min	Max	s	n
0.93	0.50	1.34	0.28	49	4.65	2.50	6.42	1.40	49
For all speeds, all ambulances, city street travel									
$\bar{x}$	Min	Max	s	n	$\bar{x}$	Min	Max	s	n
0.90	0.60	1.29	0.26	110	4.90	2.92	8.03	1.71	110
For all speeds, all ambulances, unpaved road travel									
$\bar{x}$	Min	Max	s	n	$\bar{x}$	Min	Max	s	n
1.54	0.46	2.55	1.09	27	8.44	1.87	15.45	7.06	27

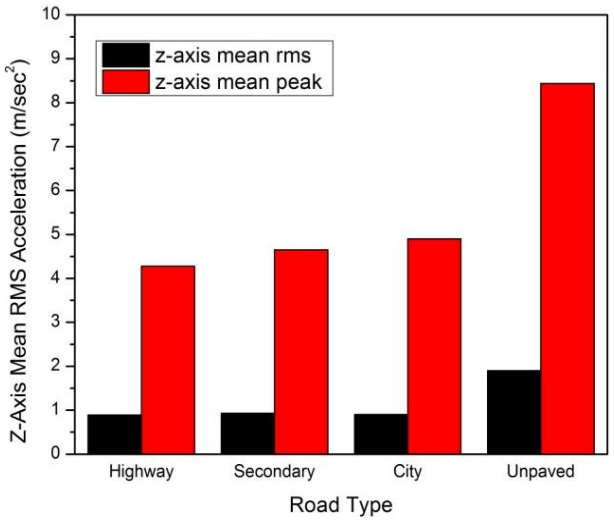

Figure 11: Graph of z-axis mean rms acceleration and mean peak acceleration for each road surface for all ambulances at all speeds

The results shown in Figure 11 correspond to what was expected to happen between the different road surfaces which were tested. The highway has relatively lower vibration magnitudes in both overall and peak values than all the other road surfaces, while unpaved roads showed the highest magnitude values.

Characterization of ambulance vibration amplitude data by vehicle speed

The data collected for each ambulance was also analyzed to evaluate the differences between the vibrations experienced when traveling within the three different speed ranges. Table 7 lists the magnitudes of the overall average z-axis vibrations and of the average peak z-axis vibrations experienced separated by the three different speed ranges tested. The results are also shown graphically in Figure 12.

Table 7: Vibration magnitudes separated by vehicle speed ranges

Overall magnitude of vibrations z-axis					Magnitude of bumps and shocks z-axis				
Mean RMS (m sec-2)					Mean peak (m sec-2)				
For all road types, all ambulances, speed ≤ 35 mph									
$\bar{x}$	Min	Max	s	n	$\bar{x}$	Min	Max	s	n
0.94	0.46	2.55	0.62	151	5.18	1.87	15.45	3.78	151
For all road types, all ambulances, speed 36 – 64 mph									
$\bar{x}$	Min	Max	s	n	$\bar{x}$	Min	Max	s	n
0.99	0.60	1.34	0.26	57	4.92	2.62	8.03	1.68	57
For all road types, all ambulances, speed ≥ 65 mph									
$\bar{x}$	Min	Max	s	n	$\bar{x}$	Min	Max	s	n
1.18	0.96	1.63	0.31	29	4.90	3.50	7.25	1.63	29

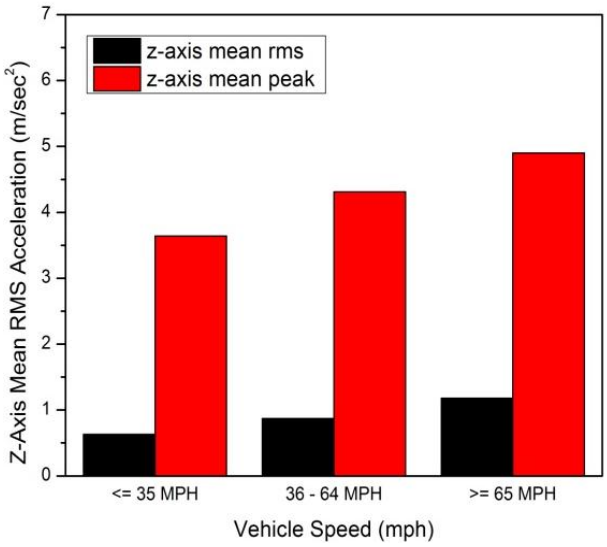

Figure 12: Graph of z-axis mean rms acceleration and mean peak acceleration for each vehicle speed range for all ambulances on all road surfaces

The results depicted in Figure 12 show that there is little significant difference between traveling over a variety of road surfaces at the three different speed ranges tested. The reason for the closeness in vibration magnitudes could be due to the fact that the most significant vibrations were experienced while traveling over unpaved roads and city streets, where road conditions and posted speed limits did not often allow for testing to be done above the 35 mile per hour range. This effectively skewed the data in such a way that the lower speed range showed relatively high vibration magnitude values.

Figures 13(a-b) show the results of the mean rms and mean peak z-axis vibration magnitude values for the different speed ranges when only considering travel over highway type road surfaces, which allows for further analysis of speed ranges as the changing variable of the experiment. In Figure 13(a) it seems that the increase in speed correlates to an increase in vibration magnitude, however Figure 13(b) does not show the same correlation as clearly.

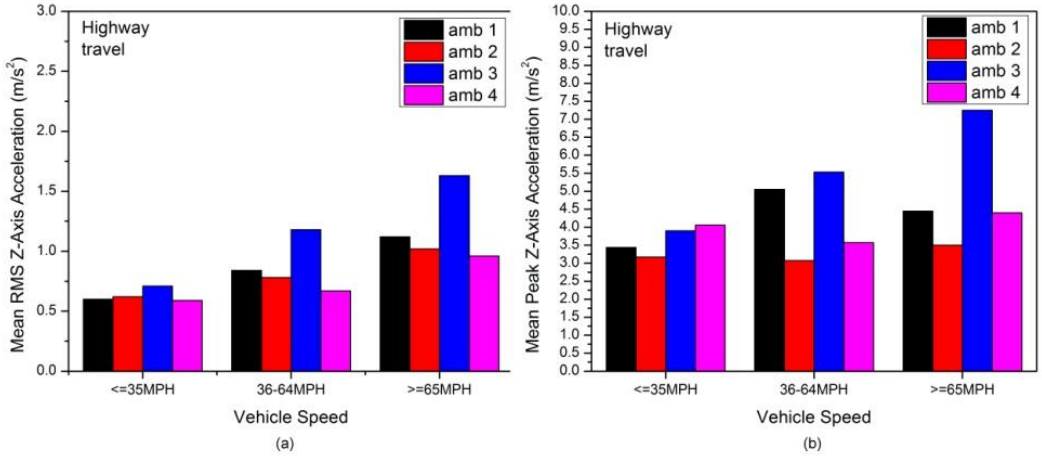

Figure 13: Graphs of (a) z-axis mean rms vibration magnitudes and (b) mean peak vibration magnitudes by three different speed ranges with all ambulances on highways

Characterization of ambulance vibration data summary and comparison

For the purpose of comparing the data collected from this experiment to the data found in other studies, the data was processed to find the minimum, maximum, and mean values for both the z-axis and the resultant axis in terms of the overall vibrations experienced and the shock vibrations experienced. The overall z-axis magnitudes from all of the ambulance tests had a range from 0.46 to 2.55 m/sec^2 with a mean value of .99 m/sec^2, while the overall resultant-axis magnitudes had a range from .66 to 2.94 m/sec^2 with a mean value of 1.33 m/sec^2. The shock vibrations experienced in the z-axis, which were likely caused by some irregularity in the road surface such as a pothole, ranged from 4.16 to 15.45 m/sec^2 with a mean value of 5.00 m/sec^2, while the resultant-axis shock vibration magnitudes ranged from 2.88 to 16.08 m/sec^2 with an average of 5.64 m/sec^2. These values are represented graphically in Figures 14 and 15.

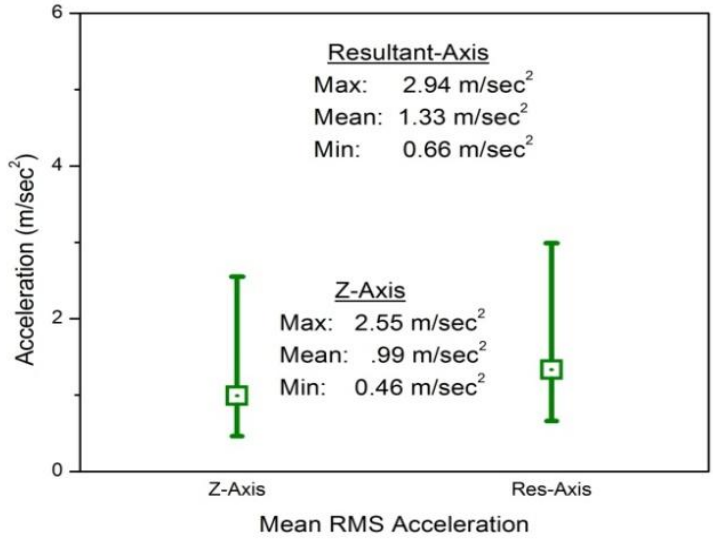

Figure 14: Graph of overall magnitude of z-axis and resultant-axis mean rms accelerations

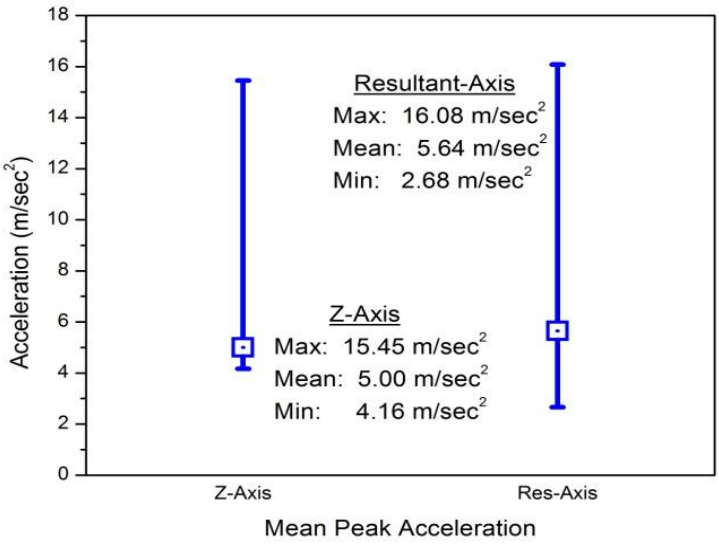

Figure 15: Graph of shock magnitude of z-axis and resultant-axis mean peak accelerations

Using these average values for both the overall vibrations and the average peak accelerations experienced in the ambulance, the data collected as part of this project was compared to data found in literature. Table 8 lists several ambulance vibration studies and shows that although there is variability in values from different studies, data collected as part of this project are within appropriate range of accelerations found in those studies.

Table 8: Comparison of vibration magnitude data

Study Authors	Max Peak accel. ($m\ s^{-2}$)	Mean R.M.S. accel. ($m\ s^{-2}$)	Road profile description	Measurement configuration
Cotnoir & Klegraefe, 2010	16.08	1.78	Highway, Secondary Roads, City Streets & Unpaved roads	Triaxial vector sum (Resultant Axis)
	15.45	1.04		Vertical axis on compartment floor
Sherwood, et. al., 1994	15	--	City & highway	Triaxial vector sum measurement on mannequin forehead, vehicle floor and base of isolette
Bellieni, et. al., 2004	11.8	1.3	City & highway	Vertical axis in isolette, on passenger seats, & on driver's seat
Shenai, et. al., 1981	5.0 – 13.0	2.2 – 6.0	Highway @ 48 mph	Vertical axis on supine infant head, abdomen, thigh
Silbergleit, et. al., 1991	3.1 – 8.1	0.7 – 1.9	Bumpy road, city road and highway	Triaxial vector sum measurement on standard backboard at head position
Mcnab, et. al., 1995	0 – 1.7	0.0 - 0.7	Bumpy road, city road and highway	Triaxial vector sum measurement from acoustical measurements
Pichard, et. al., 1970	0.16 - 0.85	--	City & highway	Z-axis, head-to-toe of recumbent patient

Data Analysis

Once the ambulance vibration data was characterized and found to be comparable to studies already completed, the data could then be correlated to the human physiological impacts associated with the amplitudes and frequencies experienced in the ambulance.

The Dynamax software that came with the Instrumented Sensor Technology accelerometer which was used for experimentation was capable of outputting the data collected as a time domain function and also had the capability of creating a power spectrum density (PSD) plot from the data. The PSD graphs showed the distribution of energy in the form of power over the frequency domain, which showed at which frequencies the energy in the vibrations peaked. Although the accelerometer device used in the experiment recorded data for all three axes, for the purpose of this project only the z-axis data was needed. Below is an example of the z-axis acceleration time domain function as well as a z-axis PSD plot. These graphs are representative of the data collected from ambulance 3 driven over a highway road surface at speeds greater than 65 miles per hour. Time domain graphs and PSD plots for more of the experimental tests are given in Appendix D of this report.

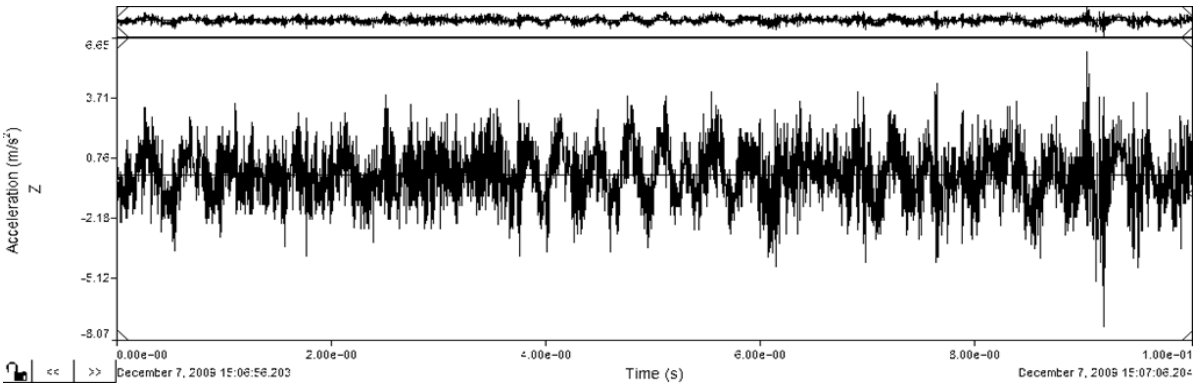

Figure 16: Z-axis acceleration time history for ambulance 3 on a highway at +65 mph

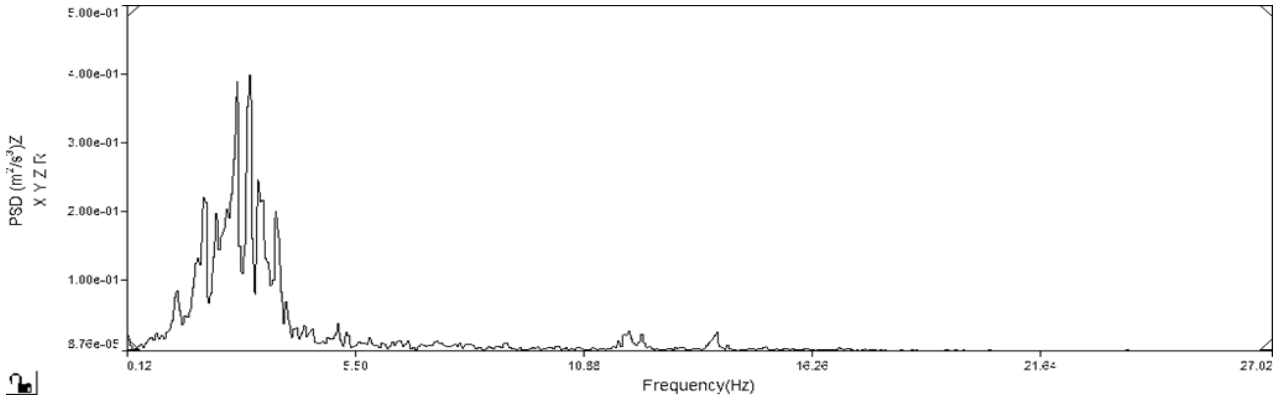

Figure 17: Z-axis power spectral density plot for ambulance 3 on highway +65mph

Though only one test run is represented in the graphs above, many of the time history graphs and PSD plots for other test runs in this experiment showed very similar results. All of the PSD plots showed that the concentration of energy experienced in the ambulances was below the 10 Hz level, with most of the highest peaks in the plots occurring between the 0.12 Hz and 5.50 Hz markers.

Human Physiological Response to Ambulance Vibrations

Effects on patient safety and comfort

The vibration data collected for this experiment had an average magnitude between 0.46 and 2.55 m/sec^2 at frequencies between 0.1 and 6 Hz. These types of vibration magnitudes and frequencies coincide with the natural frequencies of many of the human body systems, as indicated in Table 1, and can impact these systems negatively, particularly in patients who may already be in compromised situations. Some of the systems that can be affected by vibrations experienced in an ambulance have been superimposed on a PSD plot of ambulance 3 traveling on the highway at speeds greater than or equal to 65 miles per hour in Figure 18. The lines with each body system indicate the frequencies at which the particular system naturally resonates, which is where that system is most susceptible to interference from vibrations.

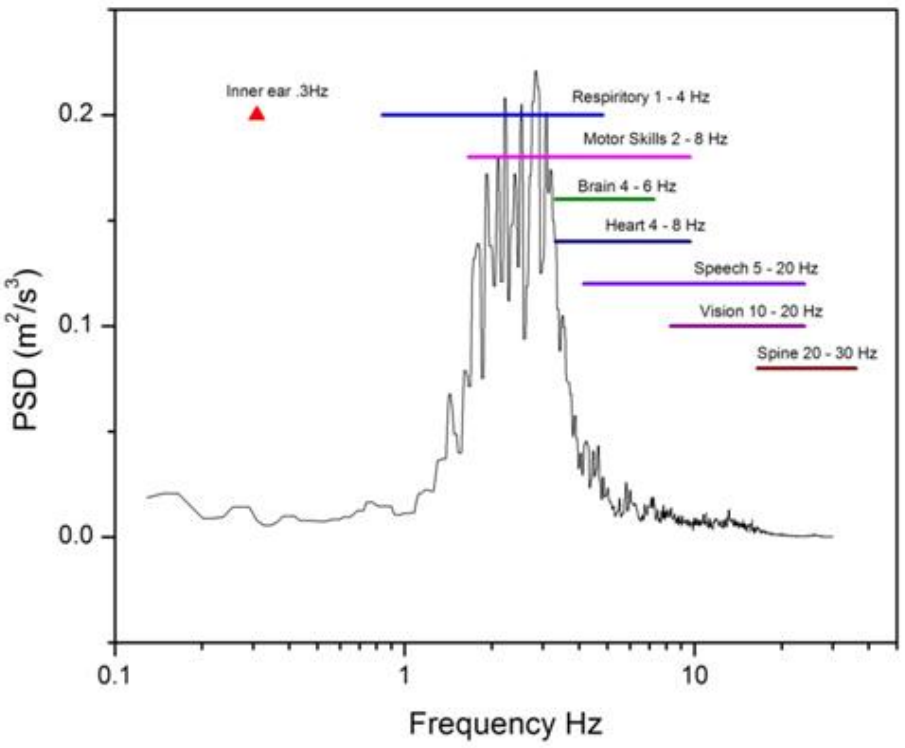

Figure 18: Physiological effects of superimposed on PSD graph of z-axis PSD from ambulance 3 on a highway at +65 mph

Although the comfort of humans exposed to the type of whole-body vibrations that are experienced in an ambulance is hard to quantify, there are general observations that have been made about the tolerance levels of humans exposed to these vibrations. Wong does provide an estimated set of guidelines for human responses to whole-body vibrations such as the ones experienced in a traveling vehicle (2008). These guidelines are represented in the graph shown in Figure 19 with the average z-axis vibration data values from this experiment superimposed within. Though the graph only shows the mean value of the vibration magnitudes reaching the "fairly uncomfortable" level presented by Wong, it is understood that the guidelines are conservative estimates that are intended to be measured using multiple axis root mean square values. In this case, the z-axis values from this experiment are lower than what would be found using all three axes to find an average.

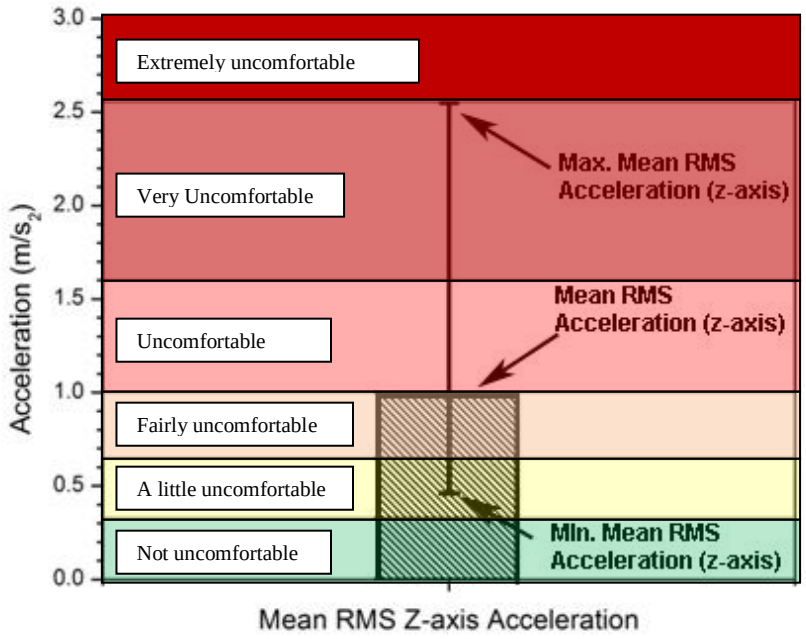

Figure 19: Effects of vehicle ride on comfort superimposed on a graph of the mean RMS z-axis accelerations

There are also guidelines set forth by the Society of Automotive Engineers (SAEJ670e, 1978) and the International Standard (ISO 2631-1978(E)), which provide the least conservative and most conservative values of human tolerance levels. These two standards are represented in Figure 20 with the yellow block representing the mean z-axis vibration magnitudes and the red block representing the mean z-axis peak vibration magnitudes. The graph shows that much of the z-axis mean peak values exceed both standards' tolerance limits, and that several of the average z-axis values exceed the SAE tolerance limit.

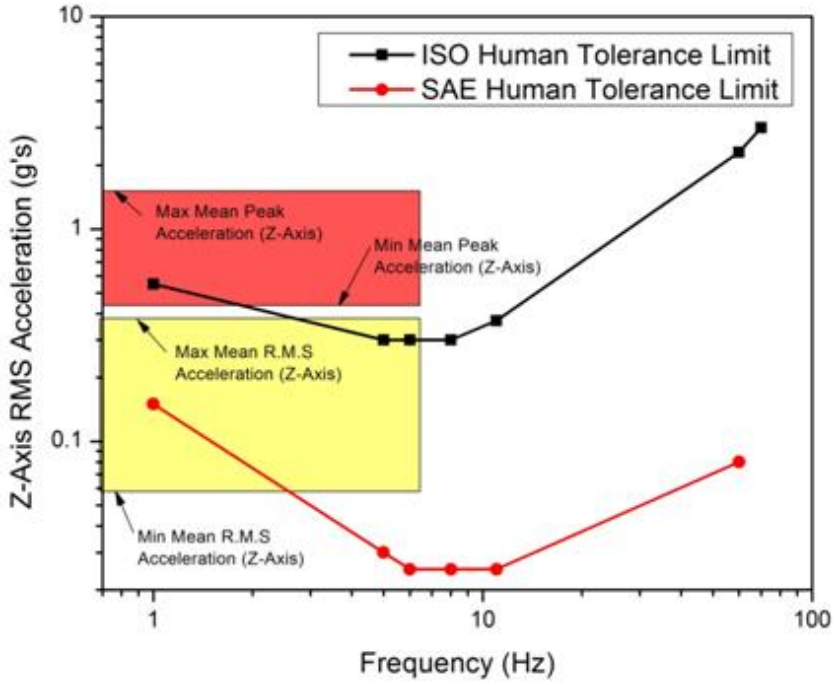

Figure 20: Human tolerance limits for vertical vibration with the mean and peak z-axis accelerations superimposed. (Human tolerance values adapted from Gillespie, 1992, p. 183)

Effects on personnel performance and patient care abilities

Because so many of the tasks performed by emergency medical personnel require the use of eye-hand coordination and fine motor skills, impedance and errors caused by the presence of whole-body vibrations can affect how the personnel interact and care for patients traveling in an ambulance. The graph in Figure 21 depicts the average tracking errors of individuals exposed to whole-body vibrations at 3.5 and 5.0 Hz frequencies. The yellow block superimposed onto the graph indicates the data collected as part of this experiment, with the dotted line representing the RMS average value.

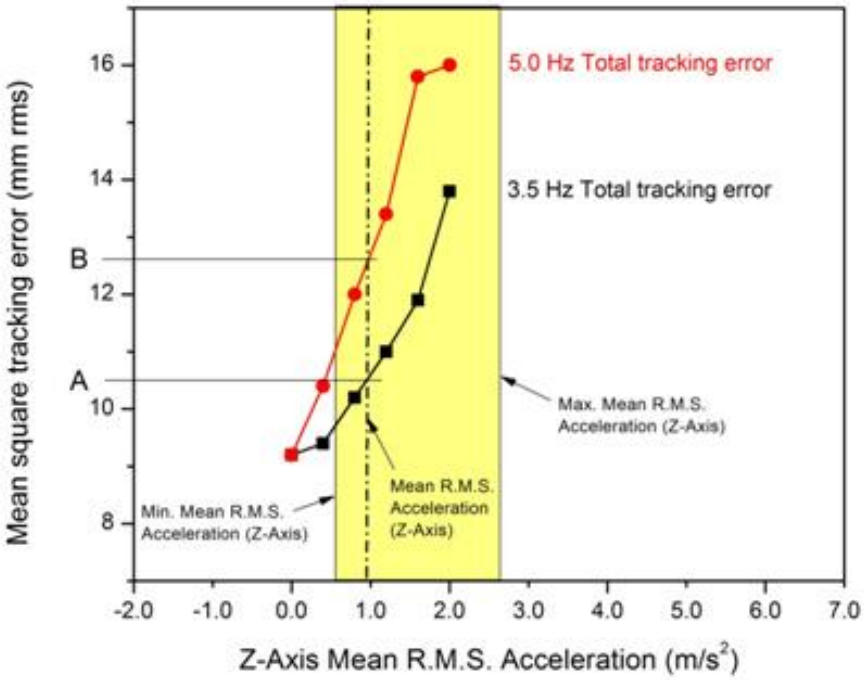

Figure 21: Average tracking error associated with whole body vibration with the mean rms z-axis accelerations superimposed. (Tracking error values adapted from Griffin, 1990, p. 153)

The intersections between the measured RMS values from this experiment and the study conducted by Lewis and Griffin show that at 3.5 Hz there was a total tracking error of approximately 10.5 millimeters and at 5.0 Hz there was a tracking error of approximately 12.5 millimeters. These tracking error values would have significant ramifications on the performance of important tasks that may need to occur in the back of an ambulance, such as inserting an intravenous line to administer medicine, or the insertion of nasal cannulas to aid patient breathing.

Another study completed by Moseley and Griffin (1986) tested the average reading errors of people subjected to various whole-body vibrations. Participants were asked to read characters that were 1.1 millimeter high from a distance of 750 millimeters while both themselves and the display were exposed to vibrations from 1.0 to 2.5 m/sec^2 over a range of frequencies from about

0.4 Hz to 4 Hz. Again, the yellow block is representative of the z-axis mean vibration magnitude values measured in this experiment and show that reading errors associated with such vibrations range from 30 up to 80 percent. Such reading errors occurring during patient transport could impact the abilities of medical personnel to read medicine labels or medical equipment read-outs and displays.

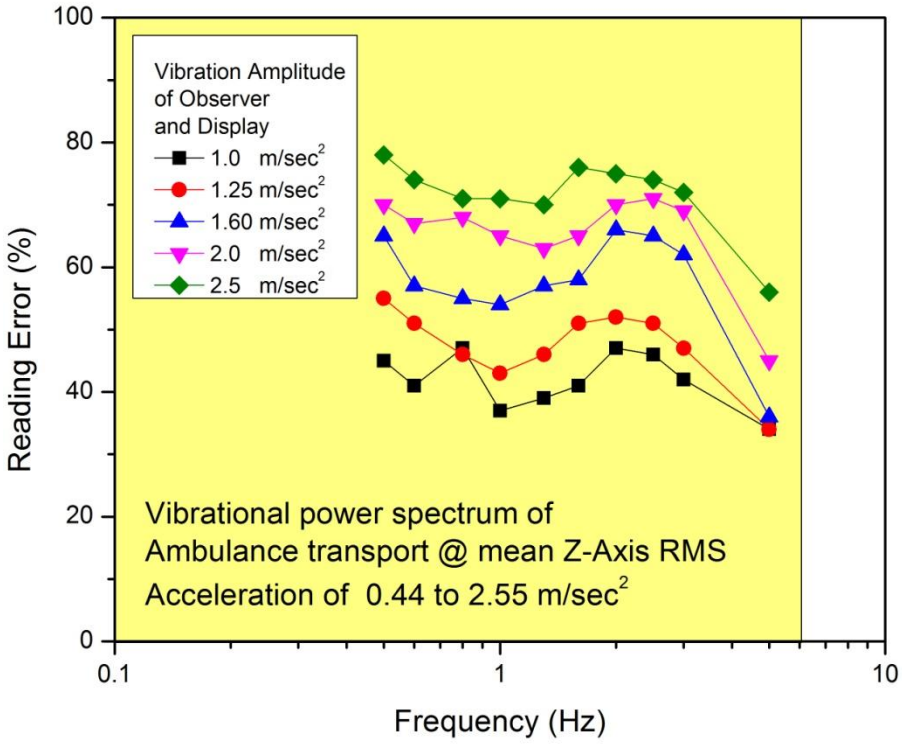

Figure 22: Vibration spectrum of z-axis excitation and associated reading errors with rms z-axis accelerations superimposed

In addition to affecting the reading abilities of medical personnel, whole-body vibrations were also shown to have impacts on writing ability in a study also conducted by Griffin (1990). Figure 23 shows some of the results from this study, with a clear degradation of legibility as acceleration magnitudes increased at the same frequency range of 4.5 Hz, a frequency level at which the data collected in this experiment shows significant vibration energy.

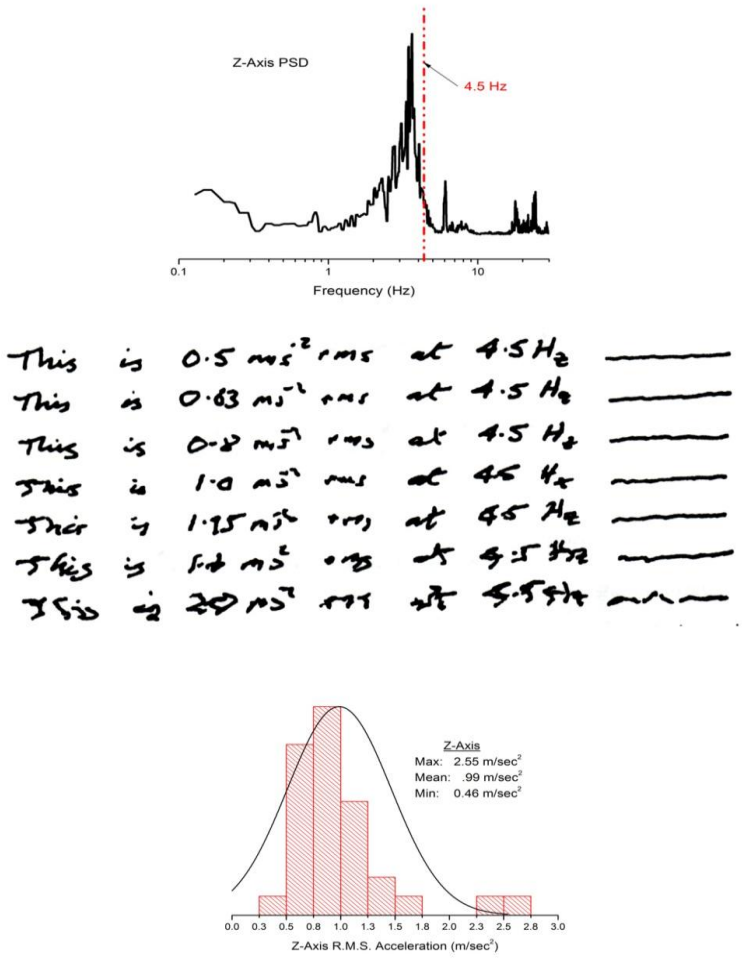

Figure 23: Amplitude and frequency of ambulance vibration and examples of associated handwriting performance (Data adapted from Griffin, 1990, p. 139)

Force Plate Model Development

The final leg of this project required the use of the vibration data collected from experimentation as an input into a designed force plate system to test its functionality and reliability as a source of vibration attenuation in an ambulance. The forcing functions found from the data gathered during experimentation allowed for analytical validation of the force plate model design.

The force plate design needed to incorporate measures that would aim to attenuate the most harmful vibrations experienced in the ambulance patient compartment. The previous sections of this report explain that the vibrations that fall into the category of being harmful to human physiology and discomfort are typically in found to have frequencies in the range of 1 to 10 Hz. Therefore, for the purpose of this project, the force plate model was designed to work to attenuate the low frequency vibrations rather than the high frequency noise vibrations shown in the data.

An analytical vehicle ride model has been developed for the ambulance and is depicted in Figure 24. This is a seven degree-of-freedom model that takes into consideration both sprung and unsprung masses in the vehicle and a number of other variable parameters.

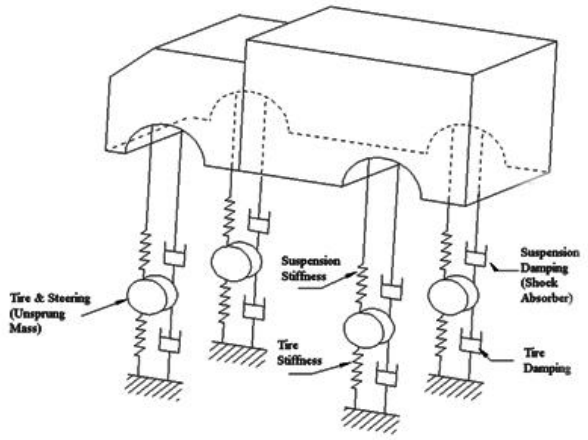

Figure 24: 7-degree-of-freedom model

This generalized ambulance model can be further simplified by reducing it to a quarter-car model and focusing in on only the vertical accelerations that are pertinent to this project. Several authors have made note that using this quarter-car model is sufficient in initial

suspension design analysis and takes into consideration all the necessary components to evaluate passenger comfort (Gobbi and Mastinu, 2001; Wong, 2008; Gillespie, 1992).

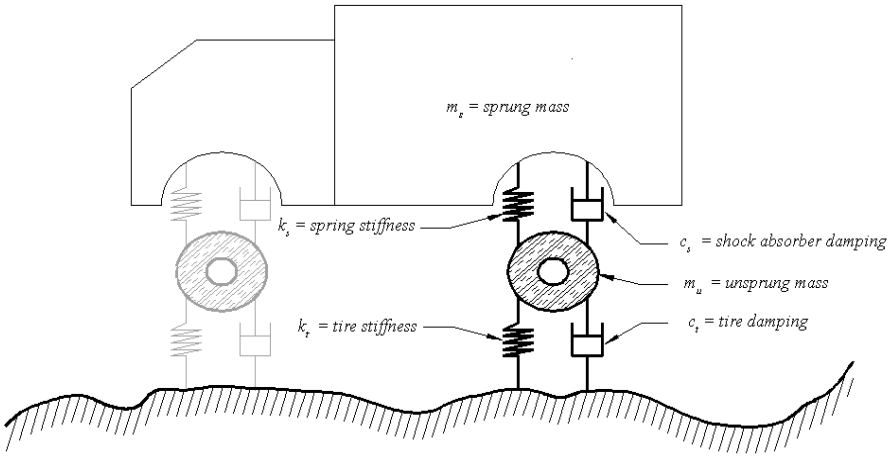

Figure 25: Quarter-car ambulance model

Treating the quarter-car model as a two-degree-of-freedom model assumes that the tires are mass-less springs, but still takes into consideration the sprung and unsprung masses of the vehicle. This type of analysis is considered adequate for evaluating systems exposed to vibration frequencies up to 50 Hz (Genta, 1997, p. 392). However, for this project, a single-degree-of-freedom model was chosen because the following assumptions could be made:

1. The vehicle vibrations of interest are only in the vertical direction.
2. The stiffness and damping effects of the tire could be neglected.
3. The tire has good traction and never leaves the road surface (tire hop is not an issue).
4. The frequencies of interest to analyze are low, typically below 10 Hz, and in the neighborhood of the natural frequency of the sprung mass.

The single-degree-of-freedom model, unlike the two degree-of-freedom model, considers the tires to be rigid bodies and does not take into consideration the unsprung mass of the vehicle. The single degree-of-freedom model is shown in Figure 26 with all of its parameter listed below.

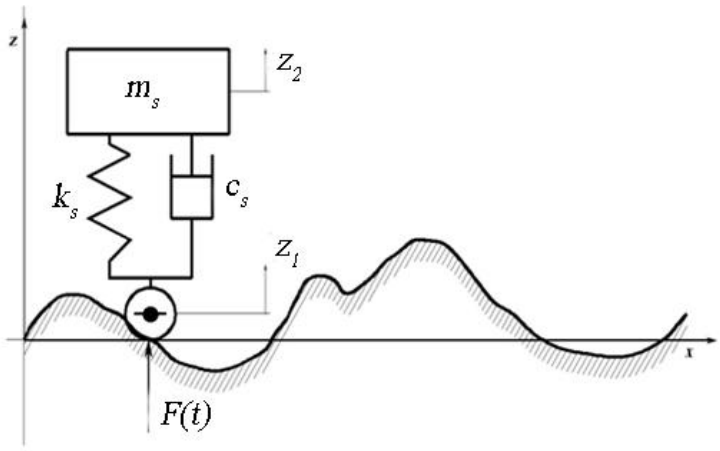

Figure 26: Single degree-of-freedom quarter-car ambulance model

For the single degree-of-freedom quarter car model:

m_s = sprung mass

k_s = suspension stiffness (leaf springs)

c_s = shock absorber damping

$z_1 =$ vertical displacement of tire at ground contact point

$z_2 =$ vertical velocity of sprung mass, starting at equilibrium position

$F(t) =$ excitation force function acting on wheel due to profile of road surface

Model parameter values for the vehicles tested as part of this project are given in Table 9.

Table 9: Ambulance quarter-car model parameters

Parameter	SI Units
m_s – sprung mass	2137 kg
m_u – unsprung mass	50 kg
k_s = suspension stiffness	110 kN/m
k_t = tire stiffness	200 kN/m
c_t = tire damping	353 N·s/m
c_s = shock absorber damping	1500 N· s/m

Using Newton's Second Law to derive an equation of motion for the sprung mass of the ambulance leads is standard practice among vehicle vibration researchers (Gobbi & Mastinu, 2001; Sun, Zhang, & Barak, 2002; Wong, 1993; Gillespie, 1992) and yields the following equations and figures.

$$\boldsymbol{F = ma} \qquad (1)$$

The free body diagram of the SDOF model is shown in Figure 27.

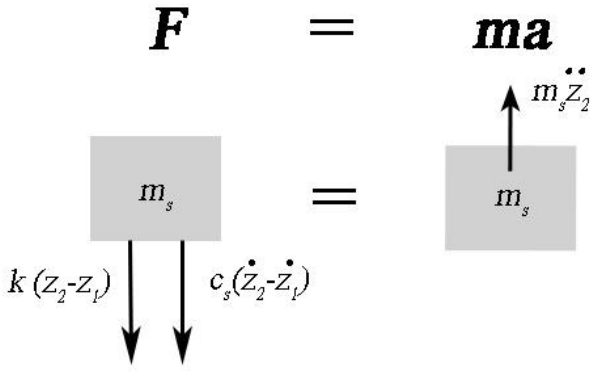

Figure 27: Free body diagram of single degree-of-freedom quarter-car model

The equation of motion for the system follows as:

$$\boldsymbol{m_s\ddot{z}_s + c_s(\dot{z}_2 + \dot{z}_1) + k_s(z_2 - z_1) = 0} \qquad (2)$$

We can define the terms $z,\ \dot{z},\ \ddot{z}$, such that they represent the relative displacements, velocities and accelerations, respectively, between the sprung vehicle mass and the tire at the road surface, leading to:

$$z = z_2 - z_1 \qquad (3)$$

$$\boldsymbol{\dot{z} = \dot{z}_2 - \dot{z}_1} \qquad (4)$$

$$\boldsymbol{\ddot{z} = \ddot{z}_2 - \ddot{z}_1} \qquad \textbf{(5)}$$

$$\boldsymbol{\ddot{z} + \ddot{z}_1 = \ddot{z}_2} \qquad \textbf{(6)}$$

Substituting equations 5.3 – 5.6 into equation 5.2, and rearranging, yields the equation of motion in terms of the forcing function input determined experimentally for this project:

$$\boldsymbol{m_s\ddot{z} + c_s\dot{z} + k_sz = -m\ddot{z}_1} \qquad \textbf{(7)}$$

Therefore, the forcing function may then be defined as:

$$\boldsymbol{F(t) = -m\ddot{z}_1} \qquad \textbf{(8)}$$

Since the ambulance sprung mass, suspension stiffness and shock absorber damping constants were known for the vehicles tested, measured values of acceleration, along with calculated velocities and displacements of the sprung mass were substituted into equation 5.7 to calculate the forcing functions for a representative sample of ambulance, road surface, and speed range experimental variables tested as part of this project. The collections of forcing functions developed are listed in Table 10 according to the variables they represent.

Table 10: Forcing function developed for model analysis

Ambualnce	Road Surface	Speed
1	Highway	<= 35 MPH
1	Highway	36 - 64 MPH
1	Highway	>= 65 MPH
1	Secondary Road	<= 35 MPH
1	City Street	<= 35 MPH
1	Unpaved Road	<= 35 MPH

The figures that follow all emerge from the same data set, the test from ambulance 1 traveling over a highway road surface in the speed range from 36 to 64 miles per hour. From the acceleration data gathered from the recording device used during the experiment, the velocity and displacement of the sprung mass of the ambulance was calculated in the time domain. All three time domain functions are shown in Figure 28 below.

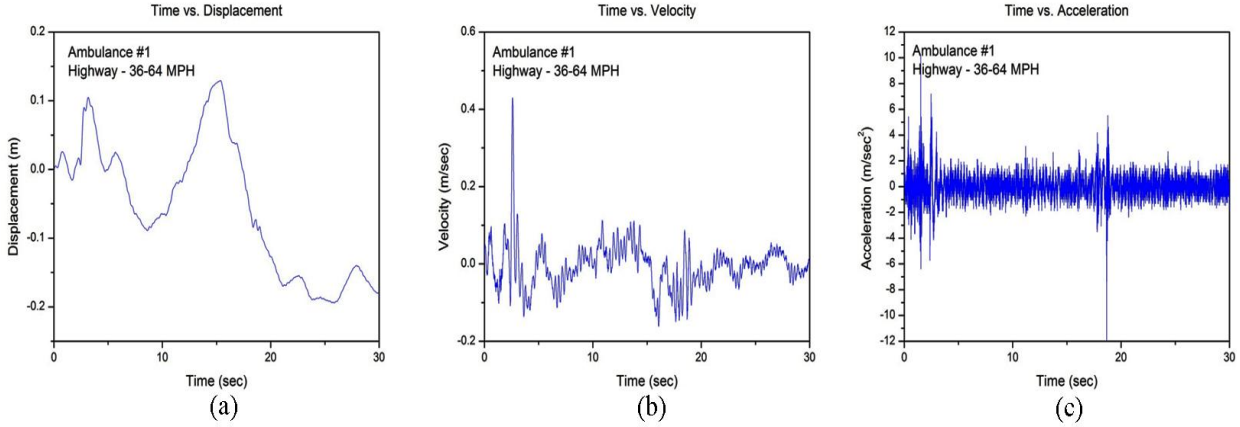

Figure 28: The z-axis (a) displacement, (b) velocity and (c) acceleration time history graphs for the sprung mass of ambulance 1

Using the values of acceleration collected through experimentation and the values calculated for the velocity and displacement, the forcing function for each of the cases was derived from the left-hand side of equation 5.7, yielding the time domain graph depicted in Figure 29. This graph clearly shows the presence of noise components in the signal, which may be attributed to vibrations from the engines and drive trains of the vehicle.

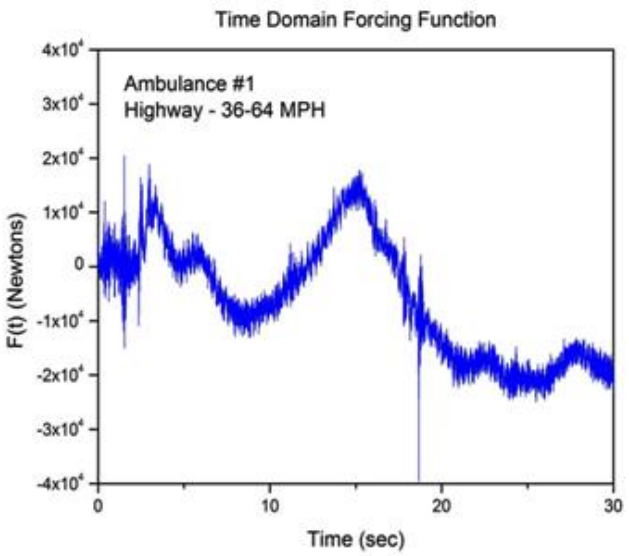

Figure 29: Time domain forcing function in the z-axis

The final analytical tool used to process and examine the data was a phase portrait plot, which is indicative of the stability and linearity of the system being examined. The phase portrait plot for this data set is presented in Figure 30, and clearly shows stability, but also multiple equilibrium points which indicate non-linearity in the system. This phase portrait further proved that the current suspension system in the ambulance is not adequate to sustain the vibrations experienced when traveling over common road surfaces.

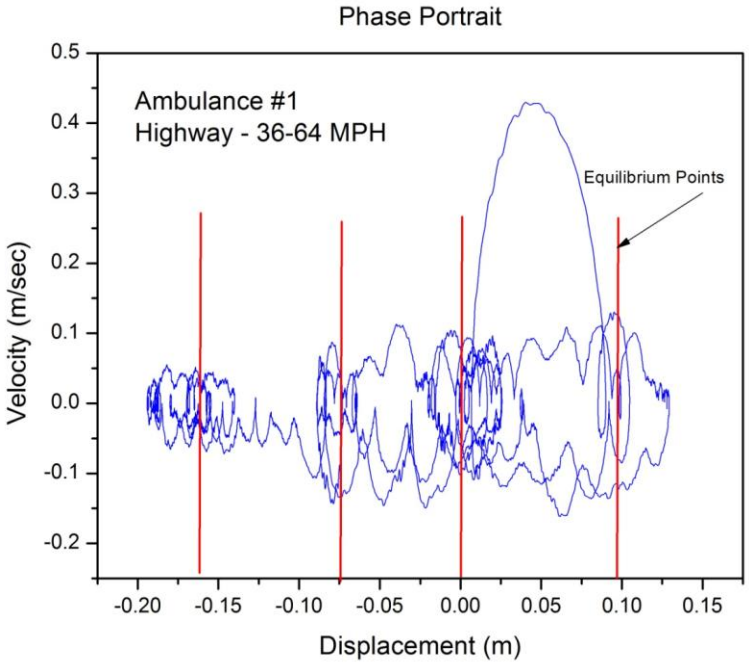

Figure 30: Phase portrait plot for ambulance 1

The current suspension system design for most Type I and Type II ambulances consists of two multi-leaf, single-stage leaf springs with a ground rating of 4286 kilograms (9450 pounds) supported by a solid axle (2008 Ford Trucks body builders layout book, 2007, p58). The ambulance is equipped with this simple and stiff suspension system because both the payload it is required to bear, reaching to between 1,800 and 2,200 kilograms (4,000 and 5,000 pounds). This loading constrains the design because prevents the use of independent suspension systems commonly found in passenger cars because they are not stiff enough to support such a heavy load.

All ambulances manufactured in the United States are built to the specifications laid out by the federal star-of-life ambulance standard, KKK-A-1822F which is put out by the U. S. General Services Administration (2007). Of particular importance to this project, there is a

specification that regulates the floor height of the ambulance module to be no higher than 34 inches from the ground. This height restriction is a major constraining factor when considering making a change to the suspension system design of the ambulance. This height constraint prevents commonly used air ride systems from being used because of their need for large volumes of working space between the axle and module floor that would be needed to support the payload.

With the given constraints on the design, choosing to keep the simple leaf spring suspension system is practical, but not ideal. In order to address the insufficiencies of the current suspension system, a type of supplementary suspension system would be a possible solution. A feasible design solution would be to implement a force plate into the floor of the ambulance compartment that would work to suppress the most harmful vibrations from the road surface by means of both passive and active attenuating devices. The force plate would fit into the floor of a typical ambulance module to support the passengers without needing to support the entire payload. Figure 31 shows how the force plate system would fit into the interior of the ambulance compartment. The force plate design would consist of two plates in between which small, active hydraulics and passive spring and damper systems would be inserted.

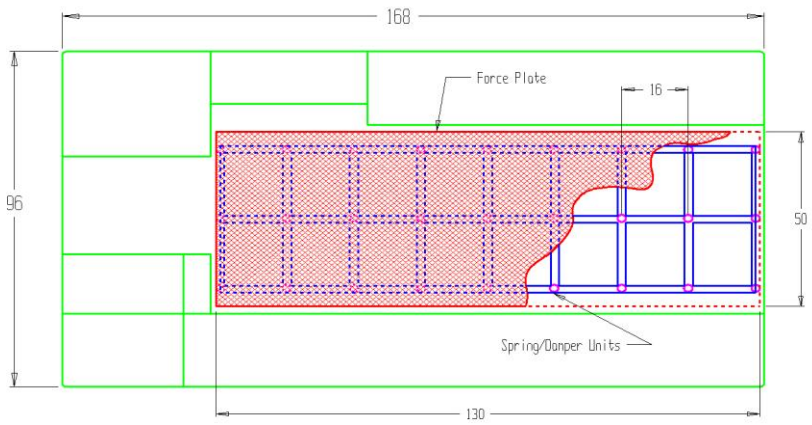

Figure 31: Top view of force plate fitted into the interior of a 167" ambulance compartment

The force plate was then modeled using the 3-D computer aided design software, Solidworks for visualization purposes. Figure 32 shows in image of this solid model. The force plate display was set to be transparent in order to be able to see the locations of the active and passive devices under the plate.

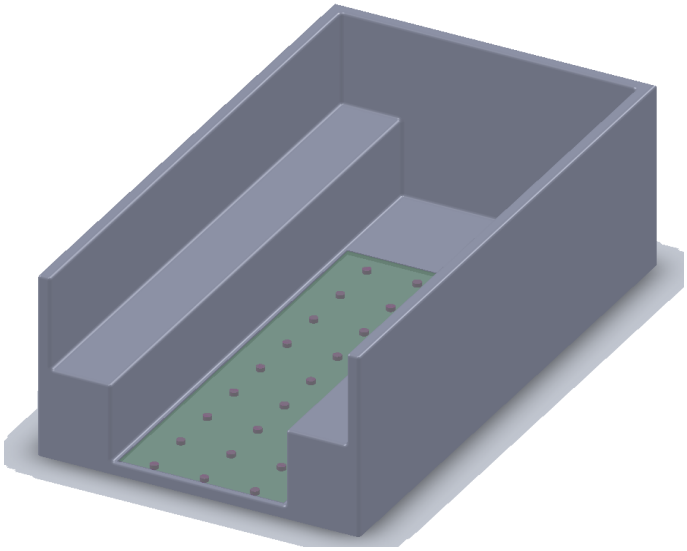

Figure 32: 3-D solid model of the force plate design

With the insertion of this supplementary suspension system, the model used previously in the chapter then changes to the representation shown in Figure 31. It is simply the single degree-of-freedom quarter-car model with the force plate system inserted on top.

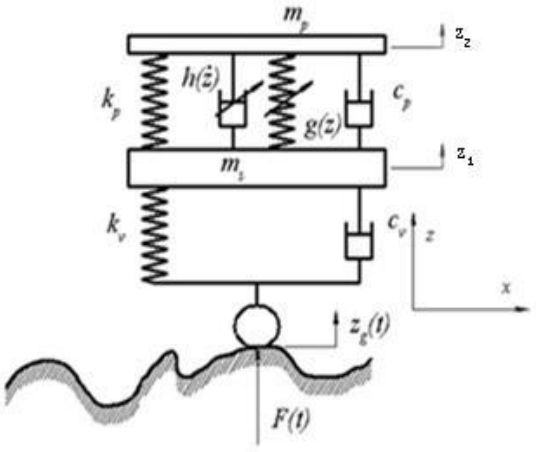

Figure 33: Force plate system model

The parameters for the model in Figure 33 are as follows:

m_s = sprung mass of vehicle
m_p = mass of force plate and supported load
k_v = stock vehicle stiffness
c_v = stock vehicle damping
k_p = passive stiffness of force plate
g(z) = active stiffness of force plate
h(z)= active damping of force plate
c_p = passive damping of force plate
$z_g(t)$= vertical displacement of tire at ground contact point
z_1= vertical displacement of ambulance, starting at equilibrium position
z_2= vertical velocity of force plate mass, starting at equilibrium position
$F(t)$ = excitation force acting on wheels due to profile of road surface

The equation of motion then also takes on a different form, which is given below.

$$m_p\ddot{z}_2 + c_p\left(1 + g(\dot{z}_1, \dot{z}_2)\right)(\dot{z}_2 - \dot{z}_1) + k_p\left(1 + h(z_1, z_2)\right)(z_2 - z_1) = u(z_1, z_2, \mu + \sigma_0\gamma(t)) \quad (9)$$

Where,

$g(\dot{z}_1, \dot{z}_2)$= non-linear damping function
$h(z_1, z_2)$ = non-linear restoring force
$u(z_1, z_2, \mu + \sigma_0\gamma(t))$ = control law
μ= deterministic divergence parameter
σ_0=noise intensity parameter
$\gamma(t)$= stochastic noise function

And,

$z = z_2 - z_1, \quad z_2 > z_1$

Additionally, the natural frequency and damping ratio of the system can be given as:

$$\omega_n = \sqrt{\frac{k_p}{m_p}} \quad , \quad \zeta = \frac{c_p}{2\sqrt{m_p k_p}}$$

Finally, substituting these into equation 9 yields the following motion equation for the complete force plate model system.

$$\ddot{z}(t) + 2\zeta\omega_n\left(1 + g(z, \dot{z})\right)\dot{z}(t) + \omega_n^2\left(1 + h(z)\right)z(t) = -\ddot{z}_1(t) + \frac{\omega_n^2}{k}u(z(t), z(t-\tau), \dot{z}(t), \mu + \sigma_0\gamma(t)) \quad (10)$$

Where:

-$\ddot{z}_1$= ambulance vertical forcing function
$z(t)$= ambulance vertical displacement
$z(t-\tau)$= ambulance vertical displacement with time delay
$\dot{z}(t)$ = ambulance vertical velocity
μ = deterministic divergence parameter
$\sigma_0\gamma(t)$= stochastic noise term

The right-hand side of this equation is the control law, which allows for design parameters for the force plate to be determined in order to best attenuate the vibrations in the ambulance to provide a safer, more comfortable ride for both patients and medical personnel. Additionally, the collection of data created by this experiment can provide a number of inputs into the function so that appropriate designs can be created for a variety of different service area profiles.

CHAPTER 6: CONCLUSIONS AND RECCOMENDATIONS

Conclusions

This project served to accomplish the following goals:

1. Vibrations experienced during a typical ambulance ride were characterized by time histories and power spectral densities to correlate human physiological responses during ambulance travel.
2. The data collected as part of the experiment was processed and analyzed to determine a mathematical design model that would adequately capture the motion of the complete suspension system with and without supplementary system designs.
3. A force plate system design, with both active and passive elements included, was explored as a possible solution to attenuating the most harmful vibrations experienced in the patient compartment of an ambulance while in motion.

Through experimentation, the magnitudes, frequencies and energy of the vibrations experienced during a typical ambulance ride were all able to be quantified, both for comparison and correlation. Four different ambulances were tested on four different road surfaces at three different speed ranges, and accelerations in the z-axis were recorded for further processing and analysis. The results of the experiment yielded average vibration magnitudes between 0.46 and 2.55 m/sec^2, with the energy of the vibrations concentrated between 0.1 and 6 Hz.

The frequencies of the vibrations measured as part of the experiment correlated to natural resonances of many of human body systems, making them vulnerable to disruption and harm, particularly in patients whose health is already compromised, as well as impeding on the

performance abilities of medical personnel trying to execute delicate medical procedures. Additionally, the average magnitudes and peak magnitudes experienced during experimentation were above generally accepted human tolerance levels for comfort.

Finally, other plots such as phase portraits and forcing functions derived from the data were used to develop a mathematical model of a possible suspension system design that included the existing suspension system and a supplementary force plate suspension design that included both passive mechanical springs and dampers as well as an active component to account for non-linearities, random events, and time delays. This model will serve as a basis to calculate the necessary parameters for a force plate design that would adequately suppress the most harmful vibrations experienced in the ambulance.

Recommendations

There is room for further analysis into detailed design requirements for space, material selections, economic and technical feasibility of this mathematical model of a force plate suspension system as a solution to attenuate harmful vibrations experienced in an ambulance that should all be explored.

In addition to furthering the work presented in this report, there is huge opportunity in the emergency medical field for more vibration research. Medical equipment could be redesigned to better withstand the affects of the vibrations experienced while traveling and other attenuation systems and designs could be worked into stretchers and mattresses, which would all positively impact the emergency service field.

BIBLIOGRAPHY

2008 Ford Trucks body builders layout book. (2007). *2008 Dimensional data E-350/450 super duty cutaway 158" wheelbase (DRW)*.

Amman, S., Pielemeier, B., Snyder, D., & Toting, F. (2001, April 30). *Road vibration investigation using the ford vehicle vibration simulator.* 2001-01-1572 presented at the SAE Noise and Vibration Conference and Exposition, Traverse City, Michigan: Society of Automotive Engineers.

Andrew, M., M, D., Yuenquan, C., Faith, G., Biraj, B., & Charles, L. (1995). Vibration and noise in pediatric emergency transport vehicles: A potential cause of morbidity? *Aviation, Space and Environmental Medicine, 66*(3), 212-219.

B. G. Kao, & P. R. Perumalswami. (1997, April 8). *A hybrid road loads prediction method with full vehicle dynamic simulation.* 971513 presented at the X International Conference on Vehicle Structural Mechanics and CAE, Troy, Michigan: Society of Automotive Engineers.

Barak, P. (1991, September 16). *Magic numbers in design of supensions for passenger cars.* Presented at the Passenger Car Meeting and Exposition, Nashville, TN: Society of Automotive Engineers.

Bellieni, C. V., Pinto, I., Stacchini, N., Cordelli, D. M., & Bagnoli, F. (2004). *Minerva Pediatrics, 56*(2), 207-212.

Brauer, R. L. (1994). *Safety and health for engineers.* New York, New York: John Wiley and Sons, Inc.

British Standards Institution 1987 BS 6841. (1987). Measurement and evaluation of human exposure to whole body vibration.

Brown, L. H., Gough, J. E., Bryan-Berg, D. M., & Hunt, R. C. (1996). Assessment of breath sounds during ambulance transport. *Annals of Emergency Medicine, 29*(2).

Brown, T. L., Mear, S. T., Moore, N. E., Kannapan, S. M., Marshek, K. M., Cuderman, J. et al. (1992, September 28). *An experimental procedure for estimating ride qulatiy for passive and semi-active suspension automobiles.* 922141 presented at the SAE Worldwide Passenger Car Conference and Exposition, Dearborn, Michigan: Society of Automotive Engineers.

Capt, J. G. C., USAF, M., Capt, J. D. W., USAF, M., William, B. H., Jr., M, D. et al. (1967). Initial cardiovascular response to low frequency whole body vibration in humans and animals. *Aerospace Medicine, 38*(5), 464-467.

Cotnoir, P., & Fofana, M. (2009, July 23). *Ambulance vibration suppression via force field domain control.* Presented at the WPI/University of Massachusetts Emergency TransCare Medical Services (ETMS) Ambulance Team, University of Massachusetts Medical Center, Worcester, MA.

Davis, J. (2003). The bleeding edge. *Wired, 11(05),* 12.

Eklund, G. (1972). General features of vibration-induced effects on balance. *Upsala Journal of Medical Science, 77,* 112-124.

Ernsting, J. (1961). *Respiratory effects of whole-body vibration. IAM Report 179* (Institute of Aviation Medicine). . Farnborough.

Genta, G. (1997). *Motor vehicle dynamics: Modeling and simulation.* River Edge, NJ: World Scientific Publishing Co. Pte. Ltd.

Gilad, I., & Bryan, E. (2007). Ergonomic evaluation of the ambulance interior to reduce paramedic discomfort and posture stress. *Human Factors, 49*(6), 1019-1032.

Gillespie, T. D. (1992). *Fundamentals of vehicle dynamics.* Warrendale, PA: Society of Automotive Engineers.

Gobbi, M., & Mastinu, G. (2001). Analytical description and optimization of the dynamic behavior of passively suspended road vehicles. *Journal of Sound and Vibration, 245*(3), 457-481.

Gobbi, M., Levi, F., & Mastinu, G. (2006). Multi-objective stochastic optimisation of the suspension system of road vehicles. *Journal of Sound and Vibration, 298*(2006), 1055-1072.

Goldman, D., & Gierke, H. (1960). *The effect of shock and vibration on man* (N0. '60-3, lecture and review series). Bethesda, Maryland: Naval Medical Research Institute.

Green, D. A., Golding, J. F., Aulukh, M., Faldon, M. C., Murphy, K. G., Bronstein, A. M. et al. (2008). Adaptation of ventilation to 'buffeting' in vehicles. *Clin. Auton. Res., 2008.*

Griffin, M. J. (1990). *Handbook of human vibration.* New York, New York: Harcourt Brace Jovanovich.

Griffin, M. J. (1998). A comparison of standardized methods for predicting the hazards of whole-body vibration and repeated shocks. *Journal of Sound and Vibration, 215*(4), 883-914.

Healthwise, Inc. (2008, March 26). *Heart Disease Health Center: Electrocardiogram*. Retrieved October 2009, from WebMD: http://www.webmd.com/heart-disease/electrocardiogram

Henderson, R. J., & Raine, J. K. (1998). A two-degree-of-freedom ambulance stretcher suspension. part 3: Laboratory and road test performance. *Proc Instn Mech Engrs, 212*(Part D: Journal of Automobile Engineering), 401-407.

Huang, Y., & Griffin, M. J. (2008). Nonlinear dual-axis biodynamic response of the semi-supine human body during longitudinal horizontal whole-body vibration. *Journal of Sound and Vibration, 312*(2008), 273-295.

Huang, Y., & Griffin, M. J. (2008a). Nonlinear dual-axis biodynamic response of the semi-supine human body during vertical whole-body vibration. *Journal of Sound and Vibration, 312*(2008).

Huang, Y., & Griffin, M. J. (2009). Nonlinearity in apparent mass and transmissibility of the supine human body during vertical whole-body vibration. *Journal of Sound and Vibration, 324*(2009), 429-452.

International Organization for Standardization 1997 ISO 2631-1. (1997). Mechanical Vibration and shock - evaluation of human exposure to whole-body vibration. Part 1: Gerneral requirements.

Johnson, T. D., Lindholm, D., & Dowd, M. (2006). Child and provider restraints in ambulances: Knowledge, opinions, and behaviors of emergency medical services providers. *Acad Emerg Med, 13*(8), 886-92.

Kinast, E. (2005, March 3). *Guest Commentary: How blood-pressure devices work.* Retrieved October 2009, from EDN: Electronics, Design, Strategy, News: http://www.edn.com/article/CA511468.html

KKK-A-1822F, F. S. f. t. S.-o.-L. A. (2007). U.S. general services administration.

Kroemer, K., & Grandjean, E. (1997). *Fitting the task to the humans, 5th ed.*. New York, New York: Taylor and Francis.

Levick, N., & Grzebieta, R. (2008a). *Development of proposed crash test procedures for ambulance vehicles.* Paper number 07-0074, Objective Safety LLC, USA.

Levick, N., & Grzebieta, R. (2008b). To evaluate crashworthiness and passive safety design and testing standards for USA and Australian ambulance vehicles. *Annals of Emergency Medicine, 51*(4), 540.

Levick, N., & Swanson, J. (2005). An optimal solution for enhancing ambulance safety: Implementing a driver performance feedback and monitoring device in ground emergency medical service vehicles. In *49th Annual Proceedings - Association for the Advancement of Automotive Medicine Sept 12-14 2005* (pp. 35-50). Boston, MA United States: Association for the Advancement of Automotive Medicine, Barrington, IL United States.

Lewis, C.H. and Griffin, M.J. (1978). Predicting the effects of dual-frequency vertical vibration on continuous manual control performance. *Ergonomics* 21:637-650.

Life Line Emergency Vehicles. (2004). 167" ESD superliner 72" headroom [Dwg. No. E4SE16772]. .

Litta-Modignani, R., Blivaiss, B. B., Magid, E. B., & Priede, I. (1964). Effects of whole-body vibration of humans on plasma an durinary coricosteroid levels. *Aerosapce Medicine, 35,* 662-667.

Loeckle, W. E. (1950). The physiological effects of mechanical vibration. In *German aviation in world war two* (US Government Printing Office, pp. Vol 2 & pp. 716-722). . Washington, DC.

Lundstrum, R., Holmlund, P., & Lindberg, L. (1998). Absorbtion of energy during vertical whole-body vibration exposure. *Journal of Biomechanics, 31*(1998), 317-326.

Macnab, M. D., Yuenquan, C., Gagnon, F., Bora, B., & Lazlo, C. (1995). Vibration and noise in pediatric emergency transport vehicles: A potential cause of morbidity? *Aviation, Space and Environmental Medicine, 66*(3), 212-219.

Maguire, B., Hunting, K., Smith, G., & Levick, N. (2002). Occupational fatalities in emergency medical services: A hidden crisis. *Annals of Emergency Medicine, 40*(6), 625-632.

Mansfield, N. J. (2006). *Literture review on low frequency vibration comfort* (Loughborough University, p. 104). Loughborough, U.K.: Collaboration in research and development of new curriculum in sound and vibration.

Margolis, D., & Asgari, J. (1991, September 16). *Multipurpose models of vehicle dynamics for controller design.* Presented at the Passenger Car Meeting and Exposition, Nashville, TN: Society of Automotive Engineers.

Matsumoto, Y., & Griffin, M. (1998). Dynamic response of the standing human body exposed to vertical vibration: Influence of posture and vibration magnitude. *Journal of Sound and Vibration, 212*(1), 85-107.

Miwa, T. (1969). Evaluation methods for vibration effect: Part 9 respsonse to sinusoidal vibration at lying posture. *Industrial Health, 7,* 116-126.

Miwa, T. (1975). Mechanical impedance of human body in various postures. *Industrial Health, 7,* 3-22.

Miwa, T. (1982). Slow vertex potentials evoked by whole-body impulsive vibrations in recumbant men. *J. Acoust. Soc. AM., 72*(1), 214-221.

Moseley, M.J., & Griffin, M.J. (1986). Effects of display vibration and whole-body vibration on visual performance. *Ergonomics*. *29*: 977-983.

Moseley, M. J., & Griffin, M. J. (1987). Whole-body vibration and visual performance: An examination of spatial filtering and time-dependency. *Ergonomics, 30,* 613-626.

Moving ambulance scope of service. (2009) (EMTLife.Com Web Forum). Retrieved 19 July 2009, from: http://www.emtlife.com/showthread.php?s=f5d37720248c66bd28c2dd73ca13db55&p=153247#post153247.

Murata, Y., & Maemori, K. (1999). Optimum design of ER dampers for ambulances. *JSME International Journal, Series C, 42*(4), 838-846.

Paddan, G. S., & Griffin, M. J. (2002). Evaluation of whole-body vibration in vehicles. *Journal of Sound and Vibration, 253*(1), 195-213.

Papagiannakis, A. T. (1997, November 17). *The need for a new pavement roughness index; RIDE*. 973267 presented at the SAE International Truck and Bus Meeting and Exposition, Cleveland, Ohio: Society of Automotive Engineers.

Parsons, K. C., & Griffin, M. J. (1983, June 6). *Methods for predicting passenger vibration discomfort.* 831029 presented at the Passenger Car Meeting, Dearborn, Michigan: Society of Automotive Engineers.

Paschold, H. (2008). Whole-body vibration. *Professional Safety, 53*(6), 52-57.

Pesterev, A. V., Bergman, L. A., & Tan, C. A. (2004). A novel approach to the calculation of pothole-induced contact forces in mDOF vehicle models. *Journal of Sound and Vibration, 275*(2004), 127-149.

Pichard, E., Poisvert, M., Hurtaud, J. P., Ivanoff, S., & Cara, M. (1970). Les accelerations et les vibrations dans la pathologie liee au transport sanitaire. *Revue Des Corps de Sante, 11,* 611-635.

Pickering, T., Hall, J., Appel, L., Falkner, B., Graves, J., Hill, M., et al. (2005). Recommendations for Blood Pressure Measurement in Humans and Experimental Animals. *Hypertension: Journal of the American Heart Association , 45,* 142-1Prasad, N. H., Brown, L. H., Ausband, S. C., Cooper-Spruill, O., Carroll, & Whitely, T. W. (1994). Prehospital blood pressures: Inaccuracies caused by ambulance noise? *Am J Emerg Med., Nov 12*(6), 617-20.

Proudfoot, S. L., Romano, N. T., Bobick, T. G., & Moore, P. H. (2003). Ambulance crash-related injuries among emergency medical services workers - United States, 1991-2002. *Journal of the American Medical Association, 289,* 1628-1629.

Pushkina, N. N. (1961). Some blood indices in subjects undergoing the effect of general (total) vibration. *Gigiena Truda I Professional'nye Zabolevanija, 6*(2006), 29-32.

Randall, J., Matthews, R., & Stiles, M. (1997). Reesonant frequencies of standing humans. *Ergonomics, 40*(9), 879-886.

Ribot, E., Roll, J. P., & Gauthier, G. M. (1986). Comparative effects of whole-body vibration on sensorimotor performance achieved with a mini-stick nad a macro-stick in force and position control modes. *Aviation, Space and Environmental Medicine, 57,* 792-799.

Roll, J. P., & Roll, R. (1987). Extraocular proprioception, body postural references and the spatial docing of retinal infromation. *Agressologie, 28,* 905-912.

Roman, J. (1958). *Effects of severe whole-body vibration on mice and methods of protection from vibration injury. WADC Technical Report 58-107* (Wright Air Development Centre No. ASTIA Document No. Ad 151070). . Wright-Patterson Air Force Base, Ohio.

Rui, Y., Saleem, Y., & Zhou, J. H. (1997). Road load simulation using effective road profile. *S.A.E. Transactions, 106*(2), 2236.

SafetyLine Institute. (2007, Jan). *Occupational health & safety practitioner reading. Human vibration: Basic characteristics.* (Government of Western Australia, Department of Consumer and Employment Protection). . Perth, Western Australia.

Schneider, S., Borok, Z., Heller, M., Paris, P., & Stewart, R. (1988). Critical cardiac transport - air versus ground. *Amer J Emerg Med, 6*(5), 449-452.

Sharp, G. R., Patrick, G. A., & Withey, W. R. (1974). The respiratory and metabolic effects of constant amplitude whole-body vibration in man. In *Vibration and combined stresses in advanced systems. Vol. Paper B-15: AGARD conference proceedings 145*.

Shenai, J. P., Johnson, G. E., & Varney, R. V. (1981). Mechanical vibration in neonatal transport. *Pediatrics, 68,* 55 - 57.

Sherwood, H. B., Donze, A., & Giebe, J. (1994). Mechanical vibration in ambulance transport. *Journal of Obstetric, Gynecologic, and Neonatal Nursing, 23*(6), 457-463.

Silbergleit, R., Dedrick, D. K., MD, Richard, E. B., & MD. (1991). Forces acting during air and ground transport on patients stabilized by standard immobilization techniques. *Annals of Emergency Medicine, 20*(8), 875-877.

Stephens, D. G. (1977, September 26). *Passenger vibration in transportation vehicles.* AMD - vol. 24 presented at the The Design Engineering Technical Conference, Chicago, Illinois: ASME.

Sterud, T., Ekeberg, O., & Hem, E. (2006). Health status in the ambulance services: A systematic review. *BMC Health Services Research, 6*(82), 1-10.

Tamboli, J., & Joshi, S. (1999). Optimum design of a passive suspension system of a vehicle sujected to actual random road excitations. *Journal of Sound and Vibration, 219*(2), 193-205.

Uchikune, M. (2002). Physiological and psychological effects of high speed driving on young male volunteers. *Journal of Ocuupational Health, 44*(4), 203-206.

Vibration Injury Network. (2001). *Review of methods for evaluating human exposure to whole-body vibration.* Appendix w4A to final report, The Institute of Sound and Vibration Research.

Waddell, G. (1975). Movement of critically ill patients within hospital. *British Medical Journal, 2,* 417-419.

Waddell, G., Scott, P. D. R., Lees, N. W., & Ledingham, I. (1975). *British Medical Journal, 1,* 386-389.

Wambold, J. C. (1997, August 4). *Vehicle ride quality -measurement and analysis.* Presented at the SAE West Coast International Meeting, Universal City, California, USA: Society of Automotive Engineers.

Wang, H., Fairbanks, R., Shah, M., Abo, B., & Yearly, D. (2008). Tort claims and adverse events in emergency medical services. *Annals of Emergency Medicine, 52*(3), 256-262.

Wasserman, D. (1996). An overview of occupational whole-body and hand-arm vibration. *Applied Occupational Environmental Hygiene, 11*(4), 266-270.

Waters, T., Rauche, C., Genaidy, A., & Rashed, T. (2007). A new framework for evaluating potential risk of back disorders due to whole body vibration and repeated mechanical shock. *Ergonomics, 50*(3), 379-395.

Weber, U., Reitinger, A., Szusz, R., Hellmich, C., Steiniechner, B., Hager, H. et al. (2009). Emergency ambulance transport induces stress in patients with acute coronary syndrome. *Emerg. Med. J., 26*(2009), 524-528.

Wickens, C., Lee, J., Liu, Y., & Becker, S. (2004). *Introduction to human factors engineering, 2nd e.*. Upper Saddle River, NJ: Pearson Prentice Hall.

Wilke, H., Neef, P., Caimi, M., Hoogland, T., & Claes, L. (1999). New in vivo measurements of pressures in the intervertebral disc in daily life. *Spine, 24*(8), 755-762.

Wong, J. Y. (2008). *Theory of ground vehicles.* Warrendale, PA: John Wiley and Sons, Inc.

Yue, Z., & Mester, J. (2007). *Studies in Applied Mathematics, 119,* 111-125.

Yue, Z., & Mester, J. (2007a). On the cardiovascular effects of whole-body vibration Part I. Longitudinal effects: Hydrodynamic analysis. *Studies in Applied Mathematics, 119,* 95-109.

APPENDIX A

Selected test ambulance & chassis specifications

Ambulance #1	
Ambulance mfg.	Horton Emergency Vehicles Co.
Date of mfg.	Oct. 2005
Ambulance type/model	F453-ICT 4x4
Chassis mfg.	Ford Motor Co.
Chassis model / yr.	F450 / 2006
Vechicle type	I
Vehicle class	1
Chassis GVWR	16000 Lbs.
Allowable. Payload per KKK-A-1822	4199 Lbs.
Tires	225/70 R19.5
Options	

Ambulance #2	
Ambulance mfg.	Life Line Emergency Vehicles
Date of mfg.	May 2001
Ambulance type/model	Type III Superliner – Floor Plan A
Chassis mfg.	Ford Motor Co.
Chassis model / yr.	E450 Super Duty
Vechicle type	III
Vehicle class	1
Chassis GVWR	14050 Lbs.
Allowable. Payload per KKK-A-1822	3390 Lbs.
Tires	225/75 R16
Options	Automatic tire chains

Ambulance #3	
Ambulance mfg.	Braun Industries, Inc.
Date of mfg.	October 2009
Ambulance type/model	Chief XL
Chassis mfg.	General Motors Corporation
Chassis model / yr.	Chevy C-4500 / 2008
Vechicle type	III
Vehicle class	5
Chassis GVWR	16500 Lbs.
Allowable. Payload per KKK-A-1822	3434 Lbs.
Tires	225/70 R19.5
Options	

Ambulance #4	
Ambulance mfg.	Life Line Emergency Vehicles
Date of mfg.	August 2009
Ambulance type/model	Type I Superliner – Floor Plan A
Chassis mfg.	Ford Motor Co.
Chassis model / yr.	Ford F-550 / 2009
Vechicle type	I
Vehicle class	1
Chassis GVWR	17950 Lbs.
Allowable. Payload per KKK-A-1822	4470 Lbs.
Tires	225/70 R19.5
Options	Air ride suspension

2006 SUPER DUTY F-250/350/450/550

STANDARD POWERTRAIN/CHASSIS EQUIPMENT SPECIFICATIONS

F-450 Chassis Cab

DRIVE:		4x2	4x4
POWERTRAIN:		Refer To The Ordering Guide For 50 States Usage	
Engine[1]	— Type	6.8L (415 CID) 3V SEFI V-10	
Transmission	— Type	Heavy-Duty Manual	
	— Speeds	6-Speed Overdrive	
Clutch Diameter		11.9" (13" With 6.0L V-8 Diesel)	
Transfer Case	— Type	—	Part-Time, 2-Speed
	— Low/High Gear Ratio	—	2.72:1/1.00:1
AXLES:			
Front Axle	— Type	Monobeam, Dana Super 60	
	— Capacity (Rating @ Ground)	7000 lbs.	
	— Hubs Type	—	Manual Locking
Rear Axle	— Type—Full-Floating	Dana	
	— Capacity (Rating @ Ground)	12,000 lbs.	
BRAKES:			
Front/Rear Disc	— Type	Dual-Piston Pin-Slider Calipers, Bolt-on Adapters, Wrap-around Tie Bars	
	— Rotor Diameter—Front/Rear	14.53"/15.35"	
Power Assist Unit	— Type	Hydro Boost	
	— Effective Diameter	1.56" Power Piston	
Anti-Lock System		4-Wheel (3-Channel)	
Parking Brake (Rear Brakes)		9.5" Drum-In-Hat (Foot-Operated, Hand Release)	
ELECTRICAL:			
Alternator	— Rating	110 Amperes, 1650 Watt	
Battery	— Type	Maintenance-Free	
	— Rating	78 Amp-hr., 750 CCA (Dual 78 Amp-hr., 750 CCA With 6.0L V-8 Diesel)	
Harnesses	— Type	7 Blunt Cut and Labeled Wires With Relays For Backup Lamps, Running Lamps and Battery Feed	
FUEL TANK:	— Capacity	40.0 Gal. (151 L) (Filler Hose Thru Hole In Frame Siderail)	
STEERING:	— Type	Power, Ford XR-50 (Includes Steering Damper)	
	— Ratio	18.0:1	
SUSPENSION:			
Frame	— Type	Ladder Type, 36,000 psi Steel With Front Blocker Beam	
	— Section Modulus (cu. in.)	10.1; 17.2 With 188.8" WB and 200.8" WB Regular Cab	
Springs, Front	— Type	Coil, Assigned Rating	
	— Rating @ Ground (min.)	Refer to page 29 for usage and ratings	
Springs, Rear	— Type	Leaf, Single-Stage Constant Rate Main and Auxiliary	
	— Rating @ Ground (min.)	Refer to page 29 for usage and ratings	
Shock Absorbers	— Gas-Type	1.38"	
Stabilizer Bar		Front and Rear	
TIRES:	— Type	Steel-Belted Radial, All-Season, BSW	
	— Size	Six, 225/70Rx19.5F	
WHEELS:	— Type and Size	Six, 10-Hole Disc, 19.5" x 6" Steel	

SPRING SPECIFICATIONS — REAR LEAF

Super Duty Series/Model	Combined Rating @ Ground (lbs.)	Number of Leaves	Total Thickness @ Pad (in.)	Overall Length (in.)	Width (in.)	Deflection Rate (lbs. per in./ spring)[1] [2]	Rating Each @ Pad (lbs. per spring)
Main Leaf & Auxiliary Spring (Including Spacer)							
F-250 Pickup[3]	7000	6	4.18	58.1	3.00	330/650/1290	3133
F-350 SRW Pickup[4]	7000	6	4.18	58.1	3.00	330/650/1290	3133
F-350 DRW Pickup	9000	6	4.37	58.1	3.00	457/902/1422	4024
F-350 SRW Chassis Cab	7280	10	4.76	55.6	3.00	617/1342	3271
F-350 DRW Chassis Cab	9750	12	5.80	55.6	3.00	1014/1644	5305
F-450 Chassis Cab	12,000	11	6.75 (Includes Top Plate)	55.6	3.00	1253/2179	5324
F-550 Chassis Cab	13,660	11	6.75 (Includes Top Plate)	55.6	3.00	1256/2129	6150
Main Leaf Only							
F-250 Pickup	6100	5	2.66	58.1	3.00	334/776	2695
F-350 SRW Pickup[5]	7000	5	2.66	58.1	3.00	330/650	3133

(1) Pickup and Box Delete models include two-stage, variable rate springs. Chassis Cab models include single-stage, constant rate springs.
(2) Lists first stage/second stage/third stage as applicable.
(3) Auxiliary rear spring available and included with Camper Package, Heavy Service Suspension Package, Snow Plow Prep Package and Heavy Service Package For Pickup Box Delete only at Job# 1. Auxiliary rear spring available and included with Camper Package and Heavy Service Package For Pickup Box Delete only at Job# 2.
(4) Auxiliary rear spring will be deleted as standard and included with Camper Package and Heavy Service Package For Pickup Box Delete only at Job# 2.
(5) Standard and available at Job# 2

2006 SUPER DUTY F-250/350/450/550

WEIGHT RATINGS

F-450 DRW Chassis Cab - GVWR/Payload/Spring & GAWR (Front Assigned)/Base Curb Weight

Cab Style/ Drive/WB (in.)	Engine/ Transmission	Maximum GVWR (lbs.) Std./Opt.	Maximum Payload (lbs.)[1] Std./Opt.	Spring/GAWR (lbs.)[2] Front (lbs.)	Spring/GAWR (lbs.)[2] Rear (lbs.)	Base Curb Weight Front (lbs.)	Base Curb Weight Rear (Lbs.)	Base Curb Weight Total (lbs.)
Regular Cab 4x2 - 140.8	6.8L/Manual	16,000/15,000	9500/8500	4800	12,000	3610	2806	6416
	6.0L/Manual	16,000/15,000	9100/8100	5200	12,000	4090	2758	6848
Regular Cab 4x2 - 164.8	6.8L/Manual	16,000/15,000	9400/8400	5600	12,000	3727	2791	6518
	6.0L/Manual	16,000/15,000	9000/8000	6000	12,000	4213	2742	6955
Regular Cab 4x2 - 188.8	6.8L/Manual	16,000/15,000	9100/8100	6500	12,000	3895	2901	6796
	6.0L/Manual	16,000/15,000	8700/7700	6500	12,000	4355	2875	7230
Regular Cab 4x2 - 200.8	6.8L/Manual	16,000/15,000	9100/8100	6000	12,000	3936	2884	6820
	6.0L/Manual	16,000/15,000	8700/7700	6500	12,000	4425	2831	7256
Regular Cab 4x4 - 140.8	6.8L/Manual	16,000/15,000	9200/8200	5200	12,000	3868	2863	6751
	6.0L/Manual	16,000/15,000	8800/7800	5600	12,000	4334	2821	7155
Regular Cab 4x4 - 164.8	6.8L/Manual	16,000/15,000	9100/8100	5600	12,000	4026	2833	6859
	6.0L/Manual	16,000/15,000	8700/7700	6000	12,000	4476	2786	7262
Regular Cab 4x4 - 188.8	6.8L/Manual	16,000/15,000	8800/7800	6500	12,000	4182	2943	7125
	6.0L/Manual	16,000/15,000	8400/7400	6500	12,000	4633	2921	7554
Regular Cab 4x4 - 200.8	6.8L/Manual	16,000/15,000	8800/7800	6500	12,000	4242	2915	7157
	6.0L/Manual	16,000/15,000	8400/7400	6500	12,000	4696	2865	7561
SuperCab 4x2 - 161.8	6.8L/Manual	16,000/15,000	9100/8100	5200	12,000	3825	2959	6784
	6.0L/Manual	16,000/15,000	8700/7700	5600	12,000	4311	2910	7221
SuperCab 4x4 - 161.8	6.8L/Manual	16,000/15,000	8800/7800	5200	12,000	4123	2998	7121
	6.0L/Manual	16,000/15,000	8400/7400	6000	12,000	4574	2950	7524
Crew Cab 4x2 - 176.2	6.8L/Manual	16,000/15,000	8900/7900	5200	12,000	3967	3033	7000
	6.0L/Manual	16,000/15,000	8500/7500	5600	12,000	4454	2980	7434
Crew Cab 4x2 - 200.2	6.8L/Manual	16,000/15,000	8800/7800	6000	12,000	4093	3008	7101
	6.0L/Manual	16,000/15,000	8400/7400	6500	12,000	4582	2955	7537
Crew Cab 4x4 - 176.2	6.8L/Manual	16,000/15,000	8600/7600	5600	12,000	4259	3078	7337
	6.0L/Manual	16,000/15,000	8200/7200	6000	12,000	4711	3030	7741
Crew Cab 4x4 - 200.2	6.8L/Manual	16,000/15,000	8500/7500	6000	12,000	4395	3043	7438
	6.0L/Manual	16,000/15,000	8100/7100	6500	12,000	4849	2993	7842

(1) Load rating represents maximum allowable weight of people, cargo and body equipment and is reduced by optional equipment weight.
(2) Gross Axle Weight Rating is determined by the rated capacity of the minimum component of the axle system (axle, computer-selected springs, wheels, tires) of a specific vehicle. Front and rear GAWR's will, in all cases, sum to a number equal to or greater than the GVWR for the particular vehicle. Maximum loaded vehicle (including passengers, equipment and payload) cannot exceed the GVW rating or GAWR (front or rear).

NOTE: Refer to page 21 for Standard Powertrain/Chassis Equipment Specifications. Refer to Option/Payload Worksheet on pages 35-39 for optional equipment weights.

NOTE: Front spring/GAWR on Chassis Cab models is assigned or specifically selected. Refer to page 32, "Chassis Cab - Optional Front Spring/GAWR Availability", for specific front spring/GAWR upgrades included in available option packages.

2006 SUPER DUTY F-250/350/450/550

TECHNICAL SPECIFICATIONS

Suspensions

FRAME SPECIFICATIONS

Cab Style	Super Duty Series/Model	Wheelbase (in.)	No. Of Crossmembers	Maximum Side Rail Section (Height x Width X Thickness) (in.)[1]	Section Modulus (cu. in.)[2]	Yield Strength (psi)
Regular Cab	F-250-350 Pickup/Box Delete	137.0	5	6.87 x 2.36 x .264	6.7	36,000
	F-350 Chassis Cab	140.8	6	7.50 x 2.74 x .280	8.7	36,000
		164.8	7	7.50 x 2.74 x .280	8.7	36,000
	F-450-550 Chassis Cab (16,000/17,950 lb. GVWR Only)	140.8	6	7.50 x 2.74 x .320	10.1	36,000
		164.8	7	7.50 x 2.74 x .320	10.1	36,000
		188.8	8	7.50 x 2.74 x .60	17.2[3]	36,000
		200.8	9	7.50 x 2.74 x .60	17.2[3]	36,000
	F-550 (19,000 lb. GVWR Only)	164.8	7	7.50 x 2.74 x .60	17.2[3]	36,000
		200.8	9	7.50 x 2.74 x .60	17.2[3]	36,000
SuperCab	F-250-350 Pickup	141.8	6	6.87 x 2.36 x .264	6.7	36,000
	F-250-350 Pickup/Box Delete	158.0	6	6.87 x 2.36 x .264	6.7	36,000
	F-350 Chassis Cab	161.8	7	7.50 x 2.74 x .280	8.7	36,000
	F-450-550 Chassis Cab	161.8	7	7.50 x 2.74 x .320	10.1	36,000
Crew Cab	F-250-350 Pickup	156.2	7	6.87 x 2.36 x .264	6.7	36,000
	F-250-350 Pickup/Box Delete	172.4	7	6.87 x 2.36 x .264	6.7	36,000
	F-350 Chassis Cab	176.2	7	7.50 x 2.74 x .280	8.7	36,000
	F-450-550 Chassis Cab	176.2	7	7.50 x 2.74 x .320	10.1	36,000
		200.2	8	7.50 x 2.74 x .320	10.1	36,000

(1) Measured to inside of metal.
(2) Cross-sectional modulus calculated at back of cab, to inside of metal.
(3) Calculated at back of cab, through the reinforced section - 17.2 SM at upper flange, 13.3 SM at lower flange.

SHOCK ABSORBER SPECIFICATIONS

Super Duty Model	Wheelbase (in.)	Usage	Front No. Used	Front Piston Dia. (in.)	Front Type	Rear[1] No. Used	Rear[1] Piston Dia. (in.)	Rear[1] Type
Pickup/Chassis Cab	All	Std.	2	1.38	Gas-Pressurized	2	1.38	Gas-Pressurized
Pickup	All	Opt.[2]	2	1.38	Gas-Pressurized	2	1.38	Gas-Pressurized

(1) Staggered rear shock absorbers with Pickup models.
(2) Included with FX4 Off-Road Package. Unique Rancho shock absorbers with white housing and red bellows.

APPENDIX B

IST EDR3C-10 Detailed specification and calibration data

CERTIFICATE OF CALIBRATION

Model Number: EDR-3C-10
Serial Number: 689
Memory: 4 MB

Hardware Version: HC11v5A
Firmware Version: 3Cv1.61
Logic Version: 9100

Internal Accelerometers:		**CH1 (*x*)**	**CH2 (*y*)**	**CH3 (*z*)**
Channel Gains (mV/cnt):		*I1V:* 0.03326	*I2V:* 0.03326	*I3V:* 0.03326
Accelerometer Sensitivities (mV/g):		*I1A:* 1.473	*I2A:* 1.427	*I3A:* 1.427
Accelerometer Measurement Range (g):		11.5	11.9	11.9
Accelerometer Measurement Resolution (g):		.023	.023	.023
Temperature Coefficient (per °C):	*ATC:*	-0.2 %	Calibration Temperature:	25 °C
Accelerometer Frequency Response:		400 Hz		
Accelerometer Resonant Frequency:		1000 Hz		

External Accelerometers:

Channel Gains (mV/cnt):	*E1V:* .9627	*E2V:* .9631	*E3V:* .9659

Temperature Sensor, Humidity and Battery Voltage:

Internal Temperature Sensor (°C per cnt):	*ITS:*	.6253
Accelerometer Temperature Sensor (°C per cnt):	*ATS:*	.6253
External Temperature Sensor (°C per cnt):	*ETS:*	N/A
Humidity Sensor:	*HSO:* 166.9	*HSG:* .1569
Battery Voltage Sensor (V/cnt):	*BVS:* .01484	

Fixed Hardware Operating Characteristics:

Accelerometer Channel Low-Pass Filter (Anti-Aliasing) 3db Cut-Off:

Internal:	90 Hz
External:	90 Hz

Power-Up Voltage:	5.02
Automatic Power-Down Voltage:	4.83
Software Power-Down:	547F

Instrumented Sensor Technology, Inc.'s calibration procedure is traceable to NIST through the following:

Temperature/Humidity Probe:	131081	Date: 04/09/09
DVM:	3146A25274	Date: 01/26/09
Accelerometer(s):	15496	Date: 05/12/09
Calibrated by: TJ Huynh		Date: 07/15/09

IST Instrumented Sensor Technology

4704 Moore Street
Okemos, Michigan 48864
517-349-8487

EDR-3 Series Recorder Specifications

	EDR-3	EDR-3C	EDR-3D
DATA ACQUISITION			
#Selectable High Speed CHs:	3 (3)	3 (3)	6 (6)
#Simultaneous High Speed CHs:	3	3	6
Digitization	10-bit	10-bit	10-bit
#Low Speed CHs:	4	4	8
#Simultaneous Low Speed CHs	4	4	8
Temperature Sensor CHs	1 (1)	1 (1)	2 (2)
Humidity Sensor CHs	(1)	(1)	(2)
Battery Voltage CHs	1	1	2
#Trigger CHs	(1)	(1)	(2)
High Speed Digitization Rate	125-3200 (4800)	125-3200	125-3200
Low Speed	1 sample every 15 sec to 1 sample every 166 hours all models		
Digitization, Agreggate MAX, sps	9600 (14400)	9600	19200
DATA STORAGE			
MegaByte- Non-volatile SRAM	1 (2,4)	1 (2,4)	2 (4,8)
DATA MANAGEMENT			
Fill & Stop Memory Mode	X	X	X
Overwrite Memory Mode	X	X	X
Sliding Window Overwrite Mode™		X	X
Sliding Window Overwrite with Event Type Partitioning			X
Sliding Window Overwrite with Channel Set Partitioning			X
Sliding Window Size	N/A	Selectable 1 min to 30 days	
# Separate Time Windows	N/A	Selectable 1 to 100	

( ) = Optional

Window Overwrite™ (SWO) is a trademark of **Instrumented Sensor Technology, Inc.**

EDR-3 Series Recorder Specifications

	EDR-3	EDR-3C	EDR-3D
DATA COMMUNICATION			
Plug & Play Serial RS-232, modem compatible	9.6kBaud	9.6 to 115kBaud	9.6 to 115kBaud
SENSORS			
Internal Accelerometer: Piezoresistive Triaxial	X	X	X
Accelerometer fs Range Choices	±2, ±5, ±10, ±20, ±50, ±100, ± 200, ±500g all models		
Accelerometer Frequency Responses			
2g, 5g fs	DC-250 Hz, DC-350 Hz		
10g, 50g fs	DC-400 Hz, DC-1000 Hz		
100g, 200g fs	DC-1500 Hz, DC-2000 Hz		
Signal Filtering: 4th Order Anti-Aliasing	60, 80, 90, 110, 140, 170, 200, 340, 420, 510, 620, 750, 930, 1120, 1915 Hz		
Standard 3dB cutoff choices	1% fs/sec all models		
Automatic Auto-Zero Offset Correction			
External Accelerometers:	Voltage mode piezoelectric, 0.5mA, 3.4V bias, 0.5mv/g to 1000 mv/g, all models		
PROGRAMMABILITY			
High Speed Sample Rate	X	X	X
Trigger selection	Internal or external channels and/or external trigger input, all models		
Triggering	X	X	X
Amplitude Threshold	X	X	X
Separate channel thresholds		X	X
Duration (time at level) Threshold	X	X	X
Separate channel thresholds		X	X
Trigger Duration Threshold	1 to 34463 samples all models		
Time Trigger Delay	0 to 35000 seconds all models		
(forced time delay between triggered recordings)	1 sample every 15 sec to 1 sample every 166 hours all models		
Time Triggered Recording			
Maximum Number of Events	5291	5291	10582
Event Length:	Fixed or Data Dependent		
Pre-trigger samples	2 to 9997 all models		
Post-trigger samples	1 to 9999 all models		
Maximum Event Length cutoff:	9999 samples all models		
Memory Modes:	FS, OW	FS, OW, SW	FS, OW, SWO, SWO-ETP,-CSP
OPERATIONAL			
Temperature Recording	Internal & external all models		
Range/Resolution	-40 to +70˚C/ ±3˚C all models		
Humidity Recording	Internal & external all models		
Range/Resolution	0 to 100% RH / ±3% RH all models		
Usable Temperature Range	1 to 60˚C all models		
Digital Clock	Month/Day/Year, Hour:Min:Sec all models		
Date & Time Tagged to each acceleration event			
Resolution/Accuracy	53 msec / ±3 min/Mo all models		
Auto ON and OFF times	X	X	X
Connectors	DB9 for RS-232 serial all models (4-pin microdot for external RS-232, aux. power, all models) (10-32 microdot for external accelerometers)		
Battery Life(Typical) Alkaline C-cell Batteries	30-40 days	20+ days	15+ days
Data Memory Backup	12+ months all models		
PHYSICAL			
Size	4.2"x 4.4" x 2.2"	4.2"x 4.4"x 2.2"	4.2"x 4.4"x 2.5"
Housing	Black Anodized Aluminum, watertight, gasket sealed		
Weight	2.2 lb	2.2 lb	2.6 lb
Operating Temperature Range	-40 to + 70˚C all models		
Shock Fragility	500g or 20 x fs, all models		

STANDARD ANALYSES
(with DM95-BASE Software package)

3-Channel Acceleration waveform graphics, histograms, temp/hum process
Resultant Acceleration waveforms
Spreadsheet tabulation of max, min, peak, duration, RMS, crest factor, velocity change, temperature, humidity, dew point, battery volt
Data editing and sorting by selected event parameters, statistical summaries
Digital filtering- low pass, high pass, bandpass

OPTIONAL ANALYSIS SOFTWARE

DM95-int Velocity and Displacement Waveforms
DM95-psd Power Spectral Density (PSD) calculation and analysis
DM95-srs Shock Response Spectrum (SRS) calculation and analysis
DM95-drop Packaging Drop height - Equivalent impact, Zero-G free fall, package trajectory animation, impact direction & type.
DM95-deriv Jerk Waveform calculation and display

HARDWARE OPTIONS			
Memory expansion	2,4 Mb	2,4 Mb	4,8 Mb
External Channel inputs	3 accel, temp, power, COM, trigger		
Relative humidity sensor	internal and/or external		
Higher digitization rates	X		
Auxiliary battery pack	X	X	X
Hand-Held remote trigger (HRT-1)	X	X	X
Remote Alarm Module (RALM-1)	X	X	X

Printed in the U.S.A. 1/99

IST Instrumented Sensor Technology
4704 Moore Street • Okemos, MI 48864 • 517/349-8487 • Fax 517/349-8469
E-Mail Address: info@isthq.com • Web Site: http://www.isthq.com

APPENDIX C

Raw vibration data collected from experimentation

Highway Road Surface Data

Table 11: Ambulance vibration amplitudes due to highway travel at speeds ≤ 35mph

Speed ≤ 35 mph - Highway									
	Mean r.m.s. accel. (m sec-2)			Maximum peak accel. (m sec-2)			Mean peak accel. (m sec-2)		
	Z-axis	Worst axis	Resultant Tri-axial sum	Z-axis	Worst axis	Resultant Tri-axial sum	Z-axis	Worst axis	Resultant Tri-axial sum
1	**0.60**	**0.60 (z)**	**0.80**	**6.92**	**6.92 (z)**	**7.48**	**3.44**	**3.44 (z)**	**3.96**
2	**0.62**	**0.62 (z)**	**0.87**	**4.81**	**4.81 (z)**	**5.58**	**3.17**	**3.17 (z)**	**3.44**
3	**0.71**	**0.71 (z)**	**0.87**	**7.90**	**7.90 (z)**	**9.13**	**3.90**	**3.90 (z)**	**4.46**
4	**0.59**	**1.80 (x)**	**1.96**	**6.38**	**6.38 (z)**	**7.69**	**4.06**	**4.06 (z)**	**5.39**

Table 12: Ambulance vibration amplitudes due to highway travel at speeds 36-64mph

Speed 36 - 64 mph - Highway									
	Mean r.m.s. accel. (m sec-2)			Maximum peak accel. (m sec-2)			Mean peak accel. (m sec-2)		
	Z-axis	Worst axis	Resultant Tri-axial sum	Z-axis	Worst axis	Resultant Tri-axial sum	Z-axis	Worst axis	Resultant Tri-axial sum
1	**0.84**	**0.84 (z)**	**0.96**	**10.32**	**10.32 (z)**	**14.63**	**5.05**	**5.05 (z)**	**6.34**
2	**0.78**	**0.78 (z)**	**0.87**	**4.13**	**4.13 (z)**	**4.21**	**3.07**	**3.07 (z)**	**3.28**
3	**1.18**	**1.18 (z)**	**1.31**	**10.80**	**10.80 (z)**	**11.05**	**5.53**	**5.53 (y)**	**6.11**
4	**0.67**	**0.67 (z)**	**0.79**	**5.94**	**5.94 (z)**	**6.38**	**3.57**	**3.57 (z)**	**4.05**

Table 13: Ambulance vibration amplitudes due to highway travel at speeds ≥ 65mph

Speed ≥ 65- Highway									
	Mean r.m.s. accel. (m sec-2)			Maximum peak accel. (m sec-2)			Mean peak accel. (m sec-2)		
	Z-axis	Worst axis	Resultant Tri-axial sum	Z-axis	Worst axis	Resultant Tri-axial sum	Z-axis	Worst axis	Resultant Tri-axial sum
1	**1.12**	**1.12 (z)**	**1.36**	**7.83**	**7.83 (z)**	**7.95**	**4.45**	**4.45 (z)**	**4.89**
2	**1.02**	**1.02 (z)**	**1.26**	**4.80**	**4.80 (z)**	**4.86**	**3.50**	**3.50 (z)**	**4.15**
3	**1.63**	**1.63 (z)**	**1.81**	**15.05**	**15.05 (z)**	**15.16**	**7.25**	**7.25 (z)**	**7.62**
4	**0.96**	**0.96 (z)**	**1.12**	**5.71**	**5.71 (z)**	**5.80**	**4.40**	**4.40 (z)**	**4.69**

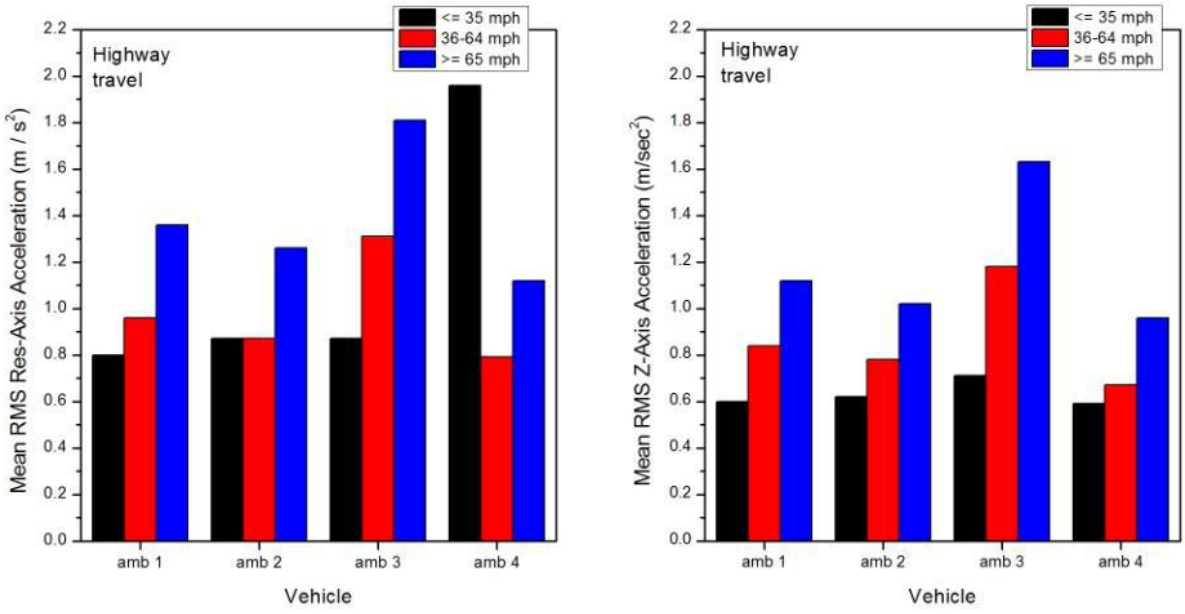

Figure 34: Overall vibration level – highway travel all ambulances all speeds

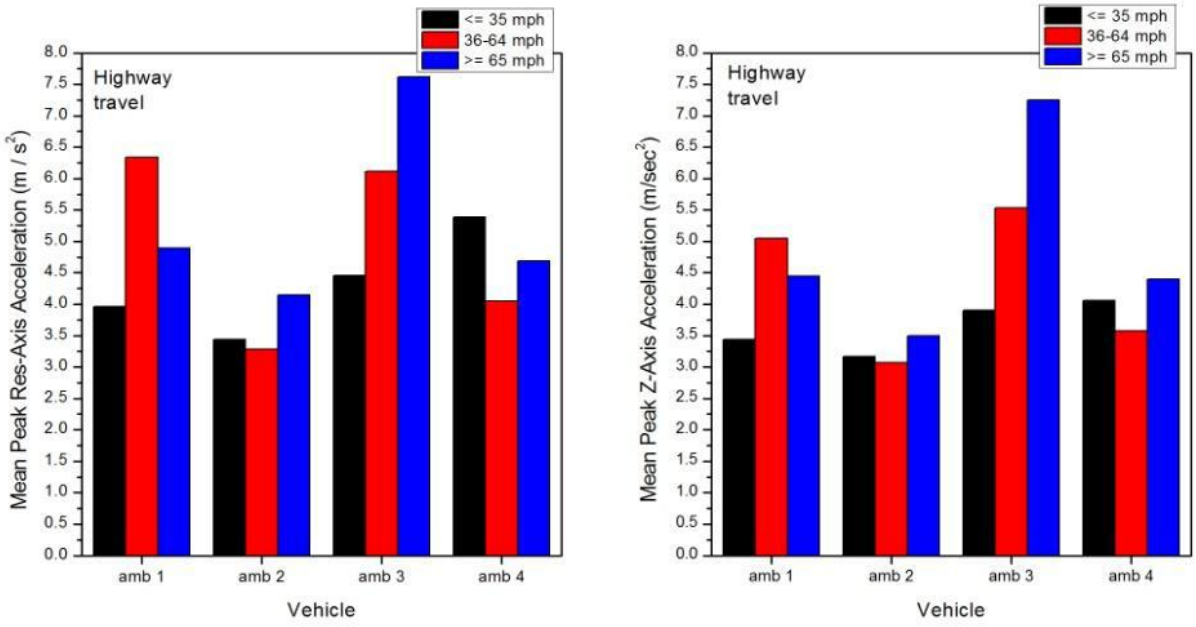

Figure 35: Mean peak vibration level – highway travel all ambulances all speeds

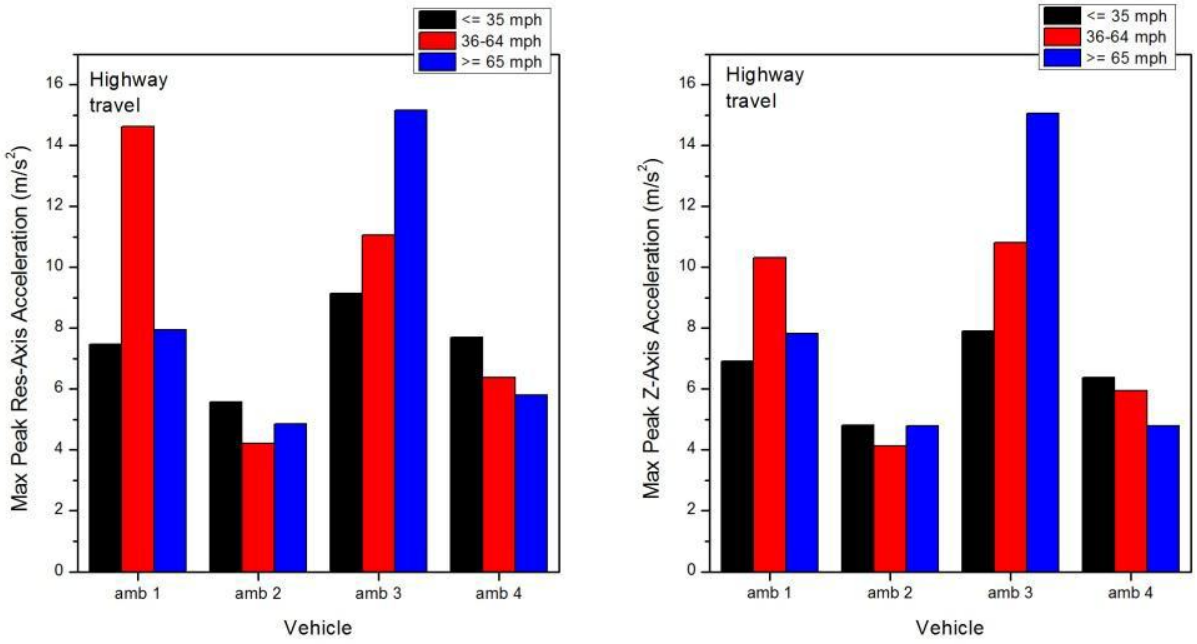

Figure 36: Max peak vibration level – highway travel all ambulances all speeds

Secondary Road Surface Data

Table 14: Ambulance vibration amplitudes on secondary roads at speeds ≤ 35mph

Speed ≤ 35 mph – Secondary roads									
	Mean r.m.s. accel. (m sec-2)			Maximum peak accel. (m sec-2)			Mean peak accel. (m sec-2)		
	Z-axis	Worst axis	Resultant Tri-axial sum	Z-axis	Worst axis	Resultant Tri-axial sum	Z-axis	Worst axis	Resultant Tri-axial sum
1	**0.91**	**0.91 (z)**	**1.23**	**8.28**	**8.28 (z)**	**8.35**	**4.46**	**4.46 (z)**	**5.14**
2	**0.88**	**0.88 (z)**	**1.16**	**9.04**	**9.04 (z)**	**9.04**	**5.21**	**5.21 (z)**	**5.56**
3	**0.99**	**0.99 (z)**	**1.10**	**9.72**	**9.72 (z)**	**9.72**	**4.99**	**4.99 (z)**	**5.23**
4	**0.50**	**0.50 (z)**	**0.66**	**3.47**	**3.47 (z)**	**3.94**	**2.50**	**2.50 (z)**	**2.66**

Table 15: Ambulance vibration amplitudes on secondary roads at speeds 36-64mph

Speed 36 - 64 mph – Secondary roads									
	Mean r.m.s. accel. (m sec-2)			Maximum peak accel. (m sec-2)			Mean peak accel. (m sec-2)		
	Z-axis	Worst axis	Resultant Tri-axial sum	Z-axis	Worst axis	Resultant Tri-axial sum	Z-axis	Worst axis	Resultant Tri-axial sum
1	**1.20**	**1.20 (z)**	**1.46**	**7.82**	**7.82 (z)**	**7.86**	**6.42**	**6.42 (z)**	**6.93**
2	**1.05**	**1.05 (z)**	**1.53**	**7.48**	**7.48 (z)**	**8.32**	**5.36**	**5.36 (z)**	**5.89**
3	**1.34**	**1.34 (z)**	**2.00**	**8.16**	**8.16 (z)**	**8.62**	**5.62**	**5.62 (z)**	**6.21**
4	**0.60**	**0.60 (z)**	**0.92**	**3.48**	**3.48 (z)**	**4.17**	**2.62**	**2.62 (z)**	**3.17**

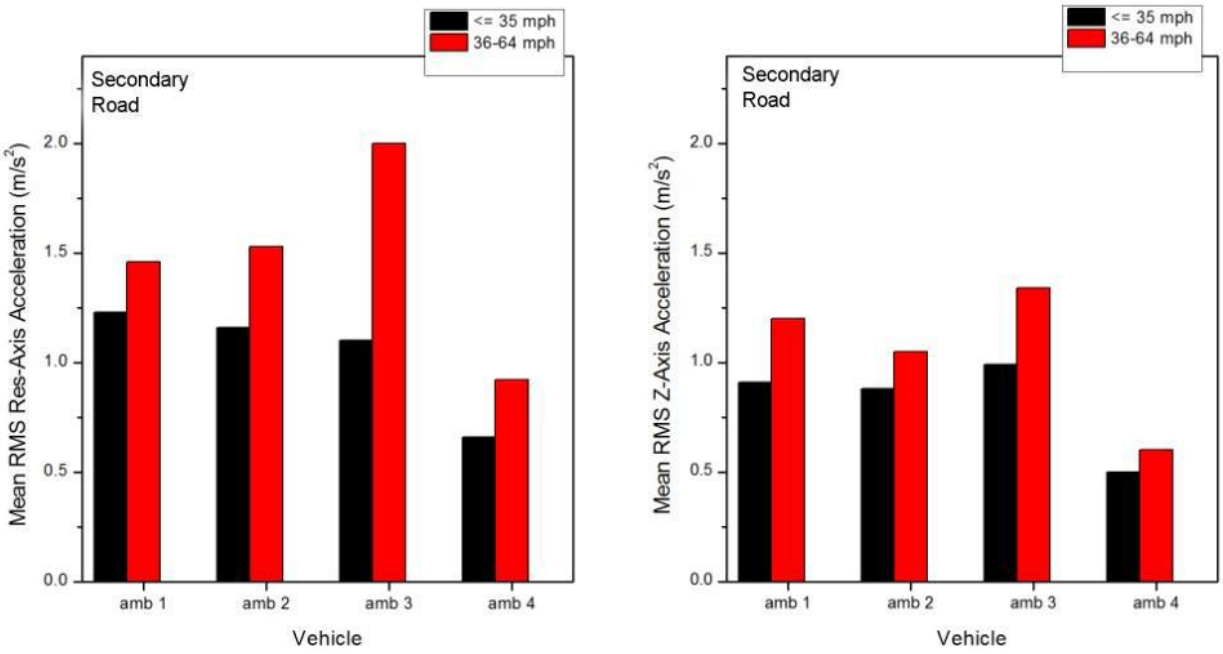

Figure 37: Overall vibration level – secondary road all ambulances all speeds

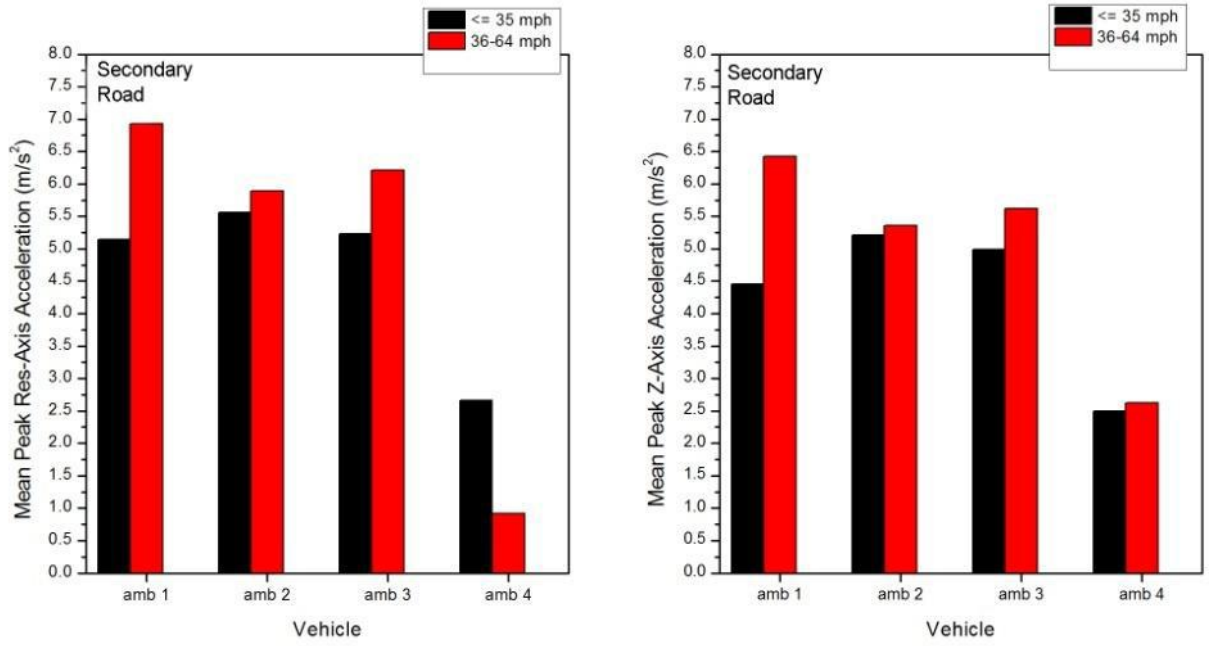

Figure 38: Mean peak vibration level – highway travel all ambulances all speeds

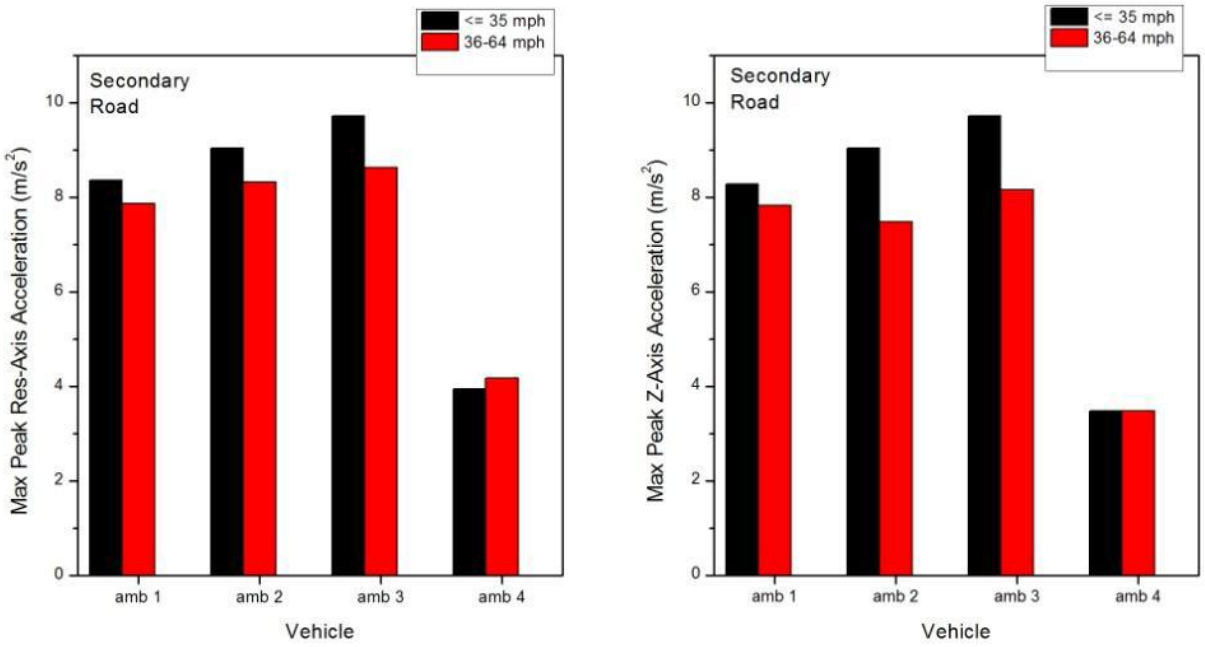

Figure 39: Max peak vibration level – highway travel all ambulances all speeds

City Street Road Surface Data

Table 16: Ambulance vibration amplitudes on city streets at speeds ≤ 35mph

Speed ≤ 35 mph – City streets									
	Mean r.m.s. accel. (m sec-2)			Maximum peak accel. (m sec-2)			Mean peak accel. (m sec-2)		
	Z-axis	Worst axis	Resultant Tri-axial sum	Z-axis	Worst axis	Resultant Tri-axial sum	Z-axis	Worst axis	Resultant Tri-axial sum
1	**0.84**	**0.92 (x)**	**1.50**	**7.60**	**7.60 (z)**	**9.62**	**4.61**	**4.61 (z)**	**5.60**
2	**0.62**	**0.64 (z)**	**1.15**	**10.38**	**10.38 (z)**	**10.48**	**3.67**	**3.67 (x)**	**4.30**
3	**0.99**	**0.99 (z)**	**1.32**	**12.04**	**12.04 (z)**	**12.14**	**5.48**	**5.48 (z)**	**5.92**
4	**0.60**	**0.60 (z)**	**0.97**	**9.79**	**9.79 (z)**	**17.87**	**3.69**	**3.69 (z)**	**4.74**

Table 17: Ambulance vibration amplitudes on city streets at speeds 36-64mph

Speed 36 - 64 mph – City streets									
	Mean r.m.s. accel. (m sec-2)			Maximum peak accel. (m sec-2)			Mean peak accel. (m sec-2)		
	Z-axis	Worst axis	Resultant Tri-axial sum	Z-axis	Worst axis	Resultant Tri-axial sum	Z-axis	Worst axis	Resultant Tri-axial sum
1	**1.24**	**1.24 (z)**	**1.75**	**7.60**	7.60 **(z)**	**8.06**	**6.61**	**6.61 (z)**	**7.36**
2	**0.88**	**0.88 (z)**	**1.00**	**6.59**	**6.59 (z)**	**6.60**	**4.21**	**4.21 (z)**	**4.46**
3	**1.29**	**1.29 (z)**	**11.09**	**11.09**	**11.09 (z)**	**11.16**	**8.03**	**8.03 (x)**	**9.56**
4	**0.77**	**0.77 (z)**	**6.62**	**4.83**	**4.83 (z)**	**6.64**	**2.92**	**2.92 (z)**	**3.70**

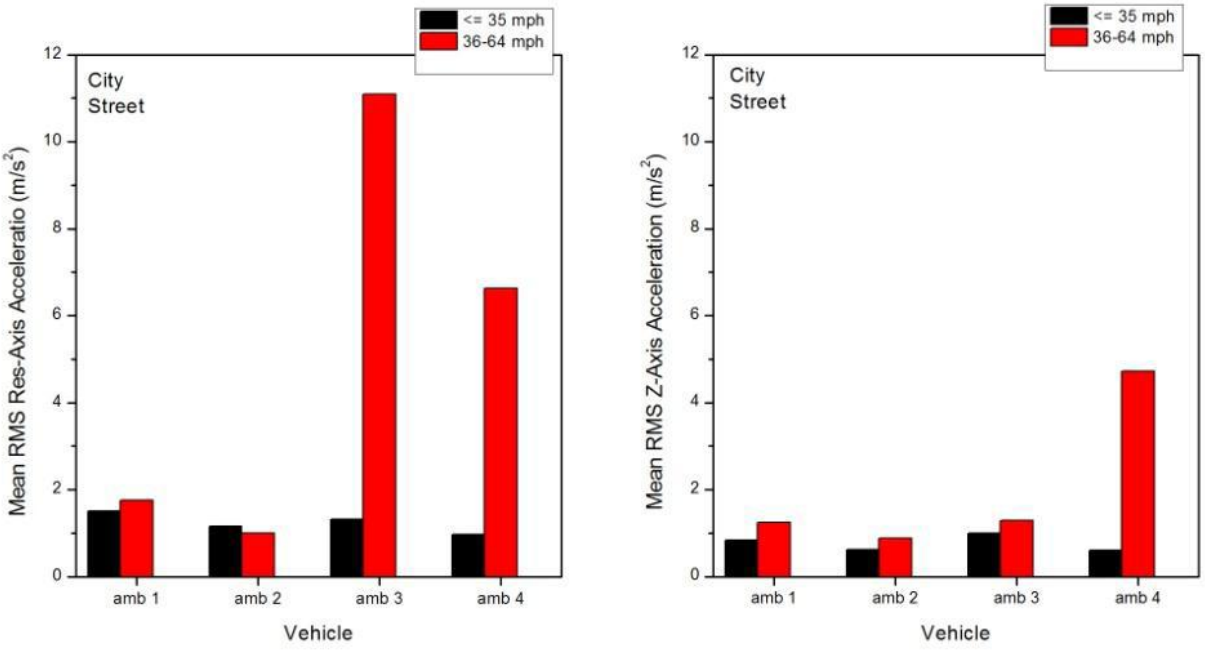

Figure 40: Overall vibration level – city street all ambulances all speeds

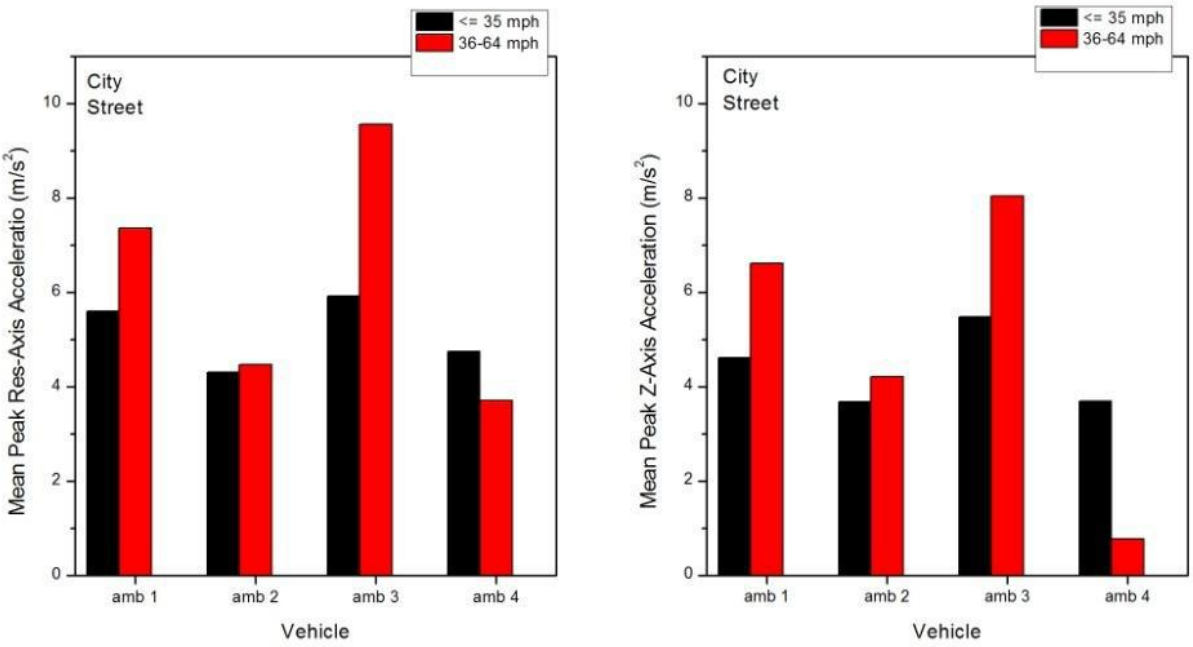

Figure 41: Mean peak vibration level – city street all ambulances all speeds

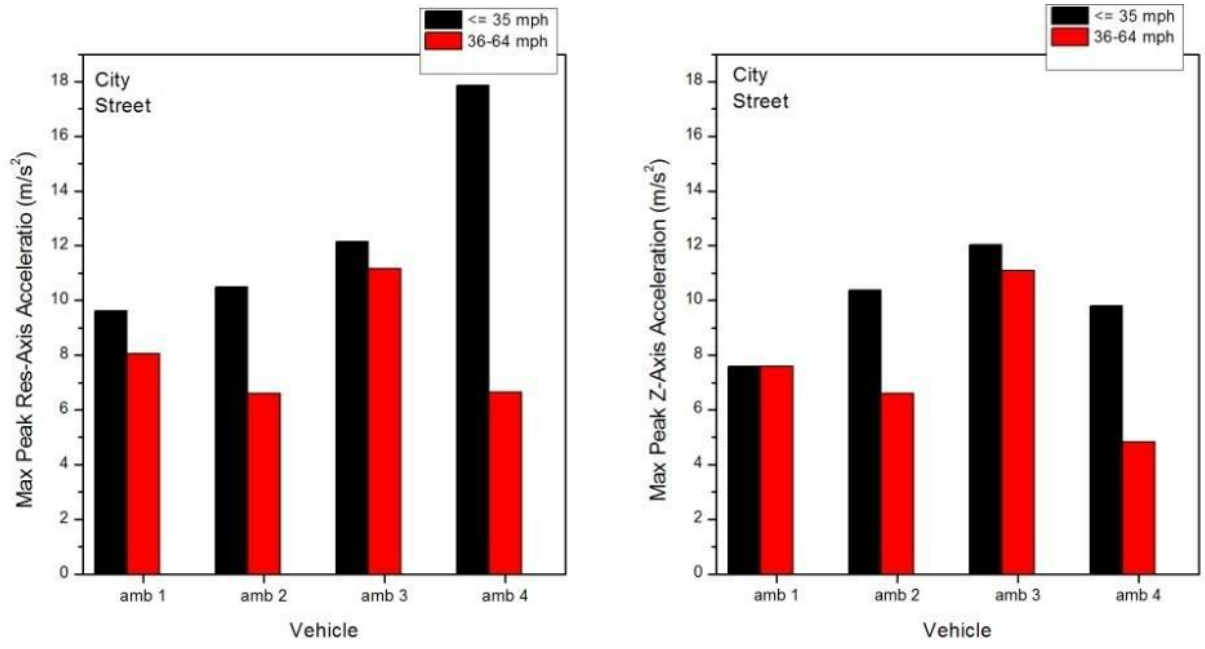

Figure 42: Max peak vibration level – city street all ambulances all speeds

Unpaved Road Surface Data

Table 18: Ambulance vibration amplitudes on unpaved roads at speeds ≤ 35mph

Speed ≤ 35 mph – Unpaved roads									
	Mean r.m.s. accel. (m sec-2)			Maximum peak accel. (m sec-2)			Mean peak accel. (m sec-2)		
	Z-axis	Worst axis	Resultant Tri-axial sum	Z-axis	Worst axis	Resultant Tri-axial sum	Z-axis	Worst axis	Resultant Tri-axial sum
1	**2.41**	**2.41 (z)**	**2.77**	**15.31**	**15.31 (z)**	**15.43**	**13.56**	**13.56 (z)**	**13.53**
2	**0.75**	**0.75 (z)**	**0.98**	**4.58**	**4.58 (z)**	**4.86**	**2.88**	**2.88 (x)**	**3.14**
3	**2.55**	**2.55 (z)**	**2.94**	**22.29**	**22.29 (z)**	**23.72**	**15.45**	**15.45 (z)**	**16.08**
4	**0.46**	**0.63 (x)**	**0.94**	**2.36**	**2.94 (x)**	**3.65**	**1.87**	**1.88 (x)**	**2.90**

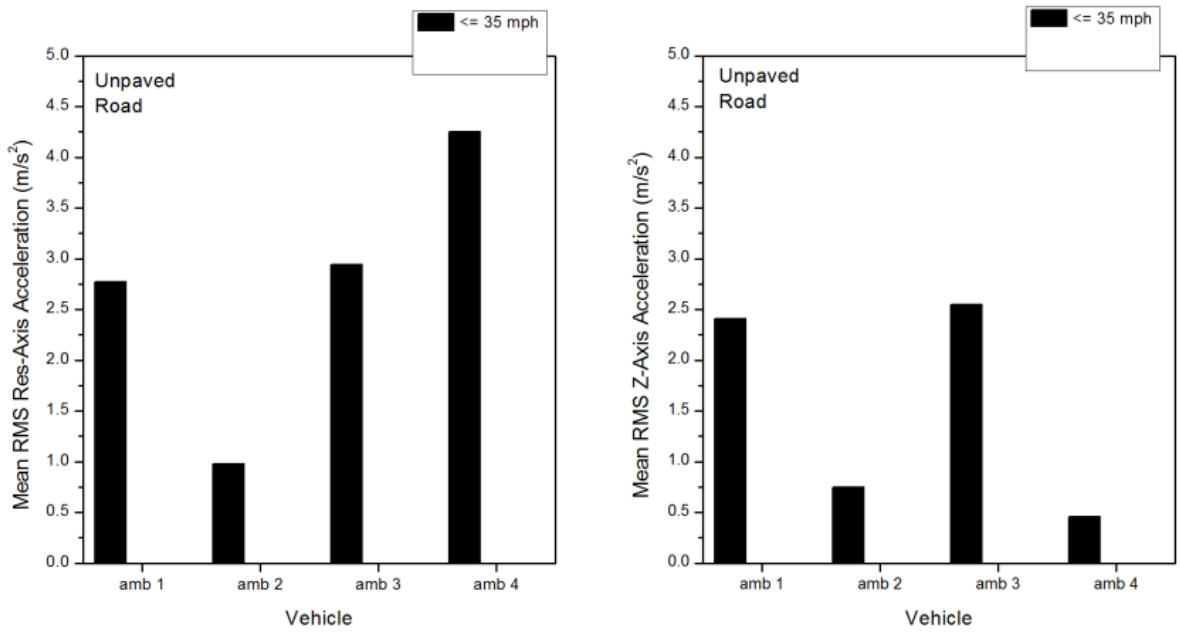

Figure 43: Overall vibration level – unpaved road all ambulances all speeds

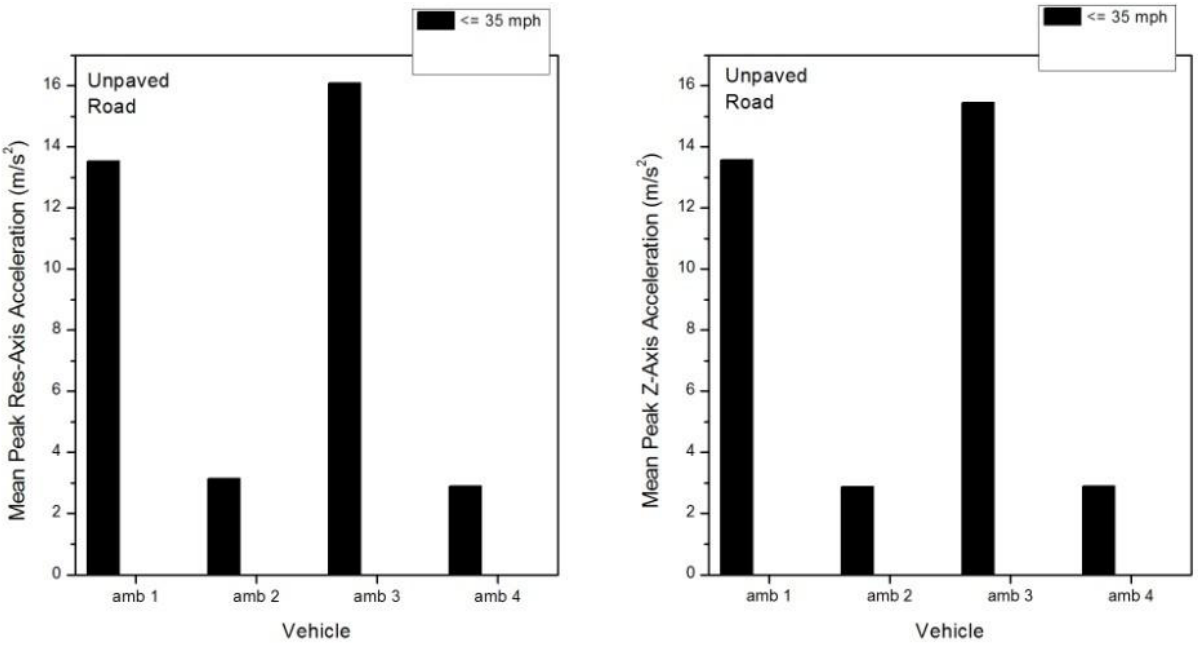

Figure 44: Mean peak vibration level – unpaved road all ambulances all speeds

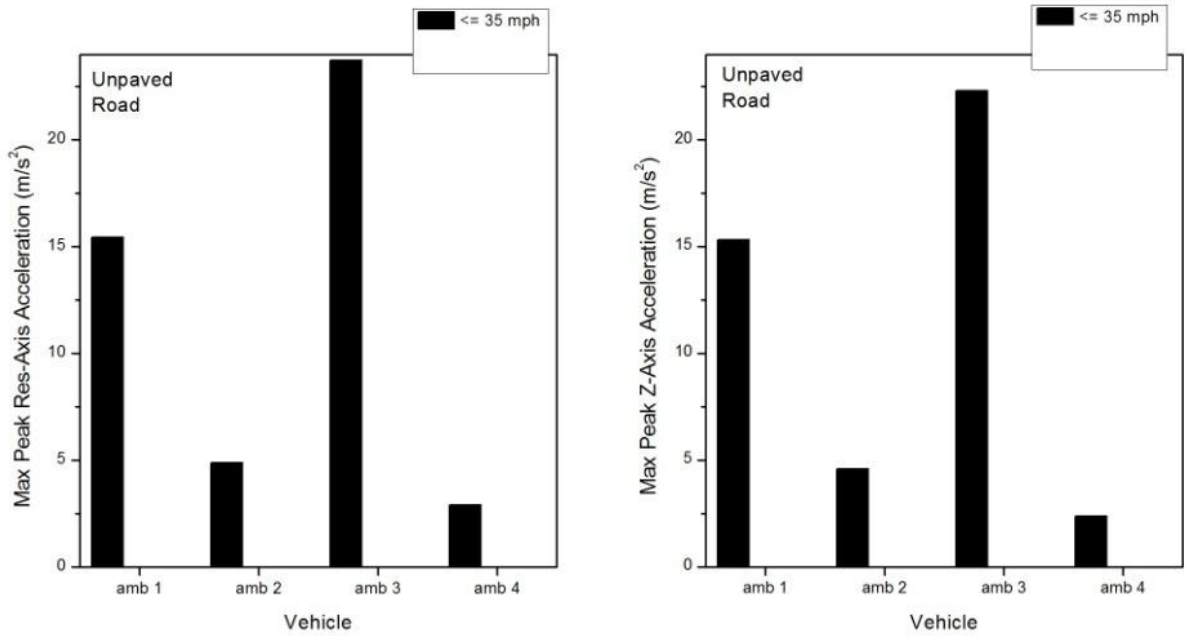

Figure 45: Max peak vibration level – unpaved road all ambulances all speeds

APPENDIX D

Vibration time history and power spectrum density graphs derived from experimental data.

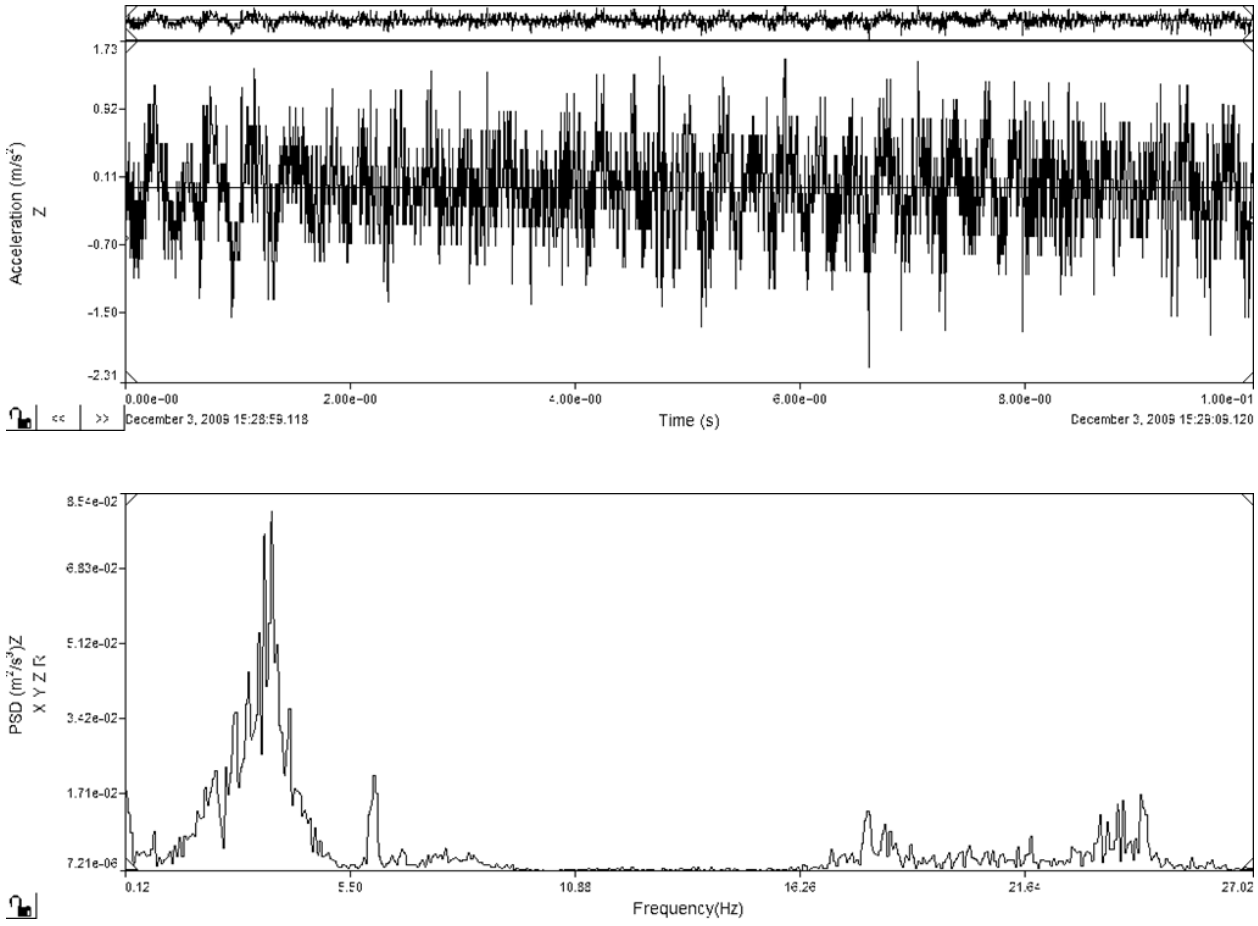

Figure 46: Ambulance #1 – Highway, 35mph, Z-Axis R.M.S., typical 10 sec event interval

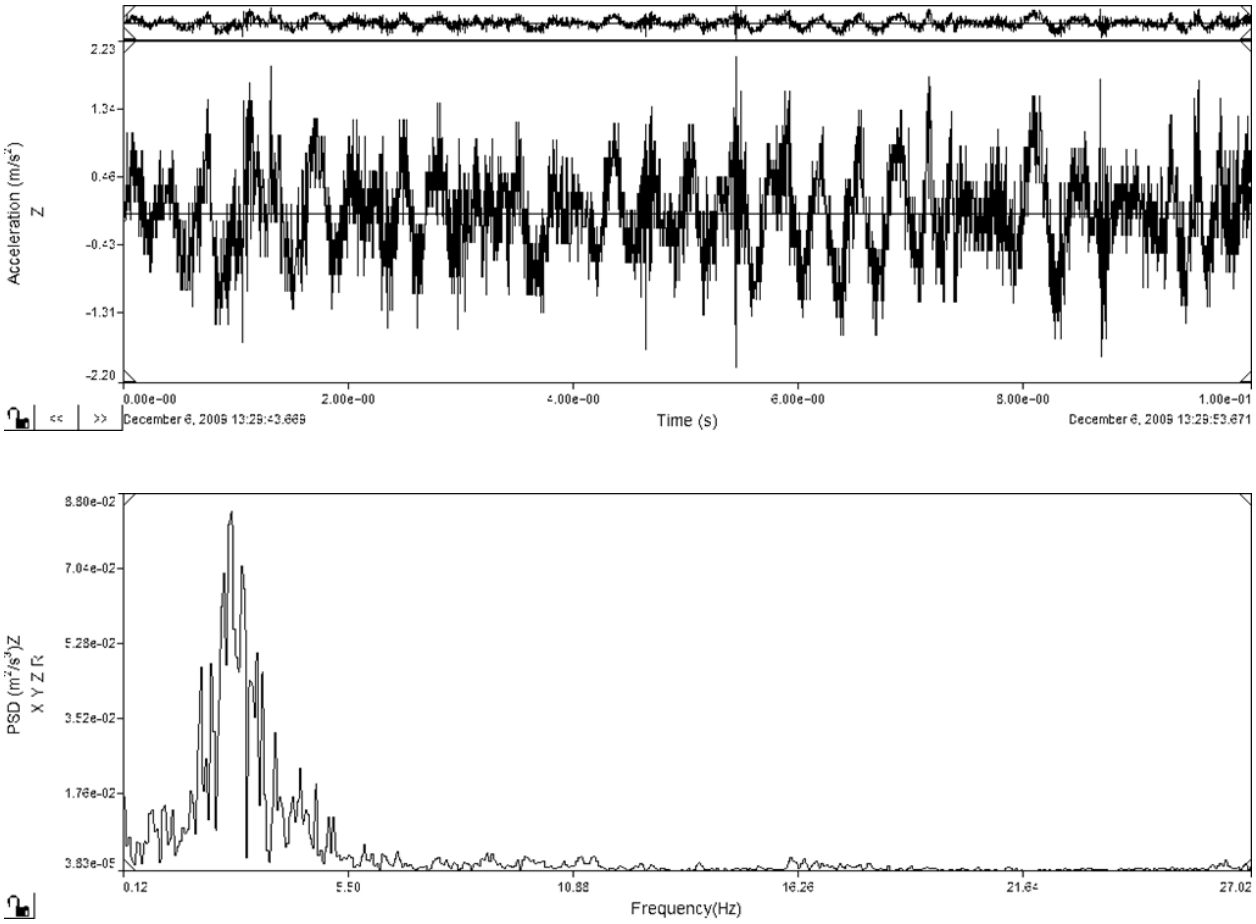

Figure 47: Ambulance #2 – Highway, 35mph, Z-axis R.M.S., typical 10 sec time interval

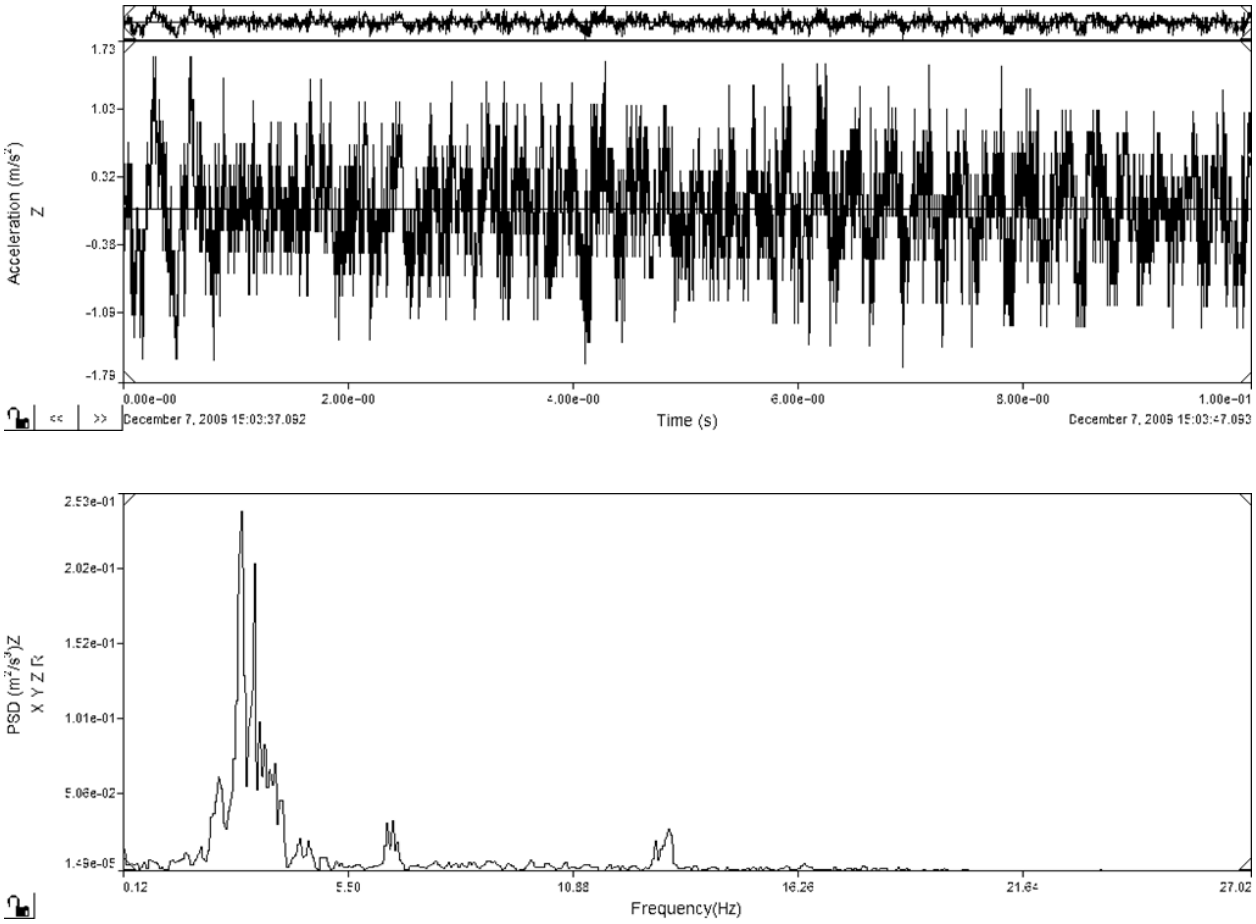

Figure 48: Ambulance #3 – Highway, 35mph, Z-axis R.M.S., typical 10 sec time interval

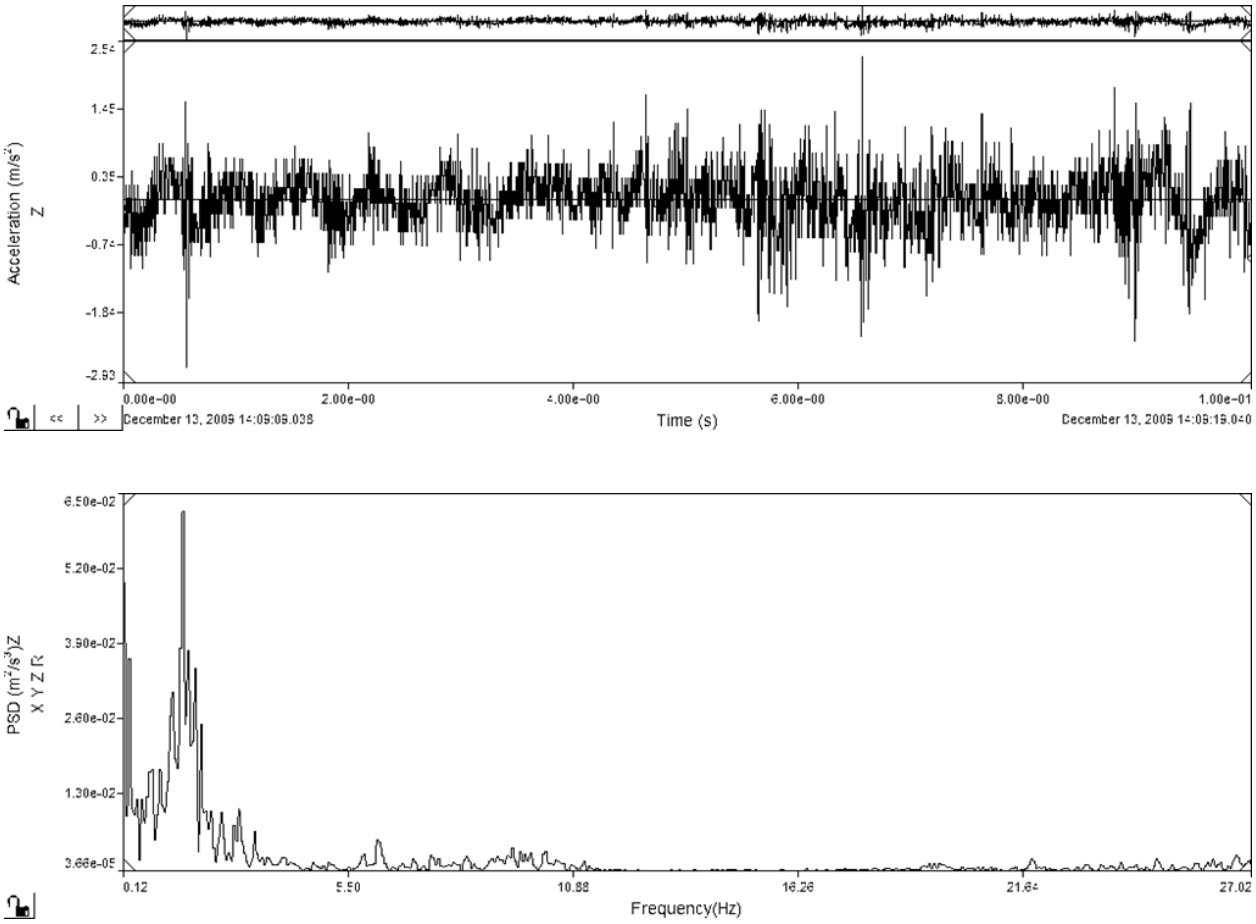

Figure 49: Ambulance #4 – Highway, 35mph, Z-axis R.M.S., typical 10 sec time interval

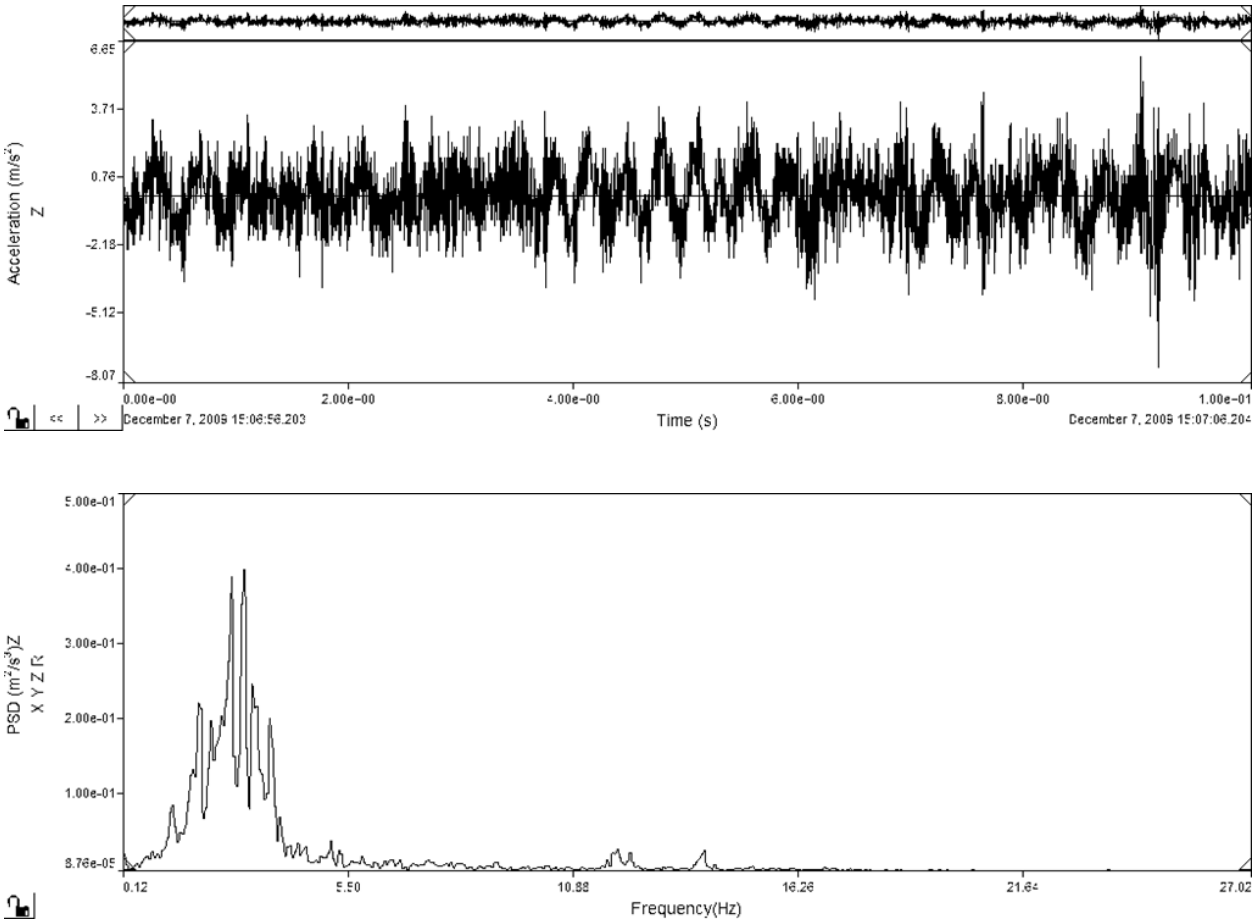

Figure 50: Highway, Ambulance #3, Z-Axis R.M.S.,≥65 mph., typical 10 sec event interval

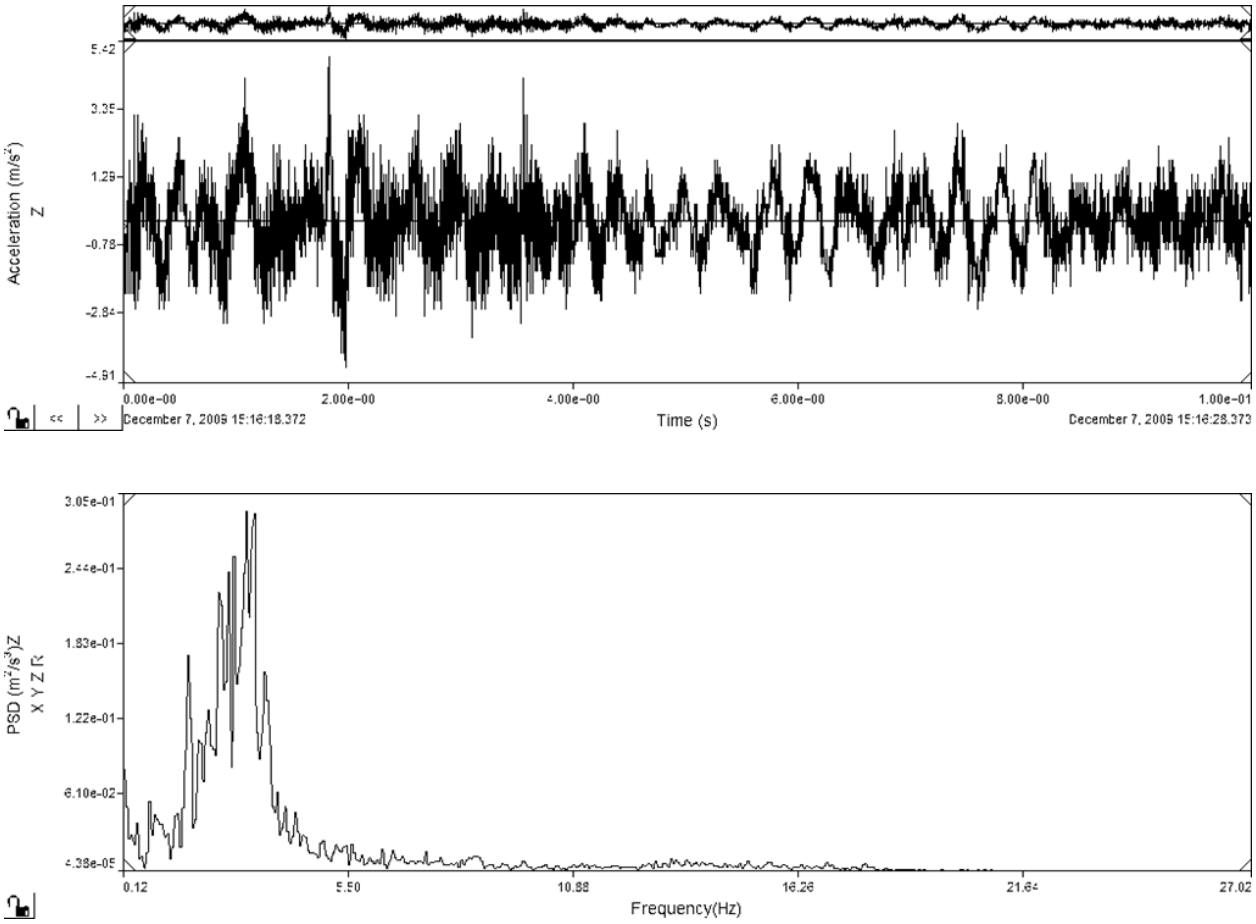

Figure 51: Secondary road , Ambulance #3, Z-Axis R.M.S.,≤35 - 64 mph., typical 10 sec event interval

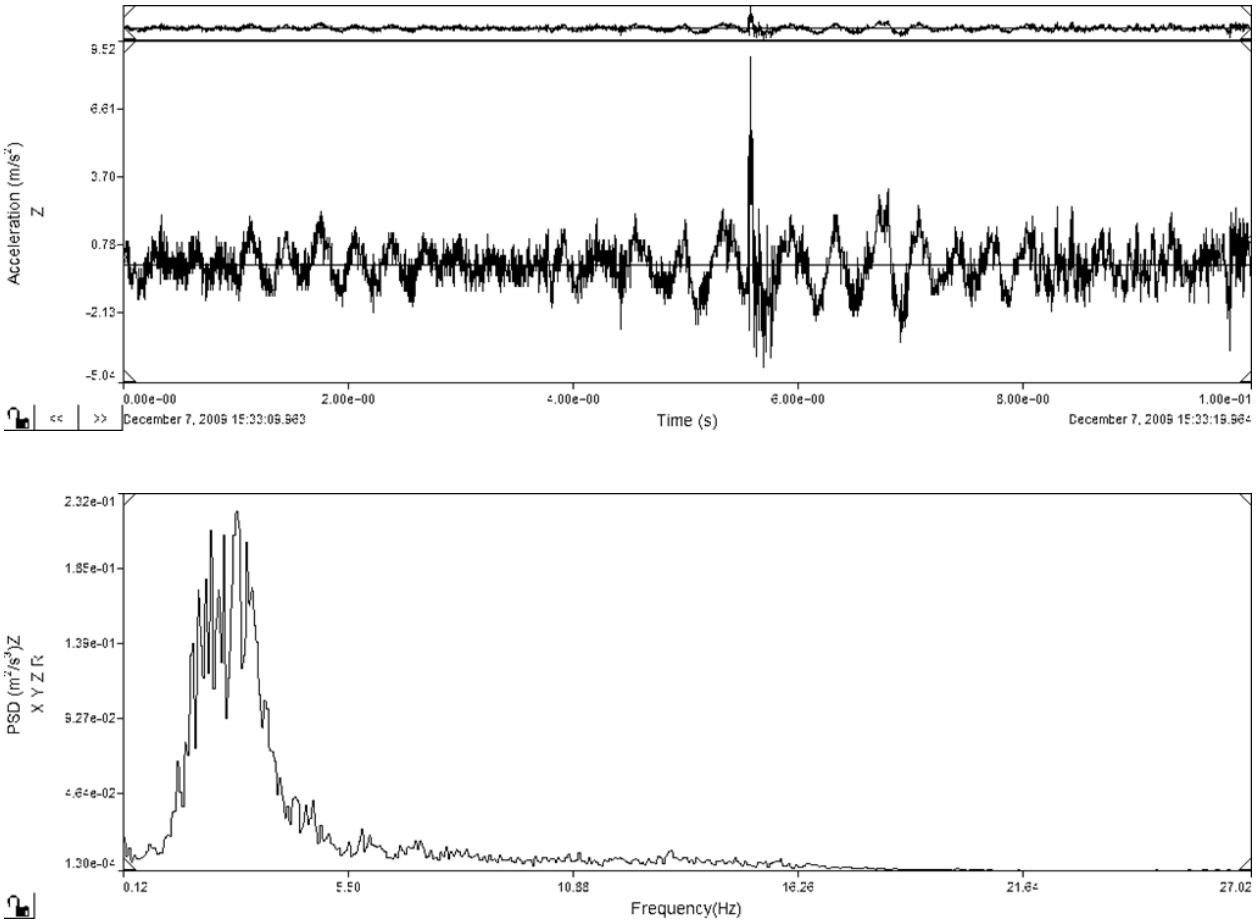

Figure 52: City Street, Ambulance #3, Z-Axis R.M.S.,≤35 - 64 mph., typical 10 sec event interval

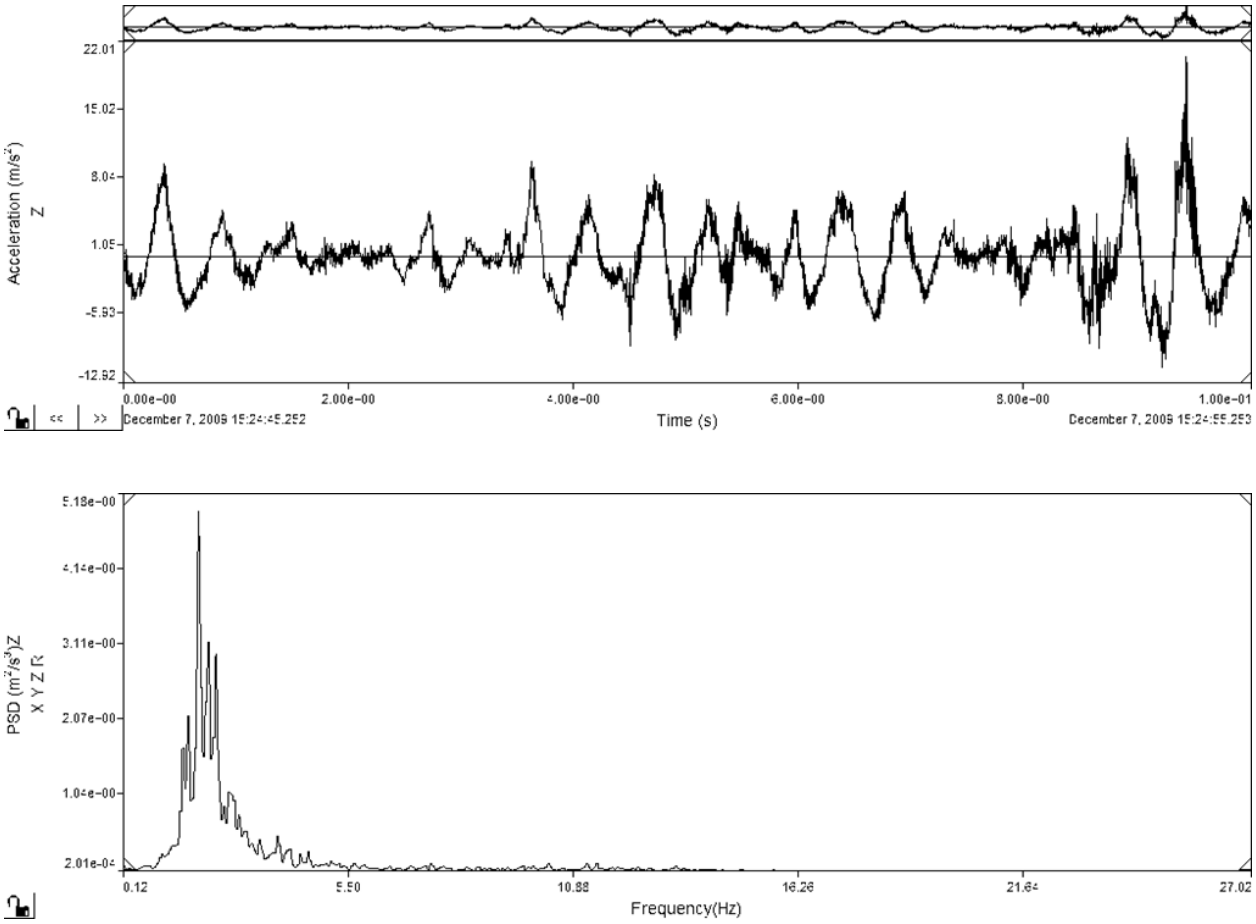

Figure 53: Unpaved Road, Ambulance #3, Z-Axis R.M.S. ≤ 35, typical 10 sec event interval

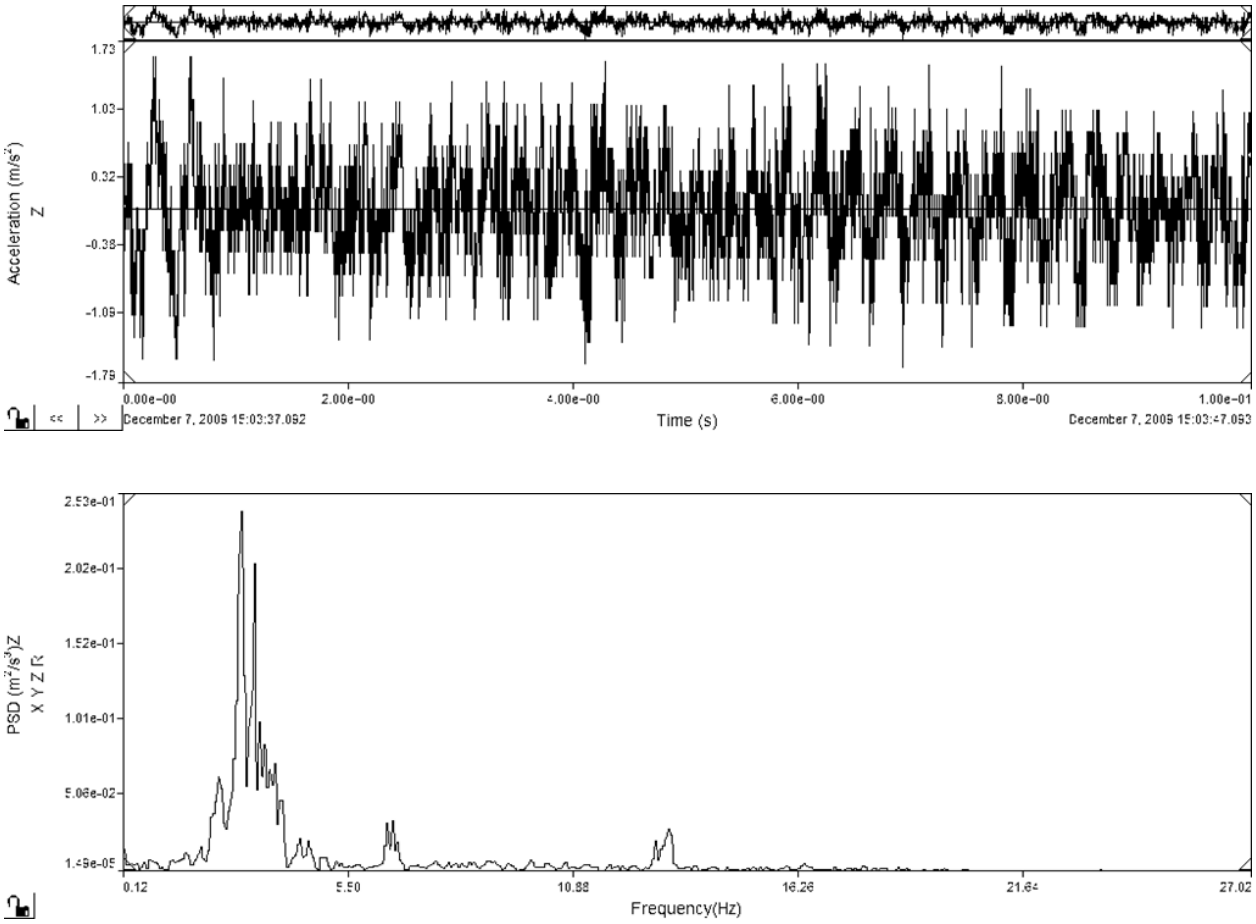

Figure 54: ≤35 mph, Highway, Ambulance #3, Z-Axis R.M.S., typical 10 sec event interval

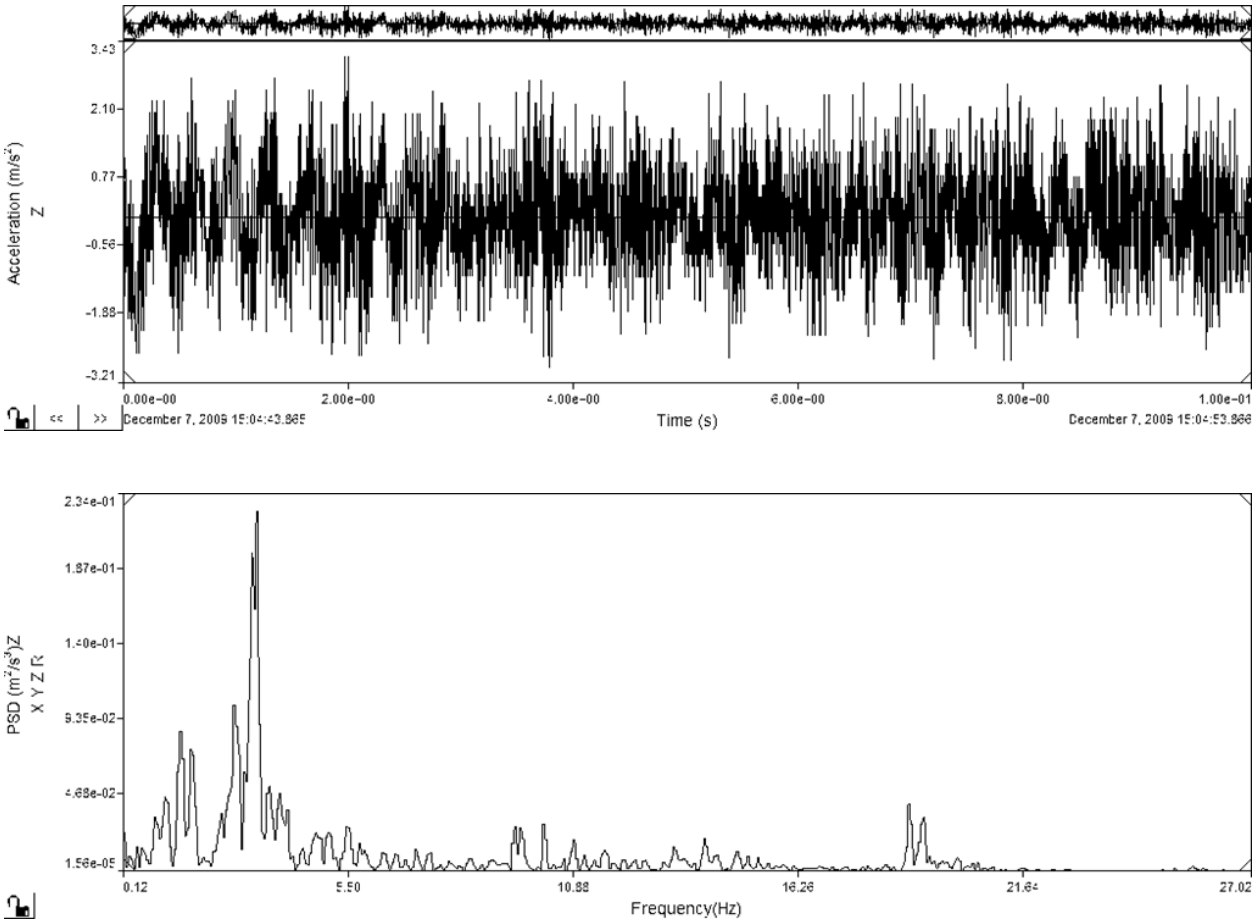

Figure 55: 36-64 mph, Highway, Ambulance #3, Z-Axis R.M.S., typical 10 sec event interval

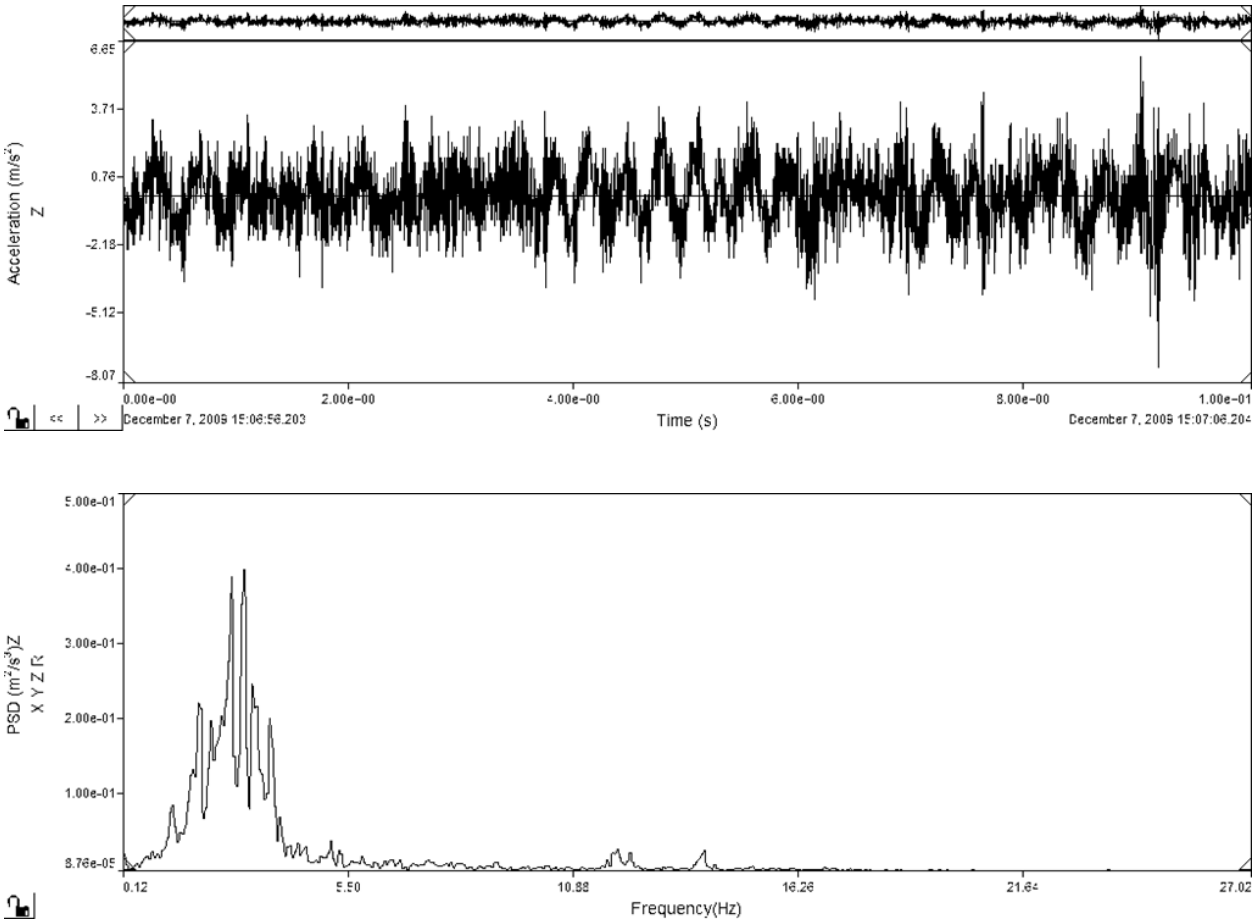

Figure 56: ≥65 mph, Highway, Ambulance #3, Z-Axis R.M.S., typical 10 sec event interval

APPENDIX E

Forcing function graphs derived from data collected during experimentation.

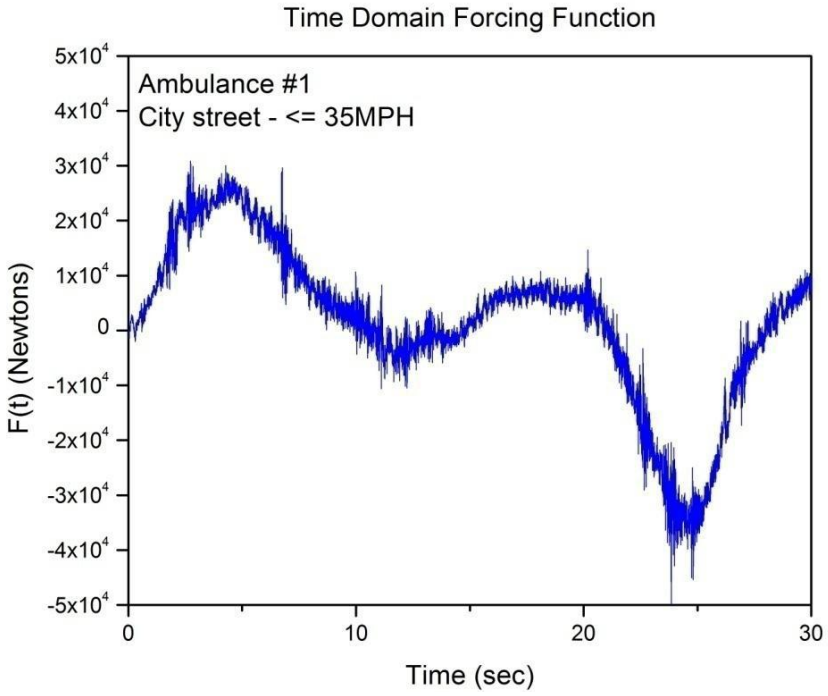

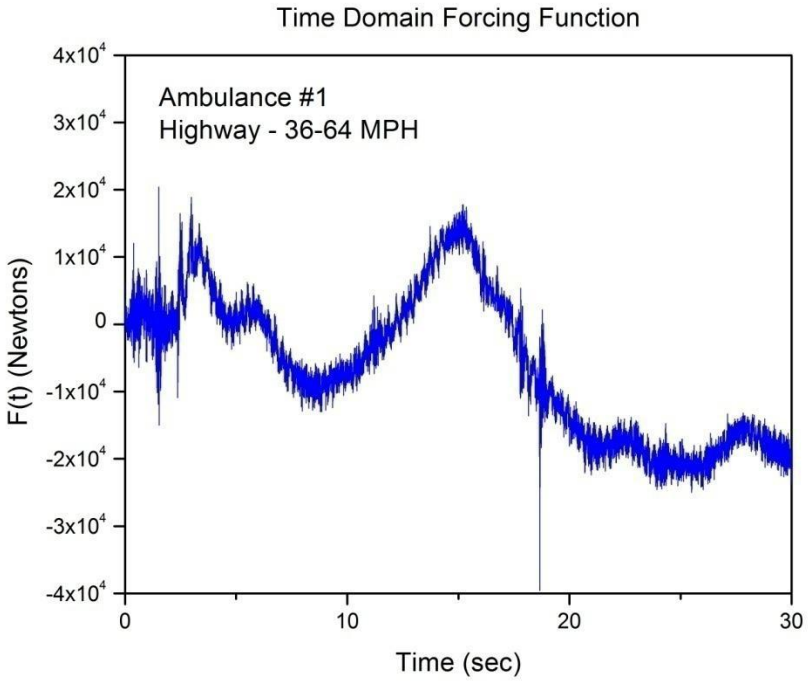

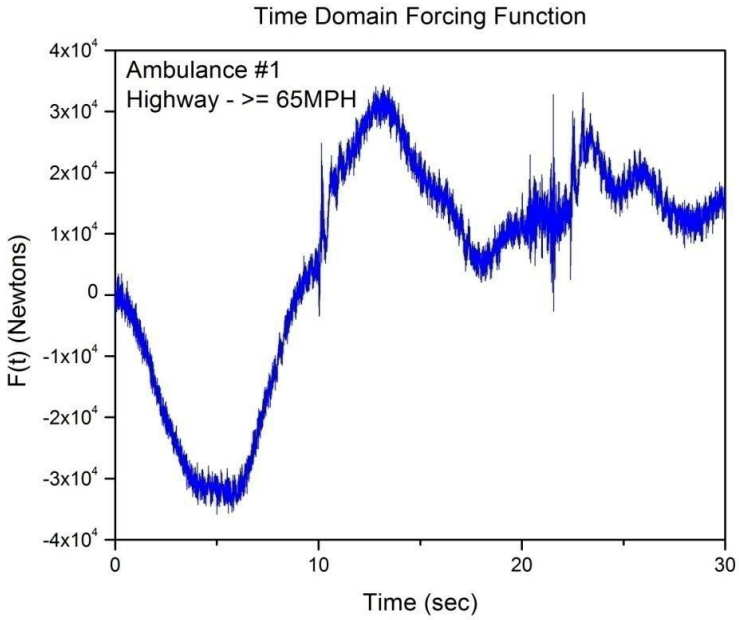
Time Domain Forcing Function
Ambulance #1
Highway - >= 65MPH
F(t) (Newtons)
Time (sec)
4x10^4
3x10^4
2x10^4
1x10^4
0
-1x10^4
-2x10^4
-3x10^4
-4x10^4
0
10
20
30

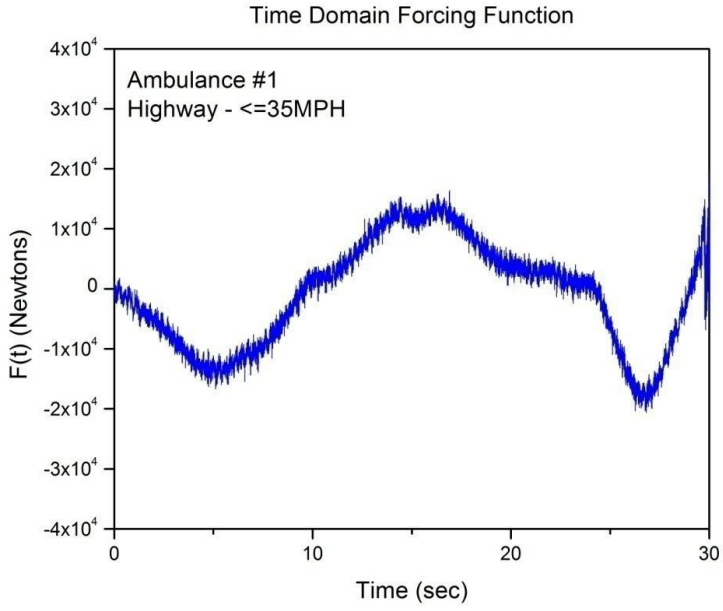
Time Domain Forcing Function
Ambulance #1
Highway - <=35MPH
F(t) (Newtons)
Time (sec)
4x10^4
3x10^4
2x10^4
1x10^4
0
-1x10^4
-2x10^4
-3x10^4
-4x10^4
0
10
20
30

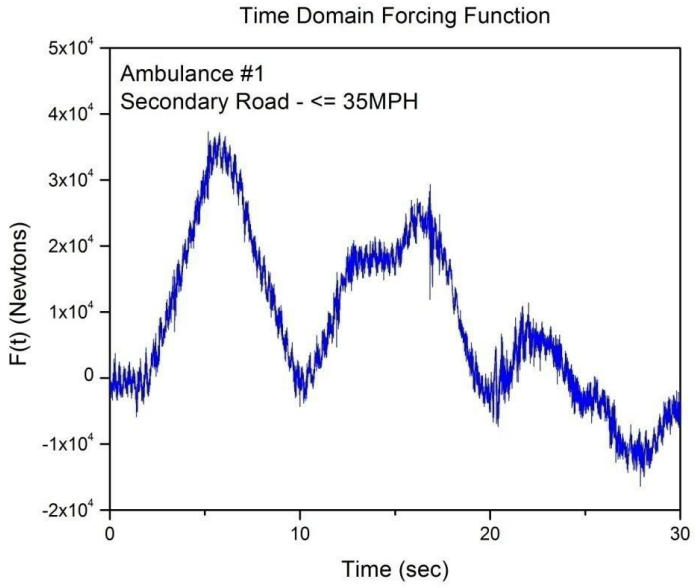
Time Domain Forcing Function
Ambulance #1
Secondary Road - <= 35MPH
F(t) (Newtons)
Time (sec)
5x10^4
4x10^4
3x10^4
2x10^4
1x10^4
0
-1x10^4
-2x10^4
0
10
20
30

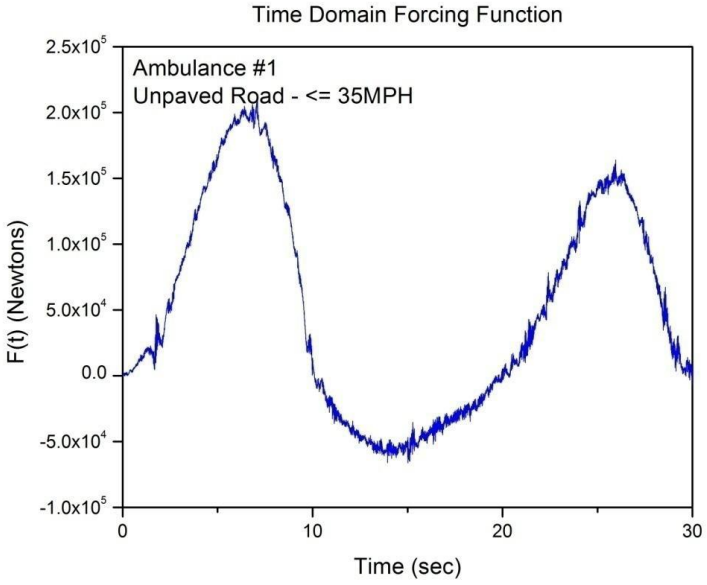
Time Domain Forcing Function
Ambulance #1
Unpaved Road - <= 35MPH
F(t) (Newtons)
Time (sec)
2.5x10^5
2.0x10^5
1.5x10^5
1.0x10^5
5.0x10^4
0.0
-5.0x10^4
-1.0x10^5
0
10
20
30